Supplementary Information

1. General Methods

CHNS Microanalysis

CHNS Analysis was performed on a Thermo EA1112 Flash CHNS-O Analyzer using standard microanalytical procedures.

Nuclear Magnetic Resonance Spectroscopy

Solution state ^{1}H and $^{13}C\{^{1}H\}$ Nuclear magnetic resonance spectra were recorded at 400 and 75 MHz respectively using a Bruker Avance 400 NMR spectrometer. Solid-state NMR experiments were performed on a 9.4 T Bruker DSX solid-state NMR spectrometer 4 mm HXY triple-resonance Magic Angle Spinning (MAS) probe in double resonance mode tuned to ^{1}H at $n_0(^{1}H)$ = 399.98 MHz and the X channel tuned to ^{13}C at $\nu_0(^{13}C)$ = 100.56 MHz. Experiments were performed at room temperature under MAS at ν_r = 12.5 kHz. ^{1}H pulses and SPINAL-64 heteronuclear decoupling decoupling[1] were performed at a radiofrequency (rf) field amplitude of 83 kHz. ^{1}H-^{13}C cross polarization (CP) MAS experiments were obtained with a ^{13}C rf field of 55 kHz, while the ^{1}H rf field amplitude was ramped to obtain maximum signal at a ^{1}H rf field of approximately 60 kHz, at a contact time of 2 ms for 16384 and 8192 scans for S2 and S3 respectively at a recycle delay corresponding to $1.3*T_1(^{1}H)$. The ^{13}C chemical shifts were referenced to the CH carbon of adamantane at 29.45 ppm.[2] Samples were packed in a zirconia rotor with a KelF cap, and NMR data were obtained and analysed using TopSpin 3.2.

Mass Spectrometry

High resolution mass spectrometry of precursors and S1, MeF1-3, PSP and MSM were performed on an Agilent Technologies 6530B accuratemass QTOF mixed ESI/APCI mass spectrometer (capillary voltage 4000 V, fragmentor 225 V) in positive-ion detection mode. Mass spectrometry of PFP was performed on an Agilent 7890B GC-MS. Mass spectrometry of MFM, S2 and S3 were performed at the National Mass Spectrometry Facility on an Xevo G2-S Atmospheric Solids Analysis Probe in positive ion detection mode.

Fourier Transformed Infra-Red Spectroscopy

Transmission FT-IR spectra were recorded on a Bruker Tensor 27 at room temperature; samples were prepared as pressed KBr pellets.

Thermogravimetric Analysis

Thermogravimetric analysis was performed on an EXSTAR6000 by heating samples at 10 °C min^{-1} under air in open platinum pans from room temperature to 800 °C.

Powder X-ray Diffraction

PXRD patterns were collected in transmission mode on samples held on thin Mylar film in aluminium well plates on a Panalytical Empyrean diffractometer, equipped with a high throughput screening XYZ stage, X-ray focusing mirror, and PIXcel detector, using Cu-Kα (λ = 1.541 Å) radiation. PXRD patterns were recorded at room temperature.

Single crystal X-ray Diffraction

SC-XRD data sets were measured on a Rigaku MicroMax-007 HF rotating anode diffractometer (Mo-Kα radiation, λ = 0.71073 Å, Kappa 4-circle goniometer, Rigaku Saturn724+ detector); or at beamline I19, Diamond Light Source, Didcot, UK using silicon double crystal monochromated synchrotron radiation (λ = 0.6889 Å, Pilatus 2M detector). Absorption corrections, using the multi-scan method, were performed with the program SADABS.[3,4] For synchrotron X-ray data, collected at Diamond Light Source (λ = 0.6889Å) data reduction and absorption corrections were performed with xia2.[5] Structures were solved with SHELXT,[6] or by direct methods using SHELXS,[7] and refined by full-matrix least squares on $|F|^2$ by SHELXL,[8] interfaced through the programme OLEX2.[9] All H-atoms were fixed in geometrically estimated positions and refined using the riding model. For full refinement details, see Tables S1-3.

Inductively Coupled Plasma Mass Spectrometry

Palladium contents were determined by by ICP-MS using a Perkin Elmer ICP MS NexION 2000. Samples (5 mg) were digested in nitric acid (70 wt. %, 10 mL) using a Perkin Elmer Microwave Titan prior to analysis and diluted to a minimum volume of 50 mL. Instrument has 1 ppb (0.0000001 wt. %) baseline with respect to the digested sample solution, therefore 'useable' limit is 10 ppm (0.001 wt. %) with respect to the sample

Static Light Scattering

SLS measurements were performed on a Malvern Mastersizer 3000 Particle Sizer, polymers were dispersed in water or in water/methanol/triethylamine (1:1:1) mixture by 10 minutes of ultrasonication and the resultant suspensions were injected into a stirred Hydro SV quartz cell, containing more of water or water/methanol/triethylamine (1:1:1) mixture, to give a laser

obscuration of 5 – 10%. Particle sizes were fitted according to Mie theory, using the Malvern 'General Purpose' analysis model, for non-spherical particles with fine powder mode turned on. An oligomer refractive index of 1.59, oligomer absorbance of 0.1 and solvent refractive index of 1.33 (water) or 1.37 (water/methanol/triethylamine) were used for fitting.

Scanning (Transmission) Electron Microscopy

Imaging of the oligomer morphology was achieved on a Tescan S8000G with secondary electron, backscatter and transmission detectors. SEM samples were dropped as powder onto conductive carbon and coated with chromium using a sputter coater. SEM images recorded at 3 keV with a beam current of 26 pA. STEM samples were dropped onto Agar Scientific holey carbon / Cu TEM grids from water suspensions. Unless otherwise stated images were recorded at 20 keV with a current of 125 pA. Images were recorded in both Bright Field (BF) mode and High Angle Dark Field (HADF) mode.

UV-Visible Absorption Spectroscopy

The UV-Visible absorption spectra of the oligomers as solutions in chloroform and the diffuse reflectance spectra of the oligomers in the solid state were recorded, at room temperature on a Shimadzu UV-2550 UV-Vis spectrometer.

Fluorescence Spectroscopy

The fluorescence spectra of the oligomers were measured with a Shimadzu RF-5301PC fluorescence spectrometer at room temperature in the solid state and as solutions in chloroform.

Time Correlated Single Photon Counting

TCSPC experiments were performed on an Edinburgh Instruments LS980-D2S2-STM spectrometer equipped with picosecond pulsed LED excitation sources and a R928 detector, with a stop count rate below 3%. An EPL-295 diodide (λ = 300.4 nm, instrument response 100 ps, fwhm) or an EPL-375 diode (λ = 370.5 nm, instrument response 100 ps, fwhm) were used as the light source. Oligomers were measured in the solid state and in chloroform solution. The instrument response was measured with colloidal silica (LUDOX HS-40, Sigma-Aldrich) at the excitation wavelength. Decay times were fitted in the FAST software using suggested lifetime estimates.

DFT Calculations

All (TD-)DFT calculations were performed using Turbomole 7.01[10] and employed besides

the parameters discussed in the main text a m3 grid throughout. The optical gap of the polymers is approximated by the excitation energy of the lowest energy vertical singlet excitation as predicted by TD-DFT.

Transient Absorption

Transient absorption experiments and photoinduced absorption measurements were carried out as described previously.[11]

Hydrogen Evolution Experiments

Water for hydrogen evolution experiments was purified using an ELGA LabWater system with a Purelab Option S filtration and ion exchange column (ρ = 15 MΩ cm) without pH level adjustment. A quartz flask was charged with the catalyst, Pd co-catalysts (if applicable) and dispersants as described and sealed with a septum. The resulting suspension was ultrasonicated until the photocatalyst was dispersed before degassing by N_2 bubbling for 30 minutes. For standard measurements the reaction mixture was illuminated with a 300 W Newport Xe light-source (Model: 6258, Ozone free) for the time specified. The lamp was cooled by water circulating through a metal jacket. Gas samples were taken with a gas-tight syringe, and run on a Bruker 450-GC gas chromatograph equipped with a Molecular Sieve 13X 60-80 mesh 1.5 m × ⅛" × 2 mm ss column at 50 °C with an argon flow of 40.0 mL min^{-1}. Hydrogen was detected with a thermal conductivity detector referencing against standard gas with a known concentration of hydrogen. Hydrogen dissolved in the reaction mixture was not measured and the pressure increase generated by the evolved hydrogen was neglected in the calculations. The rates were determined from a linear regression fit and the error is given as the standard deviation of the amount of hydrogen evolved.

External Quantum Efficiency

EQEs were measured using a 420 nm (± 10 nm, fwhm) LED. S2 or S3 (12 mg) were suspended in water/TEA/MeOH (1:1:1, 8 mL) by sonication. The mixture was transferred into a quartz cell, sealed with a septum and degassed for 30 minutes before illuminating with the LED. Light intensity was measured at the front of the cell using a ThorLabs probe and the hydrogen produced was measured as above. Efficiency was calculated as the incident photon to hydrogen conversion yield. Path length was 1 cm, illuminated area was 8 cm and light intensity varied from 15-19 W m^{-2} between experiments.

2. Synthesis

All reagents including MeF1 and S1 were obtained from Sigma-Aldrich, TCI, or Fluorochem and used as received. Water for the hydrogen evolution experiments was purified using an ELGA LabWater system with a Purelab Option S filtration and ion exchange column (ρ = 15 MΩ cm^{-1}) without pH level adjustment. Reactions were carried out under nitrogen atmosphere using standard Schlenk techniques.

3-Bromodibenzo[*b*,*d*]thiophene sulfone and 3,7-dibromodibenzo[*b*,*d*]thiophene sulfone

Dibenzo[*b*,*d*]thiophene sulfone (20.0 g, 102.4 mmol) was dissolved in concentrated H_2SO_4 (500 mL). *N*-bromosuccinimide (36.0 g, 202.2 mmol) was added in several portions over 3 hours and the mixture was stirred overnight at room temperature. The mixture was poured into ice-cold water (5000 mL) and stirred for 10 minutes. The solid was filtered off and washed repeatedly with water to give a mixture of 3,7-dibromodibezo[*b*,*d*]thiophene sulfone and 3-bromodibezo[*b*,*d*]thiophene sulfone. 3,7-Dibromodibezo[*b*,*d*]thiophene sulfone was isolated by re-crystallisation from chlorobenzene, as white crystals (22.5 g, 60.2 mmol, 59%). ^{1}H NMR (400 MHz, $CDCl_3$): δ(ppm) = 7.94 (d, *J* = 2.0 Hz, 2H), 7.78 (dd, *J* = 7.5, 2.0 Hz, 2H), 7.64 (d, *J* = 7.5 Hz, 2H). ^{13}C {^{1}H} NMR (75 MHz, $CDCl_3$): δ(ppm) = 138.93 (quaternary), 137.14, 129.63 (quaternary), 125.62, 124.64 (quarternary), 122.94. nal. Calcd for $C_{12}H_6Br_2O_2S$: C, 38.53; H, 1.62; S, 8.57 %; Found: C, 38.48; H, 1.71; S, 8.67 %. HR-MS Calcd for $[C_{12}H_6Br_2O_2S + Na]^+$: m/z = 394.8353, 396.8333, 398.8312; found: m/z = 394.8342, 396.8333, 398.8297.

The mono brominated product was purified by column chromatography of the residue material (DCM : hexane (40:60)) to give white crystals of 3-bromodibezo[*b*,*d*]thiophene sulfone (0.71 g, 2.41 mmol, 2.4%). ^{1}H NMR (400 MHz, $CDCl_3$): δ(ppm) = 7.95 (d, *J* = 2.0 Hz, 1H), 7.83 (d, *J* = 7.5 Hz, 1H), 7.79 (d, *J* = 7.5 Hz, 1H), 7.77 (dd, *J* = 8.0 and 2.0 Hz, 1H), 7.67 (d, *J* = 8.0 Hz, 1H), 7.67 (t, *J* = 7.5, 1H), 7.57 (t, *J* = 7.5, 1H). ^{13}C {^{1}H} NMR (75 MHz, $CDCl_3$): δ(ppm) = 139.22 (quaternary), 137.46 (quaternary), 136.93, 134.14, 130.74 (quaternary), 130.72, 130.49 (quaternary), 125.48, 124.24 (quaternary), 122.95, 122.34, 121.16. Anal. Calcd for $C_{12}H_7BrO_2S$: C, 48.83; H, 2.39; S, 10.86 %; Found: C, 48.82; H, 2.49; S, 10.96 %. HR-MS Calcd for $[C_{12}H_7BrO_2S + Na]^+$: m/z = 316.9248, 318.9227 ; found: m/z = 316.9243, 318.9222

3,7-Dibenzo[*b*,*d*]thiophene sulfone diboronic acid bis(pinacol) ester

3,7-Dibromodibenzo[*b*,*d*]thiophene sulfone (935 mg, 2.5 mmol), diboron pinacol ester (1.50 g, 5.9 mmol), potassium acetate (586 mg, 6.0 mmol) and [Pd(dppf)Cl_2] (27.4 mg, 0.038 mmol, 1.5 mol%) were added to a dry flask, dried under vacuum for 5 minutes and then purged with N_2. *N*,*N*-Dimethylformamide (4 mL) was added via a syringe and the solution was stirred under nitrogen at 90 °C overnight. The solution was added to water (20 mL) and the product extracted with ethyl acetate. The crude product was recrystallized from acetonitrile to give brown crystals of 3,7-dibezo[*b*,*d*]thiophene sulfone diboronic acid bis(pinacol) ester (564 mg, 1.2 mmol, 48%). ^{1}H NMR (400 MHz, $CDCl_3$): δ(ppm) = 8.28 (s, 2H), 8.05 (d, *J* = 7.5 Hz, 2H), 7.80 (d, 2H), 1.36 (s, 24H). $^{13}C\{^1H\}$ NMR ($CDCl_3$): δ(ppm) = 140.07, 137.53 (quaternary), 133.78 (quaternary), 128.42, 121.07, 84.57, 24.88. Signals for carbons bonded to boron were not observed due to C-B coupling. Anal. Calcd for $C_{24}H_{30}B_2O_6S$: C, 61.57; H, 6.46; S, 6.85 %; Found: C, 61.58; H, 6.43; S, 6.75 %. HR-MS Calcd for $[C_{24}H_{30}B_2O_6S + Na]^+$: m/z = 491.1847; found: m/z = 491.1855.

3-Dibenzo[*b*,*d*]thiophene sulfone boronic acid (pinacol) ester

3-Bromodibezo[*b*,*d*]thiophene sulfone (147 mg, 0.5 mmol), diboron pinacol ester (152 mg, 0.6 mmol), potassium acetate (293 mg, 3.0 mmol) and Pd(dppf)Cl_2 (4.8 mg, 6.5 μmols, 1.3 mol%) were added to a dry flask, dried under vaccum for 5 mins and then purged with N_2. *N*,*N*-Dimethylformamide (4 mL) was added via a syringe and the solution was stirred under nitrogen at 90 °C overnight. The solution was added to water (20 mL) and the product extracted with ethyl acetate. The crude product was recrystallized from acetonitrile to give brown crystals of 3-dibenzo[*b*,*d*]thiophene sulfone boronic acid (pinacol) ester (129 mg, 0.37 mmol, 72%). ^{1}H NMR (400 MHz, $CDCl_3$): δ(ppm) = 8.29 (s, 1H), 8.05 (d, *J* = 7.5 Hz, 1H), 7.83 (m, 2H), 7.79 (d, *J* = 7.5 Hz, 1H), 7.65 (t, *J* = 7.5, 1H), 7.55 (t, *J* = 7.5, 1H), 1.36 (s, 12H). $^{13}C\{^1H\}$ NMR ($CDCl_3$): δ(ppm) = 140.14, 138.17 (quaternary), 137.18 (quaternary), 133.80(s), 131.63(2C, quaternary), 130.77, 128.42, 122.3, 121.91, 120.73, 84.58 (quaternary), 24.89. Signals for carbons bonded to boron were not observed due to C-B coupling. Anal. Calcd for $C_{18}H_{19}BO_4S$: C, 63.18; H, 5.60; S, 9.37 %; Found: C, 62.63; H, 5.45; S, 9.11 %. HR-MS Calcd for $[C_{18}H_{19}BO_4S + Na]^+$: m/z = 365.0995; found: m/z = 365.0995.

Bis-dibenzo[*b*,*d*]thiophene sulfone (S2)

3-Bromodibenzo[*b*,*d*]thiophene sulfone (147 mg, 0.5 mmol), 3-dibenzo[*b*,*d*]thiophene sulfone boronic acid (pinacol) ester (179 mg, 0.5 mmol), toluene (10 mL), sodium carbonate solution (2 M, 5 mL) and Starks' catalyst (1 drop) and was degassed via nitrogen bubbling for 30 minutes. [$Pd(PPh_3)_4$] (8 mg, 0.007 mmol, 1.4 mol%) was added and the mixture was degassed for further 10 minutes before refluxing at 110°C for 48 hours. The mixture was allowed to cool to room temperature before pouring into methanol (150 mL). The precipitate was collected by filtration and washed with methanol, water and chloroform to give bis-dibenzo[*b*,*d*]thiophene sulfoneas an off-white powder (198 mg, 0.46 mmol, 92%). ^{1}H NMR (400 MHz, $C_2D_2Cl_4$, 373 K): δ(ppm) = 8.11 (s, 2H), 7.99 – 7.88 (unresolved m, 8H), 7.74 (t, *J* = 7.5 Hz, 2H), 7.63 (t, *J* = 7.5 Hz, 2H). ^{13}C NMR in solution was not possible due to poor solubility. Solid state $^{13}C\{^1H\}$ NMR: δ(ppm) = 137.3 (C_1, C_3, C_8), 134.0 (C_{11}), 131.9 (C_4), 130.4 (C_6, C_7), 129.2 (C_5), 125.0 (C_2), 123.1 (C_{12}), 120.3 (C_{10}), 116.7 (C_9). HR-MS Calcd for $[C_{12}H_7O_2S+H]^+$: m/z = 431.0412; found: m/z = 431.0415. Anal. Calcd for $C_{12}H_7O_2S$: C, 66.96; H, 3.28; O, 14.87; S, 14.89%; Found: C, 66.10; H, 3.54; S, 14.81%.

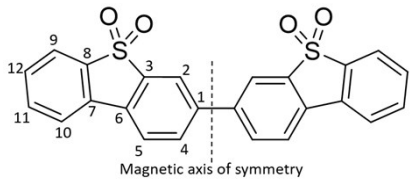

Tris-dibenzo[*b*,*d*]thiophene sulfone (S3)

3-Bromodibezo[*b,d*]thiophene sulfone (147 mg, 0.5 mmol), 3,7-dibezo[*b,d*]thiophene sulfone diboronic acid bis(pinacol) ester (117 mg, 0.25 mmol), toluene (10 mL), sodium carbonate solution (2 M, 5 mL) and Starks' catalyst (1 drop) and was degassed via nitrogen bubbling for 30 minutes. [$Pd(PPh_3)_4$] (8 mg, 0.007 mmol, 1.4 mol%) was added and the mixture was degassed for further 10 minutes before refluxing at 110 °C for 48 hours. The mixture was allowed to cool to room temperature before pouring into methanol (150 mL). The precipitate was collected by filtration and washed with methanol and water. Purification by Soxhlet extraction using methanol, followed by chloroform gave tris-dibenzo[*b,d*]thiophene sulfone as a green-yellow powder (143 mg, 0.22 mmol, 89%). NMR in solution was not possible due to poor solubility in chloroform, DMSO and tetrachloroethane. Solid state $^{13}C\{^1H\}$ NMR: δ(ppm) = 140.1 (C_5, C_{15}), 139.8 (C_8), 136.8 (C_1, C_{13}), 133.3 (C_{11}), 131.5 (C_4, C_7, C_{16}), 130.3 (C_5, C_6, C_{17}, C_{18}), 124.5 (C_2, C_{14}), 122.3 (C_{12}),

120.5 (C_{10}), 116.5 (C_9). HR-MS Calcd for $[C_{36}H_{20}O_6S_3+H]^+$: m/z = 645.0500; found: m/z = 645.0509. Anal. Calcd for $C_{36}H_{20}O_6S_3$: C, 67.07; H, 3.13; O, 14.89; S, 14.92%; Found: C, 65.81; H, 3.23; S, 14.58%.

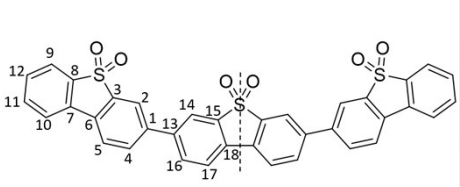

9,9,9',9'-Tetramethyl bifluorene (MeF2)

A flask was charged with 9,9-dimethylfluoren-2-yl boronic acid pinacol ester (320 mg, 1 mmol), 2-bromo-9,9-dimethylfluorene (273 mg, 1 mmol), toluene (10 mL), sodium carbonate solution (2 M, 5 mL) and Starks' catalyst (1 drop) and was degassed via nitrogen bubbling for 30 minutes. $[Pd(PPh_3)_4]$ (17.3 mg, 0.015 mmol, 1.5 mol%) was added and the mixture was degassed for further 10 minutes before refluxing at 110 °C for 48 hours. The mixture was allowed to cool to room temperature before being poured into water (30 mL). The organic phase was extracted with chloroform (30 mL), washed with brine (20 mL) and dried with magnesium sulfate, filtered, and the solvents were removed under reduced pressure. The crude product was recrystallized using a two-solvents mixture of dichloromethane/ *n*-hexane to give 9,9,9',9'-tetramethyl bifluorene as white crystals (298 mg, 77%). ^{1}H NMR (400 MHz, $CDCl_3$): δ(ppm) =1.52-1.53 (m, 12H), 7.31-7.39 (m, 4H), 7.47 (dd, *J* = 7.0, 1.5 Hz, 2H), 7.64 (dd, *J* = 7.0, 2.0 Hz, 2H), 7.70 (s, 2H), 7.76 (dd, *J* = 7.0, 1.5 Hz, 2H), 7.81 (d, *J* = 7.0Hz, 2H). ^{13}C{^{1}H} NMR ($CDCl_3$): δ(ppm) = 27.6, 47.1, 120.4, 121.5, 122.8, 126.4, 127.2, 127.4, 138.5, 139.0, 140.9, 154.0, 154.4, 120.2. Anal. Calcd (for $C_{15}H_{13}$): C, 93.22; H, 6.78%; Found: C, 91.52; H, 6.64%. HR-MS Calcd for $[C_{30}H_{26}]^+$: m/z = 386.2035; found: m/z = 386.2028.

MeF3, 9,9,9',9',9'',9''-Hexamethyl terfluorene

A flask was charged with 2,7-dibromo-9,9-dimethylfluorene (353 mg, 1 mmol), 2-(9,9-dimethylfluoren-yl boronic acid pinacol ester (640 mg, 2 mmol), toluene (20 mL), sodium carbonate solution (2 M, 10 mL) and Starks' catalyst (1 drop) and was degassed via nitrogen bubbling for 30 minutes. $[Pd(PPh_3)_4]$ (17.3 mg, 0.015 mmol, 1.5 mol%) was added and the mixture was degassed for further 10 minutes before refluxing at 110 °C for 48 hours. The mixture was allowed to cool to room temperature before being poured into water (60 mL).

The organic phase was extracted with chloroform (60 mL), washed with brine (20 mL) and dried with magnesium sulfate, filtered, and the solvents were removed under reduced pressure. The crude product was recrystallized using a two-solvents mixture of dichloromethane/ n-hexane to give the pure product as white crystals (521mg, 0.901 mmol, 90%). ^{1}H NMR (400 MHz, $CDCl_3$): δ(ppm) = 7.84 (d, *J* = 8.0 Hz, 2H), 7.81(d, J 8.0 Hz, 2H), 7.77 (dd, *J* = 6.5, 1.5 Hz, 2H), 7.72 (dd, *J* = 4.0, 1.5 Hz, 4H), 7.65-7.68 (m, 4H), 7.47 (dd, *J* = 6.5, 1.5 Hz, 2H), 7.31-7.39 (m, 4H), 1.65 (s, 6H), 1.58 (s, 12H). ^{13}C{^{1}H} NMR (75 MHz, $CDCl_3$): δ (ppm) = 154.6, 154.3, 153.9, 140.8 (2x), 138.9, 138.4, 138.1, 127.2, 127.0, 126.4, 126.3, 122.6, 121.4, 120.4, 120.3, 120.1, 47.1, 47.0, 27.4, 27.3. Anal. Calcd (for $C_{45}H_{38}$): C, 93.38; H, 6.62%; Found: C, 92.55; H, 6.52%. HR-MS Calcd for $[C_{45}H_{38}]^{+}$: m/z = 578.2974; found: m/z = 578.2969.

3,7-Diphenyldibenzo[*b*,*d*]thiophene sulfone (PSP)

A flask was charged with the 3,7-dibromodibenzo[*b*,*d*]thiophene 5,5-dioxide (374 mg, 1.0 mmol), phenylboronic acid (366 mg, 3 mmol), Starks' catalyst (2 drops), toluene (50 mL), aqueous K_2CO_3 (25 mL, 2 M) and the mixture was degassed with nitrogen. Then $[Pd(PPh_3)_4]$ (35 mg, 3 mol%) was added and the reaction was heated to 110 °C for 2 days. After cooling to room temperature the layers were separated, and the aqueous phase was extracted with toluene. The combined organic phases were filtered over a plug of SiO_2 and the plug was thoroughly washed with dichloromethane. The combined organic phases were reduced to around 20 mL and the filters that formed were filtered off giving the product as white crystals in 76% yield (280 mg). ^{1}H NMR (400 MHz, $CDCl_3$): δ (ppm) = 8.06 (s, 2 H), 7.88 (d, *J* = 1.0 Hz, 4H), 7.65 (d, *J* = 7.5 Hz, 4H), 7.50 (t, *J* = 7.5 Hz, 4H), 7.44 (t, *J* = 7.5 Hz, 2H). ^{13}C{^{1}H} NMR ($CDCl_3$): δ (ppm) = 143.8, 138.8, 138.7, 132.6, 130.2, 129.2, 128.6, 127.1, 121.9, 120.8. Anal. Calcd for $C_{24}H_{16}O_2S$: C, 78.24; H, 4.38; O, 8.68; S, 8.70%; Found: C, 77.48; H, 4.35; S, 8.64%. HR-MS Calcd for $[C_{24}H_{16}O_2S+Na]^{+}$: m/z = 391.0769; found: m/z = 391.0767.

3,7-Dimesityldibenzo[*b*,*d*]thiophene sulfone (MSM)

A flask was charged with mesitylboronic acid (328 mg, 2 mmol), 3,7-dibromodibenzo[*b*,*d*]thiophene sulfone (374 mg, 1 mmol), toluene (20 mL), potassium

carbonate solution (2 M, 7 mL) and Starks' catalyst (1 drop) and was degassed via nitrogen bubbling for 30 minutes. [$Pd(PPh_3)_4$] (15 mg) was added and the mixture was degassed for further 10 minutes before refluxing at 110 °C for 48 hours. The mixture was allowed to cool to room temperature before being poured into water (50 mL). The organic phase was extracted with chloroform (50 mL), washed with brine (40 mL) and dried with magnesium sulfate, filtered, and the solvents were removed under reduced pressure. The crude product was purified by column chromatography in light petroleum ether : ethyl acetate (75:25 gradient to 30:70) and was then recrystallized using a two-solvents mixture of dichloromethane/*n*-hexane to give the pure product as white crystals (201 mg, 44%). ^{1}H NMR (400 MHz, $CDCl_3$): δ (ppm) = 7.88 (d, *J* = 7.5 Hz, 2H), 7.63 (d, *J* = 1.0 Hz, 2H), 7.44 (dd, *J* = 7.5 and 1.0 Hz, 2H), 6.97 (s, 4H), 2.35 (s, 6H), 2.04 (s, 12H). $^{13}C\{^1H\}$ NMR ($CDCl_3$): δ (ppm) = 144.0, 138.4, 137.7, 136.6, 135.7, 135.2, 130.1, 128.5, 123.1, 121.6, 21.1, 20.8. Anal. Calcd (for $C_{30}H_{28}O_2S$): C, 79.61; H, 6.24; O, 7.07; S, 7.08%; Found: C, 79.01; H, 6.14; S, 6.98%. HR-MS Calcd for $[C_{30}H_{28}O_2S + Na]^+$: m/z = 475.1708; found: m/z = 475.1707.

3,7-Diphenylfluorene (PFP)

A flask was charged with the 2,7-dibromo-9*H*-fluorene (1.22 g, 3.77 mmol), phenylboronic acid (1.38 g, 11.31 mmol), Starks' catalyst (2 drops), toluene (50 mL), aqueous K_2CO_3 (25 mL, 2 M) and the mixture was degassed with nitrogen. Then [$Pd(PPh_3)_4$] (35 mg, 3 mol%) was added and the reaction was heated to 110 °C for 2 days. After cooling to room temperature the layers were separated, and the aqueous phase was extracted with chloroform. The combined organic phases were filtered over a plug of SiO_2 and the plug was thoroughly washed with chloroform. The combined organic phases were evaporated to dryness and the product recrystallized from toluene to give the product as white crystals in 74% yield (888 mg). ^{1}H NMR (400 MHz, $CDCl_3$): δ (ppm) = 7.87 (d, *J* = 7.5 Hz, 2H), 7.80 (d, *J* = 1.5 Hz, 2H), 7.67 (dd, *J* = 1.5 and 7.5 Hz, 4H), 7.64 (d, *J* = 7.5 Hz, 2H), 7.47 (t, J 7.5 Hz, 4H) 7.36 (tt, *J* = 7.5 and 1.5 Hz, 2H) 4.03 (s, 2H). $^{13}C\{^1H\}$ NMR ($CDCl_3$): δ (ppm) = 144.2, 141.5, 140.6, 139.9, 128.8, 127.2, 127.1, 126.1, 123.8, 120.2, 37.2. Anal. Calcd for $C_{25}H_{18}$: C, 94.30; H, 5.70%; Found: C, 94.46; H, 5.72%. GC-MS Calcd for $[C_{25}H_{18}]^+$: m/z = 318; found m/z = 318.

3,7-Dimesitylfluorene (MFM)

A flask was charged with the 2,7-dibromo-9*H*-fluorene (972 mg, 3.0 mmol), 2,4,6-trimethylphenylboronic acid (1.48 g, 9 mmol), Starks' catalyst (3 drops), toluene (150 mL), aqueous K_2CO_3 (75 mL, 2 M) and the mixture was degassed with nitrogen. Then $[Pd(PPh_3)_4]$ (105 mg, 3 mol%) was added and the reaction was heated to 110 °C for 2 days. After cooling to room temperature the layers were separated, and the aqueous phase was extracted with toluene. The combined organic phases were dried over $MgSO_4$, filtered, and the solvents were removed under reduced pressure. The crude product was then recrystallized from acetonitrile to give the product as light brown crystals in 48% yield (653 mg). ^{1}H NMR (400 MHz, $CDCl_3$): δ (ppm) = 7.85 (d, *J* = 7.5 Hz, 2H), 7.32 (s, 2H), 7.16 (d, *J* = 7.5 Hz, 2H), 6.97 (s, 4H), 3.98 (s, 2H) 2.35 (s, 6H), 2.05 (s, 12H). ^{13}C{^{1}H} NMR (75 MHz, $CDCl_3$): δ (ppm) = 143.6, 140.0, 139.6, 139.4, 136.5, 136.2, 128.1, 128.0, 125.9, 119.7, 37.1, 21.1, 20.8.Anal. Calcd for $C_{31}H_{30}$: C, 92.49; H, 7.51%; Found: C, 91.88; H, 7.60%. HR-MS Calcd for $[C_{31}H_{30}+H]^+$: m/z = 404.2426, 404.2460; found: m/z = 403.2422, 404.2457.

3. Nuclear Magnetic Resonance Spectra

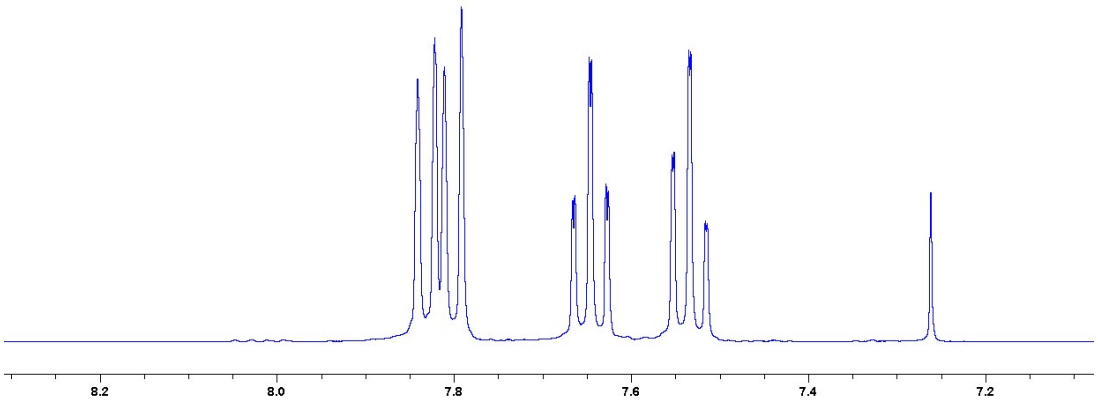

Figure S1: ^{1}H NMR spectrum of S1, dibenzo[*b*,*d*]thiophene sulfone in $CDCl_3$. X-axis displays chemical shift in ppm.

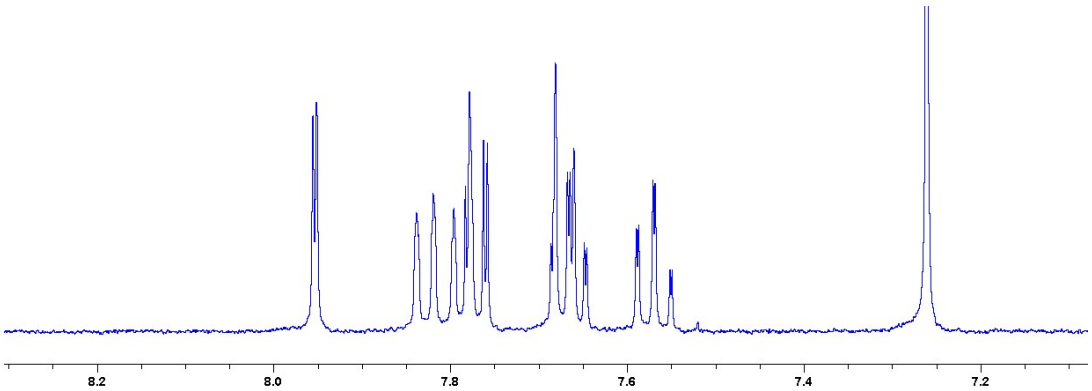

Figure S2: ^{1}H NMR spectrum of 3-bromodibenzo[*b*,*d*]thiophene sulfone in $CDCl_3$. X-axis displays chemical shift in ppm.

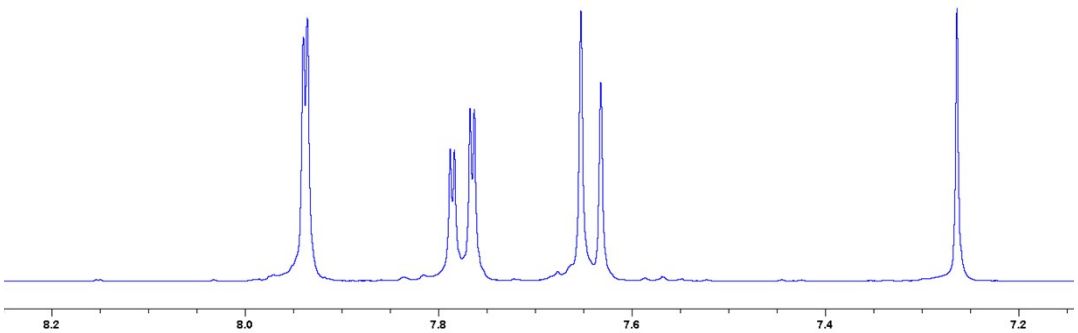

Figure S3: ^{1}H NMR spectrum of 3,7-dibromodibenzo[*b*,*d*]thiophene sulfone in $CDCl_3$. X-axis displays chemical shift in ppm.

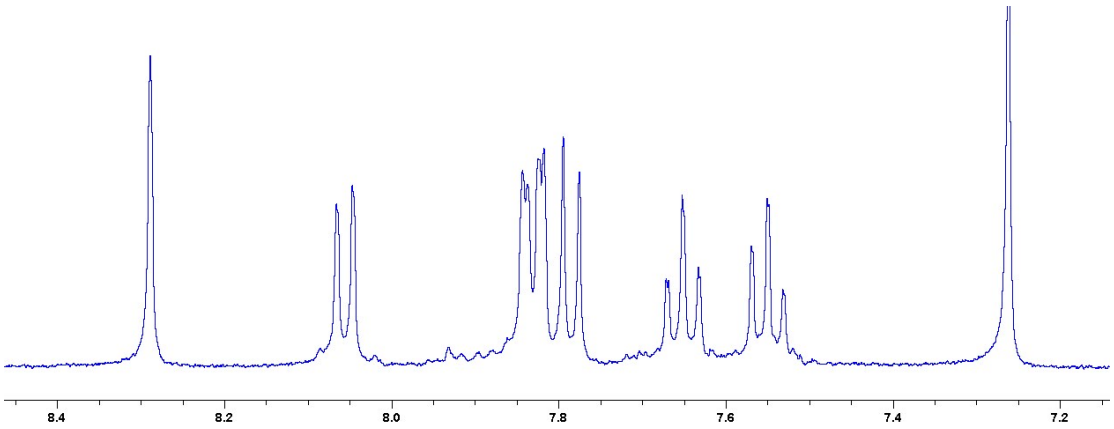

Figure S4: ^{1}H NMR spectrum of 3-dibenzo[*b*,*d*]thiophene sulfone boronic acid pinacol ester in $CDCl_3$. X-axis displays chemical shift in ppm.

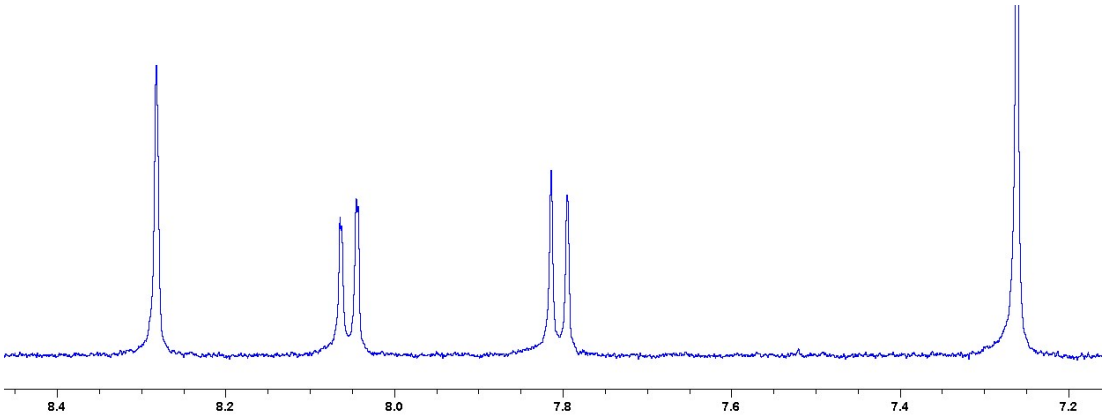

Figure S5: ^{1}H NMR spectrum of 3,7-dibenzo[*b*,*d*]thiophene sulfone diboronic acid bispinacol ester in $CDCl_3$. X-axis displays chemical shift in ppm.

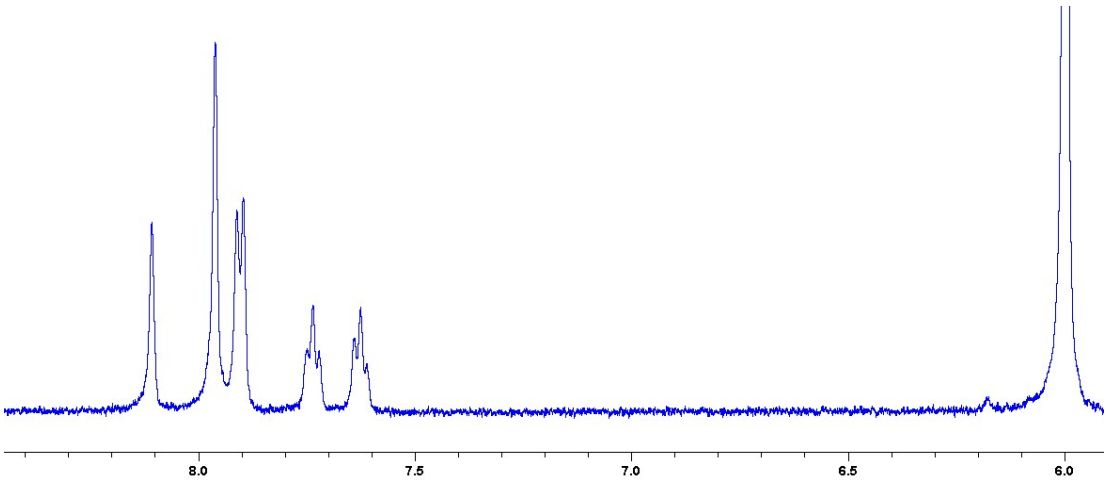

Figure S6: ^{1}H NMR spectrum of S2, bis-dibenzo[*b*,*d*]thiophene sulfone in $C_2D_2Cl_4$ at 373 K. X-axis displays chemical shift in ppm.

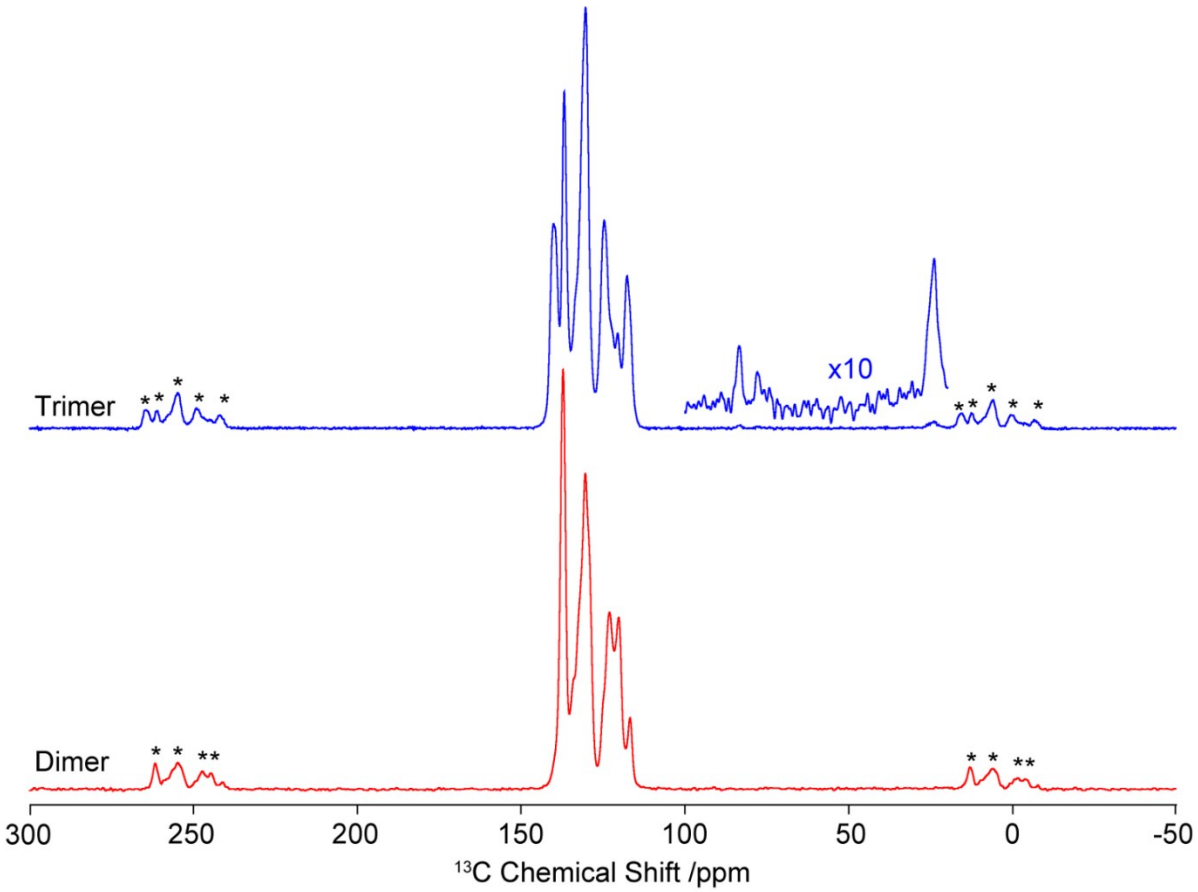

Figure S7: ^{13}C solid state NMR spectra of S2, bis-dibenzo[*b*,*d*]thiophene sulfone (red) and S3, tris-dibenzo[*b*,*d*]thiophene sulfone.

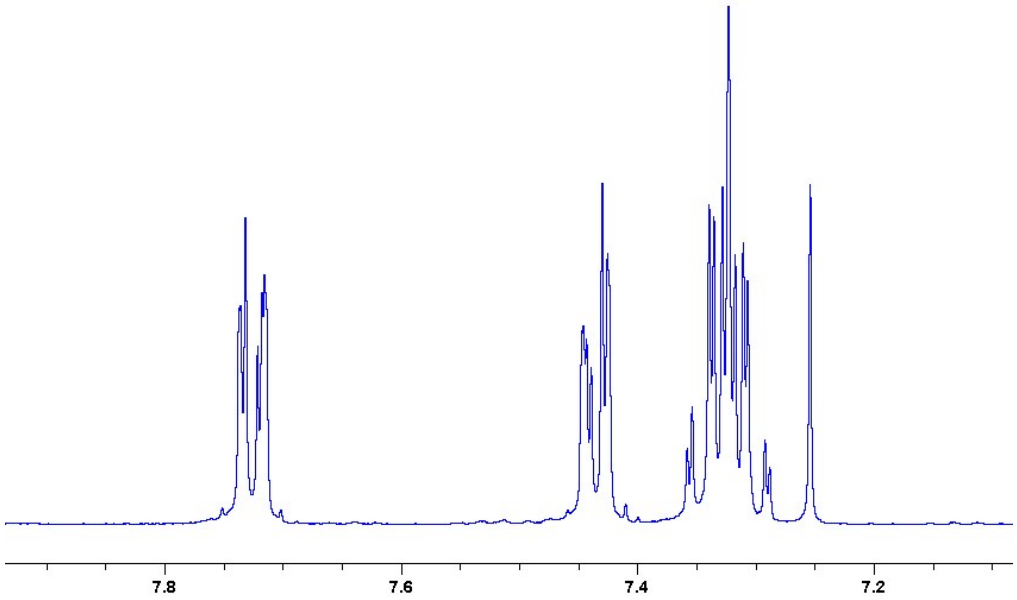

Figure S8: ^{1}H NMR spectrum of MeF1 in $CDCl_3$. X-axis displays chemical shift in ppm.

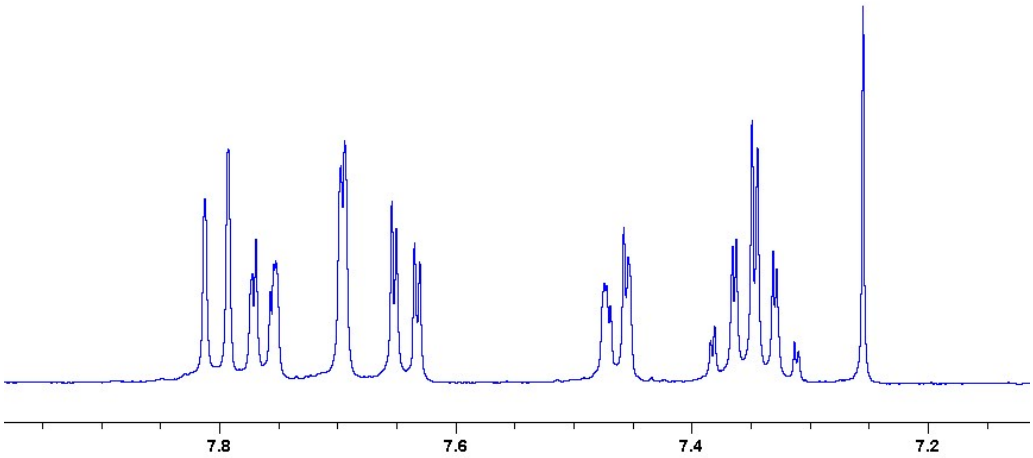

Figure S9: ^{1}H NMR spectrum of MeF2 in $CDCl_3$. X-axis displays chemical shift in ppm.

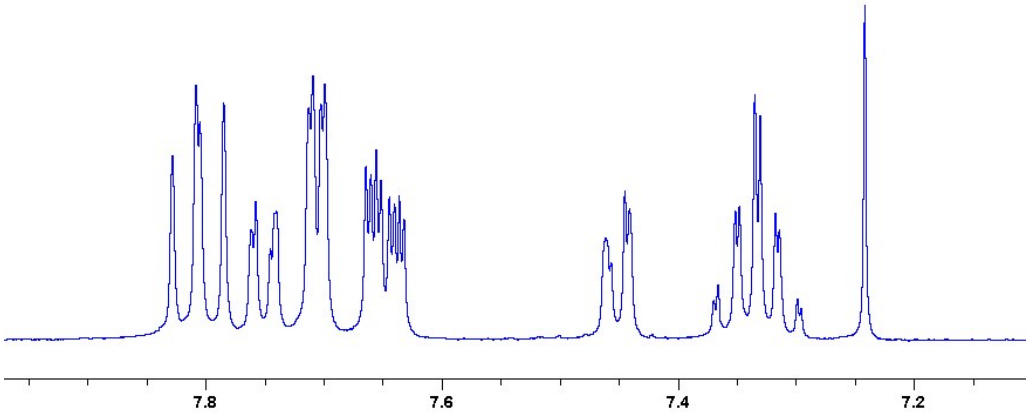

Figure S10: ^{1}H NMR spectru of MeF3 in $CDCl_3$. X-axis displays chemical shift in ppm.

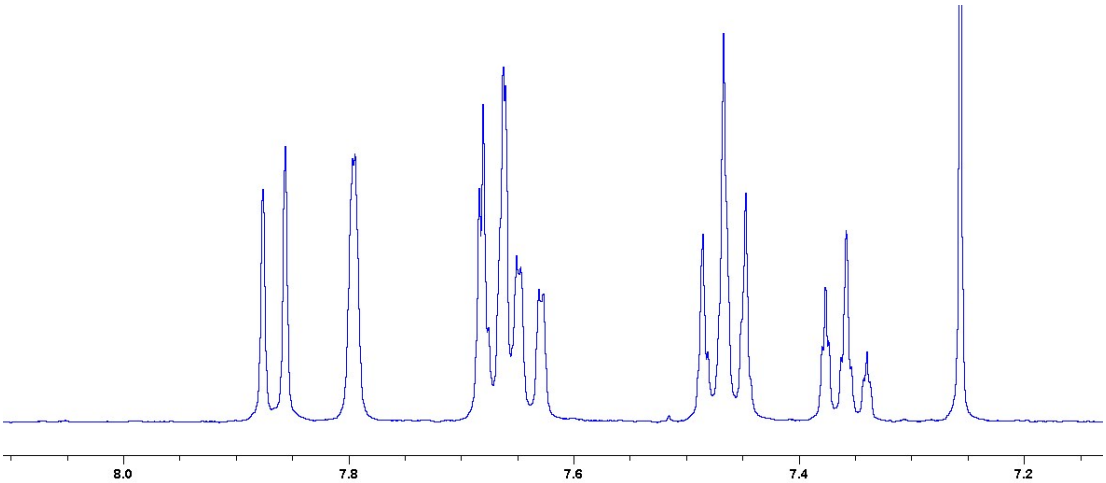

Figure S11: ^{1}H NMR spectrum of PSP in $CDCl_3$ X-axis displays chemical shift in ppm.

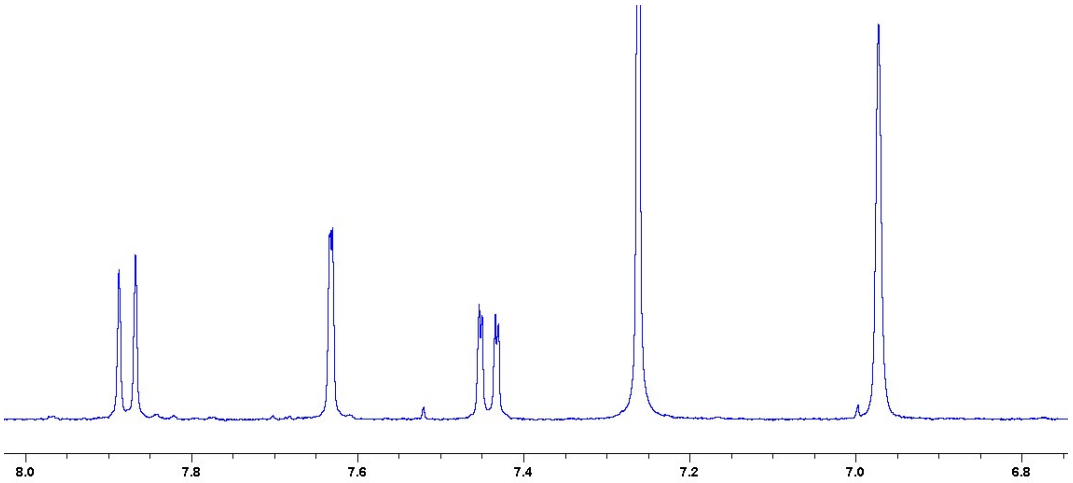

Figure S12: ^{1}H NMR spectrum of MSM in $CDCl_3$ X-axis displays chemical shift in ppm.

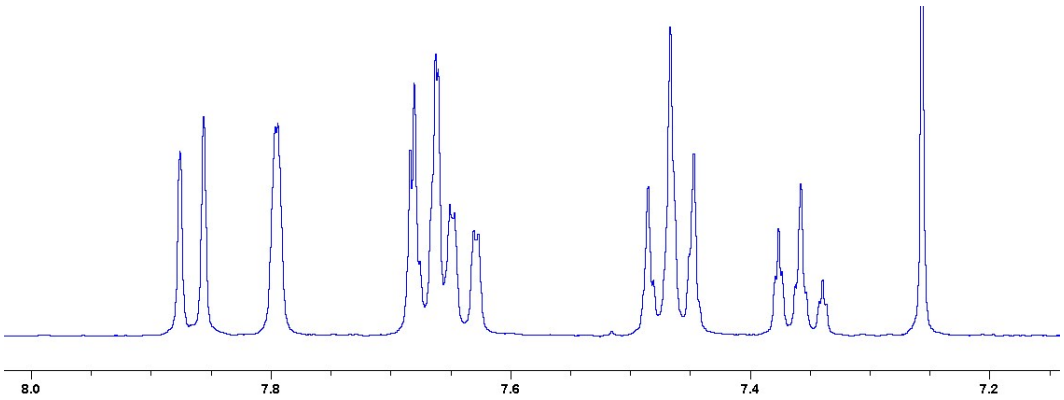

Figure S13: ^{1}H NMR spectrum of PFP in $CDCl_3$ X-axis displays chemical shift in ppm.

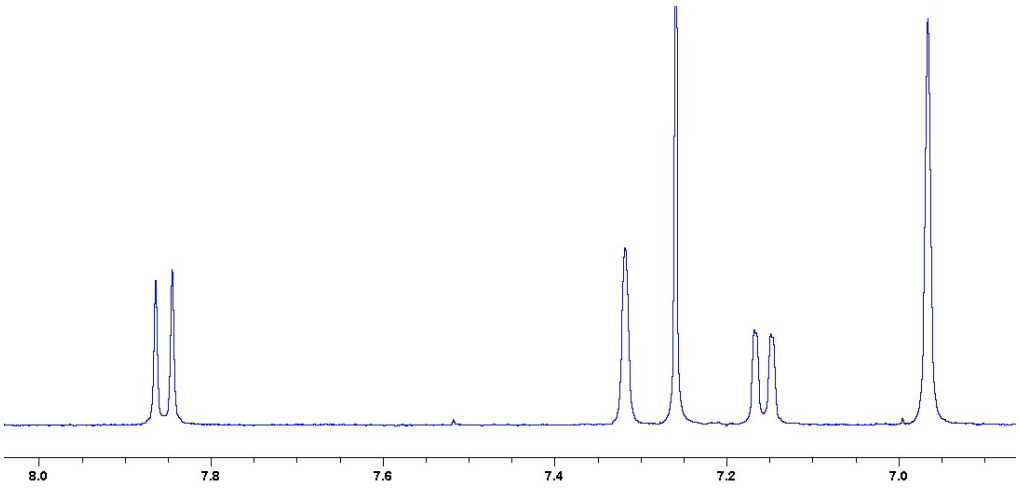

Figure S14: ^{1}H NMR spectrum of MFM in $CDCl_3$ X-axis displays chemical shift in ppm.

4. Single Crystal X-Ray Diffraction

Table S1. Single crystal X-ray refinement details for MeF1, MeF2, and MeF3.

	MeF1	MeF2	MeF3[a]
Crystallisation Conditions	Received from supplier as crystalline sample	DCM / *n*-hexane	DCM / *n*-hexane
Space Group	$I4_1/a$	$P\bar{1}$	$P2_1/n$
Wavelength [Å]	Mo-Kα	Mo-Kα	Mo-Kα
Collection Temperature	100 K	100 K	298 K
Formula	$C_{15}H_{14}$	$2(C_{30}H_{26})$	$2(C_{45}H_{38})$
Mr	194.26	773.01	1157.5
Crystal Size (mm)	0.53 x 0.43 x 0.32	0.28 x 0.09 x 0.04	0.41 x 0.29 x 0.09
Crystal System	Tetragonal	Triclinic	Monoclinic
a [Å]	21.5488(14)	8.3173(13)	19.5956(5)
b [Å]		9.6055(17)	22.8016(4)
c [Å]	9.6725(6)	13.200(2)	16.5804(4)
α [°]		100.545(5)	
β [°]		92.275(4)	109.790(3)
γ [°]		90.001(5)	
V [Å^3]	4491.4(6)	1035.9(3)	6970.8(3)
Z	16	1	4
D_{calcd} [g cm^{-3}]	1.149	1.239	1.103
μ [mm^{-1}]	0.065	0.070	0.062
F(000)	1664	412	2464
2θ range [°]	3.78 – 61.98	4.31 – 46.61	4.77 – 52.74
Reflections collected	25139	11415	145548
Independent reflections, R_{int}	3576, 0.0572	2982, 0.1043	14055, 0.0544
Obs. Data [$I > 2\sigma$]	2650	412	7267
Data / restraints / parameters	3576 / 0 / 138	2982 / 0 / 352	14055 / 1309 / 1077
Final R1 values ($I > 2\sigma(I)$)	0.0478	0.0700	0.0955
Final R1 values (all data)	0.0671	0.1297	0.1680
Final wR(F^2) values (all data)	0.1338	0.2008	0.2548
Goodness-of-fit on F^2	1.049	1.033	1.572
Largest difference peak and hole [e.A^{-3}]	0.153 / -0.247	0.183 / -0.225	0.693 / -0.244
CCDC	1999752	1999748	1999755

[a] In the crystal structure of MeF3, one of the fluorene trimers was disordered over two position (50:50 occupancy split) and both parts were refined with constrained aromatic geometries (AFIX 66 in SHELX) and bond distance restraints (DFIX in SHELX). In addition, due to disordered, the structure was refined with a rigid bond restraint (RIGU in SHELX).

Table S2. Single crystal X-ray refinement details for PSP, PFP, MSM, and MFM.

	PSP[a]	PFP[b]	MSM[c]	MFM
Crystallisation Conditions	DCM / toluene	toluene	DCM / *n*-hexane	acetonitrile
Space Group	$P2_1/n$	$P2_1/n$	*Ia*	$P\bar{1}$
Wavelength [Å]	Mo-Kα	Mo-Kα	Mo-Kα	Mo-Kα
Collection Temperature	293 K	150 K	150 K	100 K
Formula	$C_{24}H_{16}O_2S$	$C_{25}H_{18}$	$2(C_{30}H_{28}O_2S)$	$2(C_{31}H_{30})$
Mr	368.43	318.39	905.16	805.10
Crystal Size (mm)	0.14 x 0.05 x 0.03	0.45 x 0.11 x 0.04	0.10 x 0.08 x 0.02	0.27 x 0.04 x 0.04
Crystal System	Monoclinic	Monoclinic	Monoclinic	Triclinic
a [Å]	9.362(3)	7.9704(15)	15.642(5)	8.5024(8)
b [Å]	9.511(2)	5.7466(10)	17.335(3)	11.1377(10)
c [Å]	20.202(5)	36.314(7)	18.046(3)	26.180(2)
α [°]				83.462(7)
β [°]	99.403(11)	95.924(4)	98.641(5)	84.924(7)
γ [°]				89.341(7)
V [Å^3]	1774.6(8)	1654.4(5)	4837.7(19)	2453.4(4)
Z	4	4	4	2
D_{calcd} [g cm^{-3}]	1.379	1.278	1.243	1.090
μ [mm^{-1}]	0.199	0.072	0.159	0.061
F(000)	768	672	1920	864
2θ range [°]	4.08 – 46.48	4.51 – 52.76	3.28 – 43.93	3.68 – 46.51
Reflections collected				30026
Independent reflections, R_{int}	2755, 0.0789	3387, 0.0412	5280	7071, 0.1343
Obs. Data [$I > 2\sigma$]	2012	2863	4007	3474
Data / restraints / parameters	2755 / 0 / 245	3387 / 0 / 227	5280 / 578 / 608	7071 / 3 / 571
Final R1 values ($I > 2\sigma(I)$)	0.0814	0.0524	0.0883	0.0682
Final R1 values (all data)	0.1240	0.0636	0.1178	0.1666
Final wR(F^2) values (all data)	0.1573	0.1309	0.2131	0.1792
Goodness-of-fit on F^2	1.208	1.065	1.046	0.994
Largest difference peak and hole [e.A^{-3}]	0.298 / -0.391	0.219 / -0.206	0.753 / -0.409	0.194 / -0.203
CCDC	1999749	1999747	1999756	1999753

[a] X-ray data for PSP was refined as a 2-component twin (HKLF 5) with the BASF refined to 0.504(3), after scaling the X-ray data in TWINABS. [b] X-ray data for PFP was refined as a 2-component twin (HKLF 5) with the BASF refined to 0.667(2), after scaling the X-ray data in TWINABS. [c] X-ray diffraction data for MSM was weakly diffracting and twinned. X-ray data was detwinned using the TwinRotMat function in Platon and refined as a 2-component twin (HKLF 5) with the BASF refined to 0.337(7). Due to disorder, a 0.95 Å resolution limit was applied during refinement and structure was refined with a rigid-bond restraint (RIGU in SHELX).

Table S3. Single crystal X-ray refinement details for S1, S2, and S3.

	S1	S2[a]	S3
Crystallisation Conditions	Received from supplier as crystalline sample	sublimation	sublimation
Space Group	*C*2/*c*	$P\bar{1}$	$P\bar{1}$
Wavelength [Å]	Mo-Kα	Mo-Kα	0.6889
Collection Temperature	298 K	298 K	298 K
Formula	$C_{12}H_8O_2S$	$2(C_{24}H_{14}O_4S_2)$	$2(C_{36}H_{20}O_6S_3)$
Mr	216.24	860.94	1289.40
Crystal Size (mm)	0.12 x 0.06 x 0.04	0.09 x 0.06 x 0.01	0.09 x 0.03 x 0.006
Crystal System	Monoclinic	Triclinic	Triclinic
a [Å]	10.1221(8)	7.3833(13)	7.6704(19)
b [Å]	13.8377(11)	8.4946(16)	16.878(3)
c [Å]	7.1345(5)	15.020(3)	23.693(5)
α [°]		94.371(5)	71.258(16)
β [°]	91.650(2)	93.590(6)	84.16(2)
γ [°]		90.853(5)	78.786(18)
V [Å^3]	998.89(13)	937.3(3)	2846.6(11)
Z	4	1	2
D_{calcd} [g cm^{-3}]	1.438	1.525	1.504
μ [mm^{-1}]	0.296	0.316	0.283
F(000)	448	444	1328
2θ range [°]	4.99 – 58.30	4.81 – 52.80	2.50 – 51.69
Reflections collected	6680		37013
Independent reflections, R_{int}	1349, 0.0374	3813	11880, 0.1731
Obs. Data [$I > 2\sigma$]	1139	2510	5372
Data / restraints / parameters	1349 / 0 / 69	3813 / 0 / 272	11880 / 0 / 811
Final R1 values ($I > 2\sigma(I)$)	0.0454	0.0653	0.0854
Final R1 values (all data)	0.0518	0.1041	0.1546
Final wR(F^2) values (all data)	0.1401	0.1804	0.2427
Goodness-of-fit on F^2	1.088	1.057	0.945
Largest difference peak and hole [e.A^{-3}]	0.316 / -0.332	0.306 / -0.413	0.596 / -0.354
CCDC	1999750	1999751	1999754

[a] X-ray data for S2 was detwinned using the TwinRotMat function in Platon and refined as a 2-component twin (HKLF 5) with the BASF refined to 0.198(3).

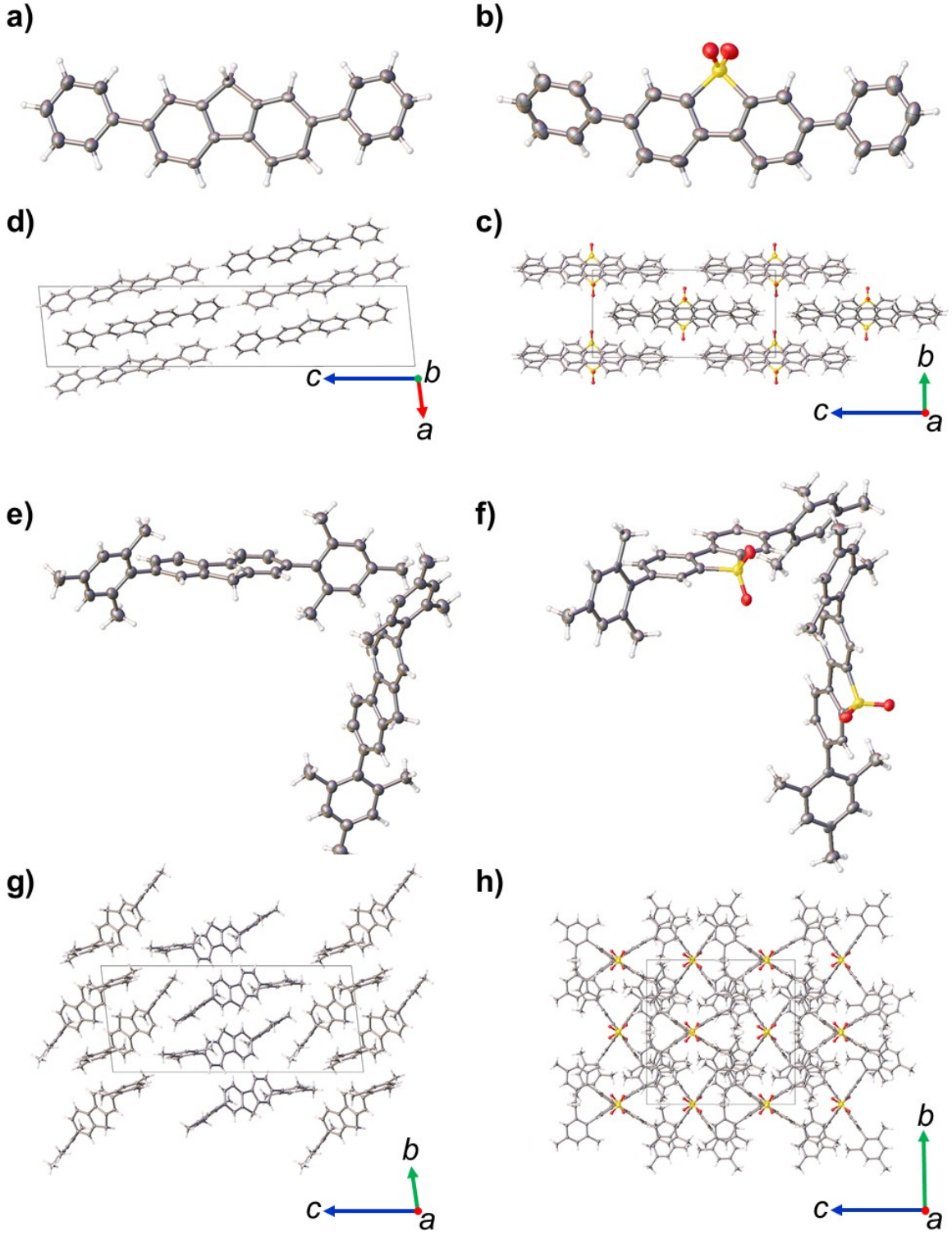

Figure S15: Displacement ellipsoid plots from the single crystal structures of; a) PFP, b) PSP, e) MFM, f) MSM; ellipsoids displayed at 50% probability level. Crystal packing in the single crystal structures of; c) PFP, d) PSP, g) MFM, h) MSM. Grey = carbon, white = hydrogen, yellow = sulfur; red = oxygen.

5. Powder X-Ray Diffraction

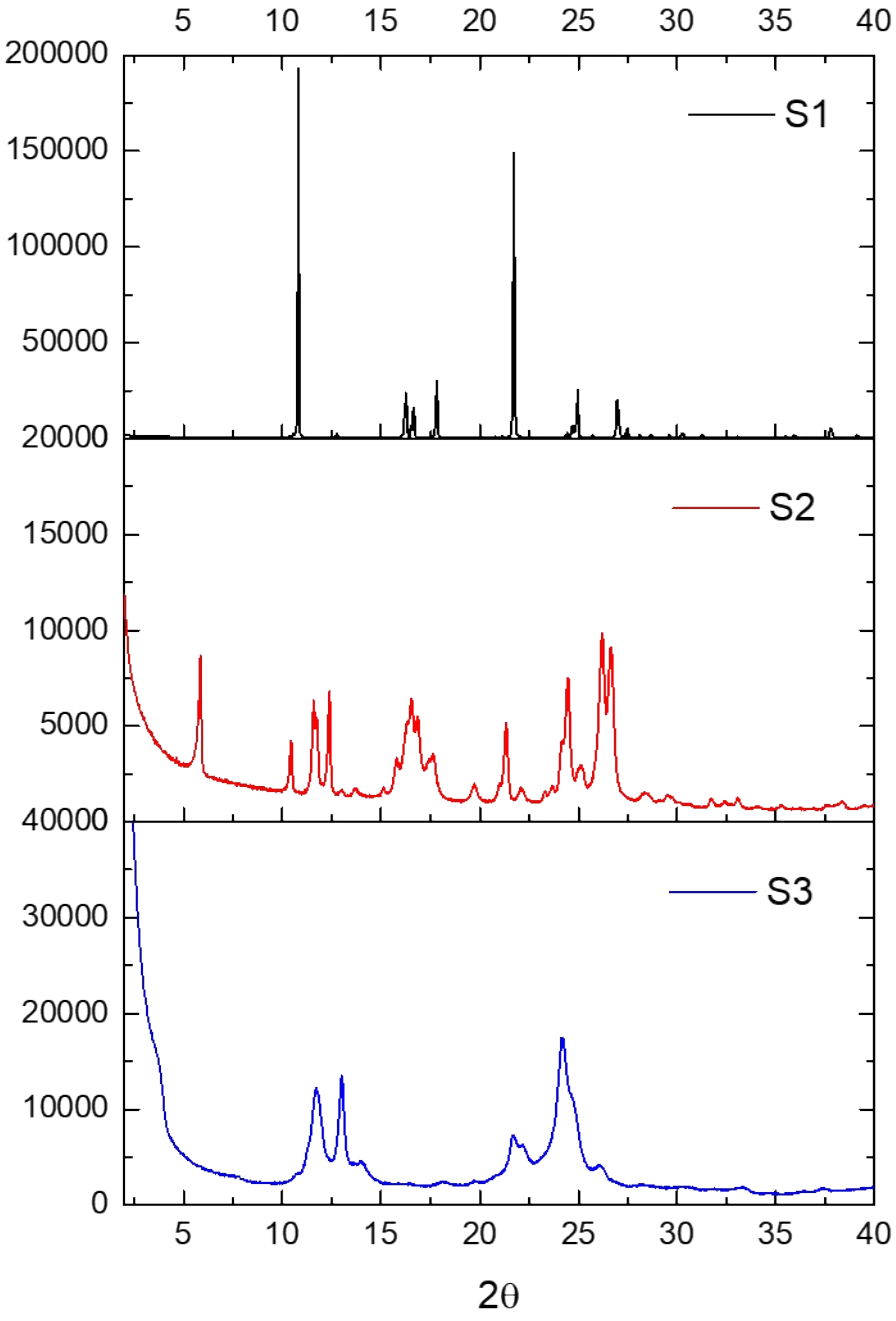

Figure S16: Powder X-ray diffraction pattern of S1, S2 and S3 as synthesised.

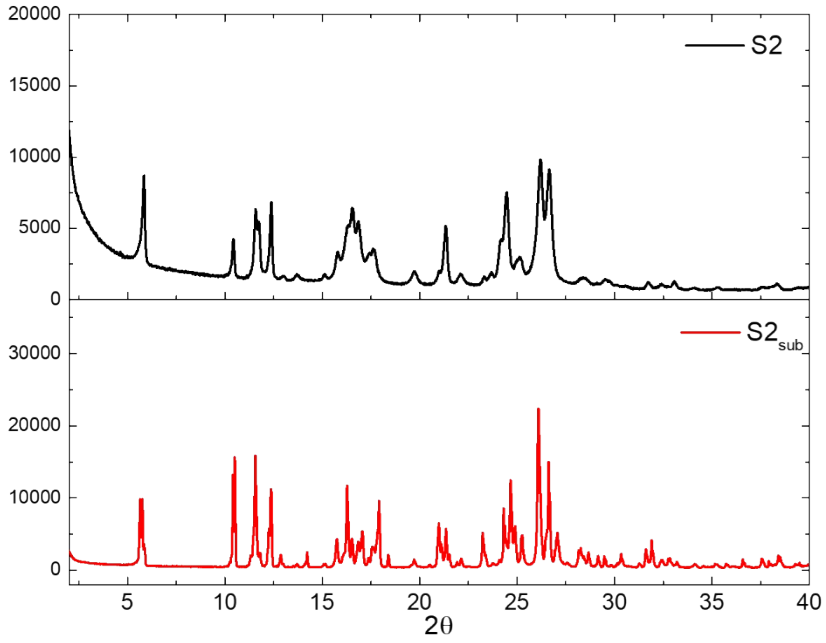

Figure S17: Powder X-ray diffraction pattern of S1, S2 and S3 as synthesised.

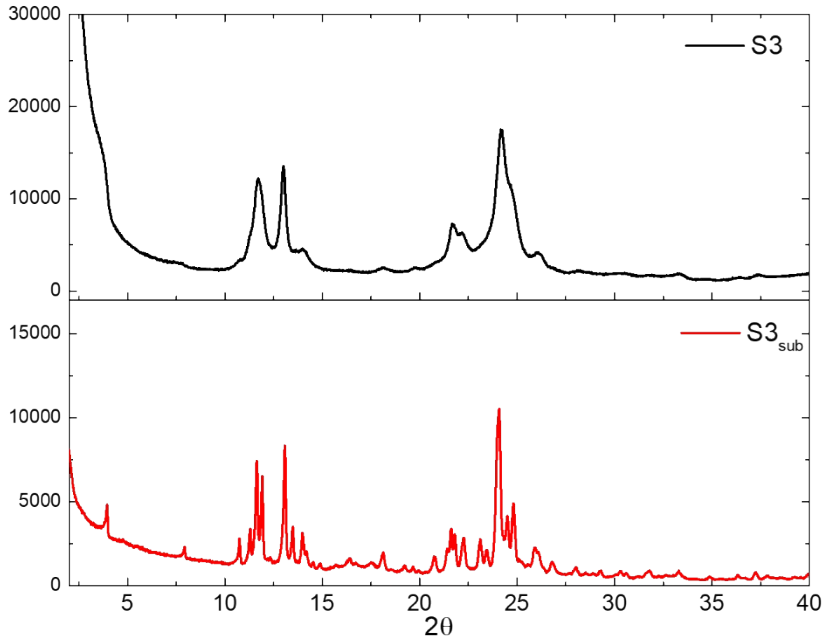

Figure S18: Powder X-ray diffraction pattern of S3 and as synthesised (black) and after sublimation (red).

6. Scanning Electron Microscopy

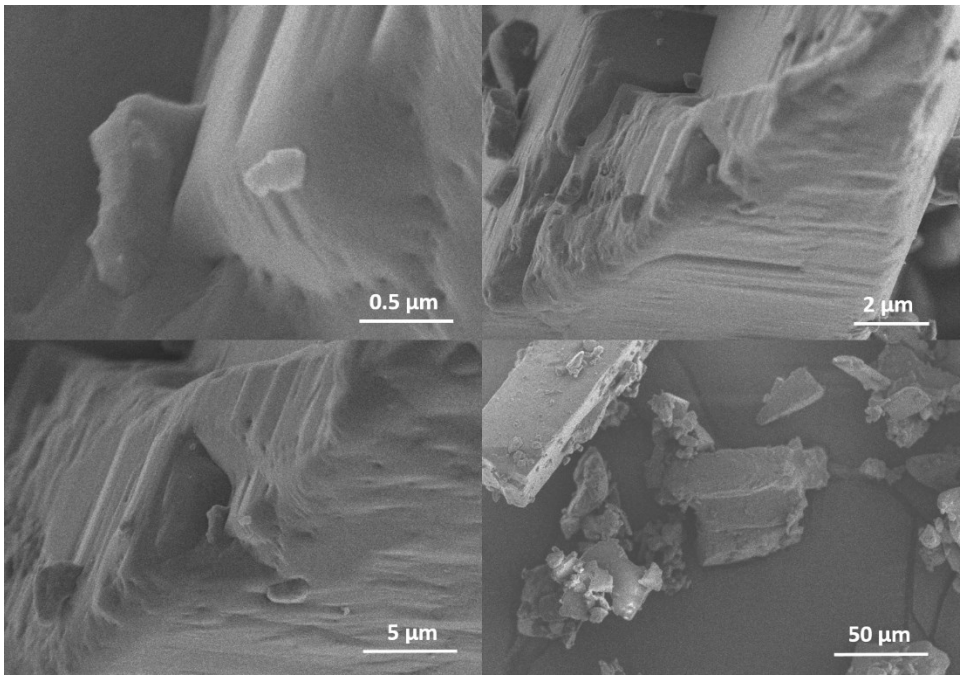

Figure S19: SEM images of S1 recorded at 3 keV.

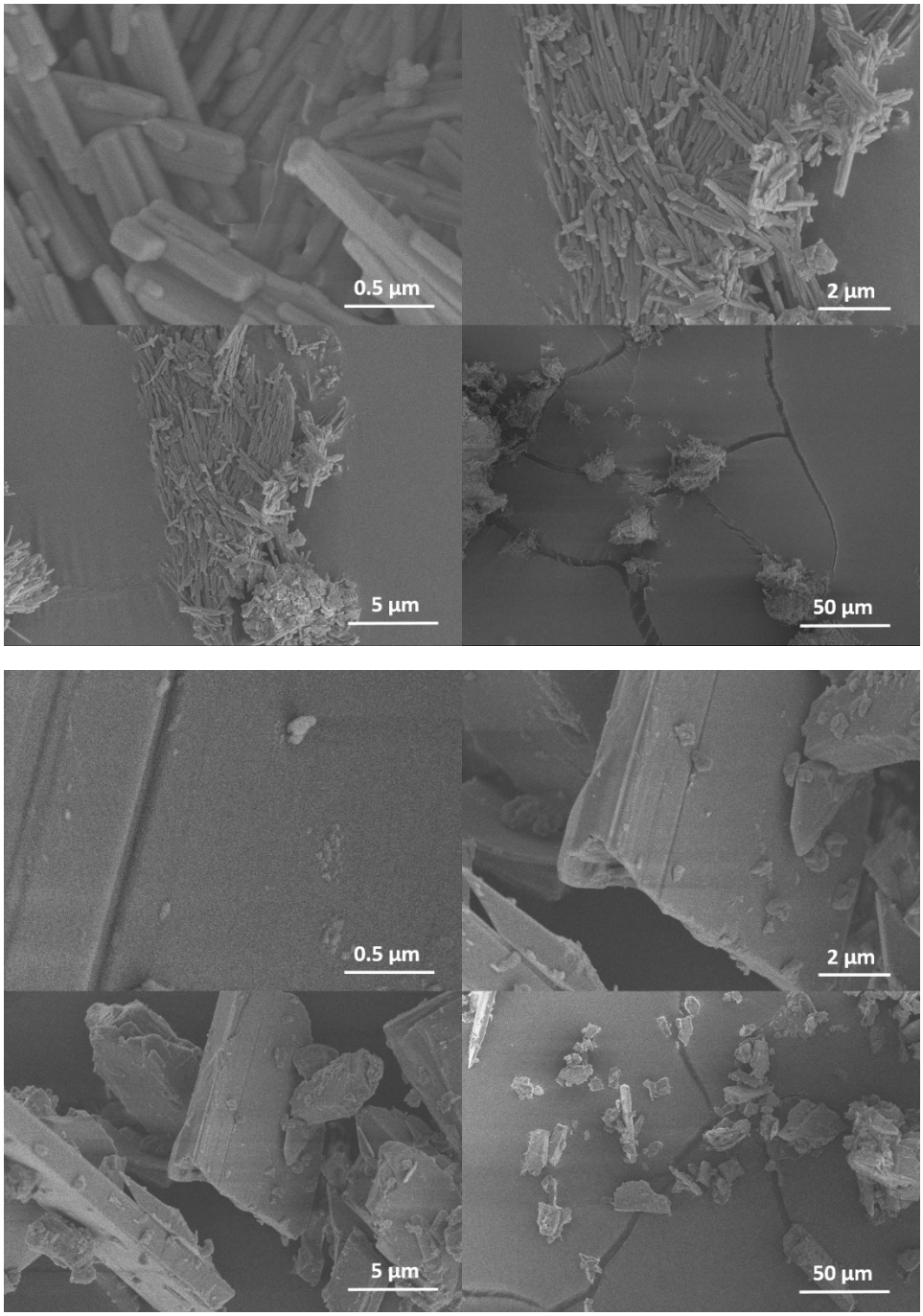

Figure S20: SEM images of S2 as synthesised recorded at 3 keV (top). SEM images of S2 sublimed recorded at 3 keV (bottom).

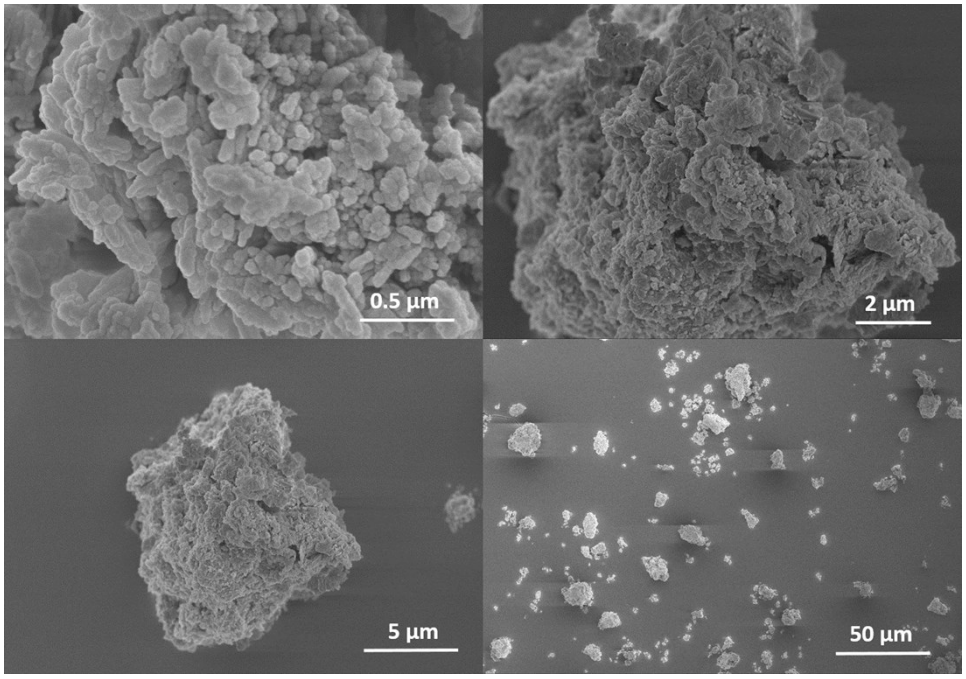

Figure S21: SEM images of S3 as synthesised recorded at 3 keV.

7. Fourier-Transform Infrared Spectroscopy

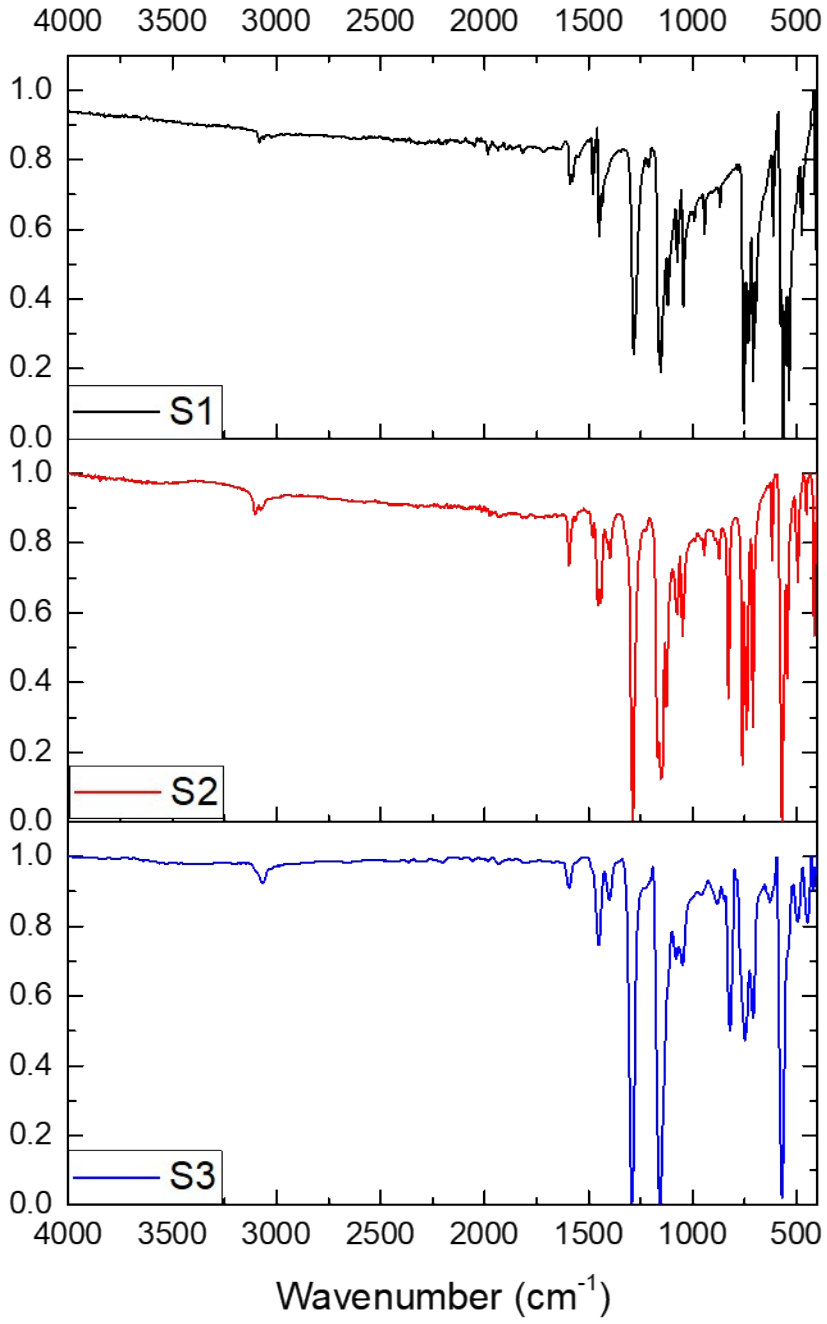

Figure S22: Fourier-transform Infrared spectra of S1, S2 and S3.

8. UV-Vis and Photoluminescence Spectroscopy

Molar extinction coefficients (ε_{Molar}) were calculated using Equation 1 below, with absorption (A) recorded at the maxima for each material in chloroform, at a range of different concentrations (c), in a cell of path length (l) 1 cm. Values were calculated from a concentration / absorption graph with at least 4 points and R^2 values of over 0.99.

$$\varepsilon_{Molar} = \frac{A}{lc} \quad \text{(Equation 1.)}$$

Average extinction coefficients ($Average\ \varepsilon_{Molar}$), discussed in section 16, were calculated by averaging of absorption values over the 275-400 nm range (values collected every 0.5 nm) for each concentration. Values were calculated from a concentration / average absorption graph with at least 4 points and R^2 values of over 0.99.

Mass extinction coefficients (ε_{Mass}) were calculated by dividing the molar extinction coefficients (ε_{Molar}) by the molar mass (m_r) of each material, Equation 2, and represents the absorption of the oligomers per unit mass (m).

$$\varepsilon_{Mass} = \frac{\varepsilon_{Molar}}{m_r} = \frac{A}{lcm_r} = \frac{AV}{l\,m} \quad \text{(Equation 2.)}$$

Average mass extinction coefficients ($Average\ \varepsilon_{Mass}$) were calculated by dividing the average molar extinction coefficients ($Average\ \varepsilon_{Molar}$) by the molar mass ($m_r$) of each material.

Photoluminescent quantum yields (Φ) were calculated using standard techniques,[12] Equation 3 using the quantum yield of a standard (Φ_s), the integrated fluorescence emission of the oligomers (I_x) and the standard (I_s), the absorption of the oligomers (A_x) and the standard (A_s) at the excitation wavelength and the refractive index of the solvent used for the oligomers (η_x) and the standard (η_s). The oligomers were measured in chloroform (η_x= 1.46),[13] a quinine sulfate standard in $H_2SO_{4(aq)}$ (0.5 M) was used (Φ_s= 0.546, η_s= 1.346),[12] and values were calculated from an absorption / emission graph with at least 4 points and R^2 values over 0.99.

$$\Phi = \frac{No.\ photons\ emitted}{No.\ photons\ absorbed} \times (100\%) = \Phi_s \frac{I_x A_s}{A_x I_s}\left(\frac{\eta_x^2}{\eta_s^2}\right) \times (100\%) \quad \text{(Equation 3.)}$$

Absorption corrected activity (ACA) values, Equation 4, discussed in section 16, were calculated by dividing the hydrogen evolution rates (HER) of the oligomers in μmol $h^{-1}g^{-1}$, by the average mass extinction coefficients in $cm^2\,g^{-1}$.

$$ACA = \frac{HER}{Average\ \varepsilon_{Mass}} \quad \text{(Equation 4.)}$$

Table S4. Optical properties of the oligomers.

Material	λ_{onset} solid-state[a] (nm)	λ_{max} chloroform (nm)	ε_{Molar}[b] chloroform (M^{-1} cm^{-1})	ε_{Mass}[c] chloroform (cm^2 g^{-1})	λ_{em} solid-state (nm)	λ_{em} chloroform (nm)	Φ[d] chloroform (%)
PSP	426	323	35,300	96	438	409	76
MSM	386	301	18,800	80	387	390	65
PFP	437	331	40,300	127	423	357, 373	94
MFM	341	279, 312	29,800	74	333, 372	334	8
MeF1	332	269, 307	16,500	85	326	312	10
MeF2	405	330	42,800	111	428	363	94
MeF3	430	355	71,100	123	446	394	100
S1	382	285, 323, 362	7,400	34	394	361	11
S2	444	316, 333	-[e]	-[e]	460	373, 389	73
S3	471	322, 344	-[e]	-[e]	492	393, 414	77

[a] From diffuse reflectance spectroscopy of solid powder; [b] Molar extinction coefficient, see above; [c] Mass extinction coefficient, see above; [d] Photoluminescence quantum yield see above; [e] Not measured due to insolubility in chloroform and other common organic solvents.

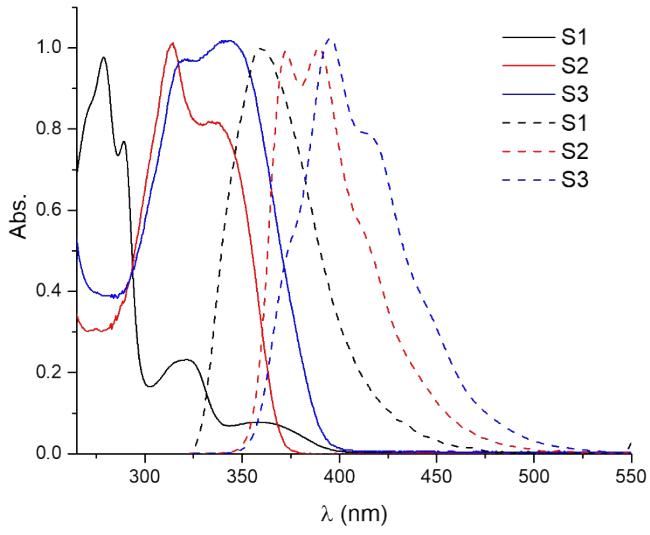

Figure S23: UV-Vis (solid) and photoluminescence spectra (dashed) in chloroform of S1, S2 and S3.

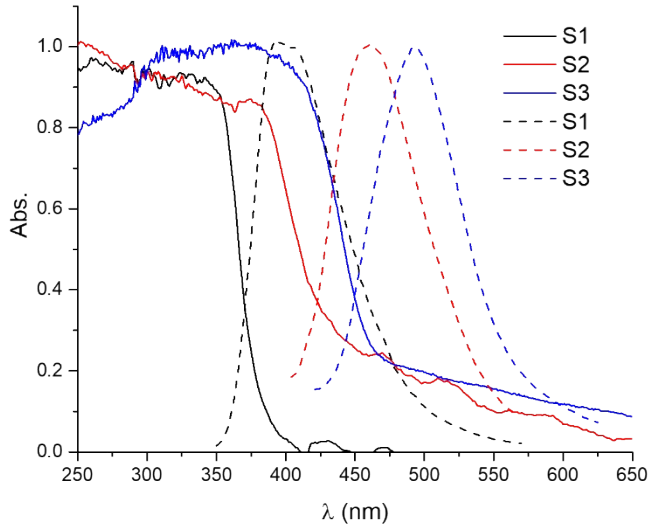

Figure S24: UV-Vis (solid) and photoluminescence spectra (dashed) in the solid state of S1, S2 and S3.

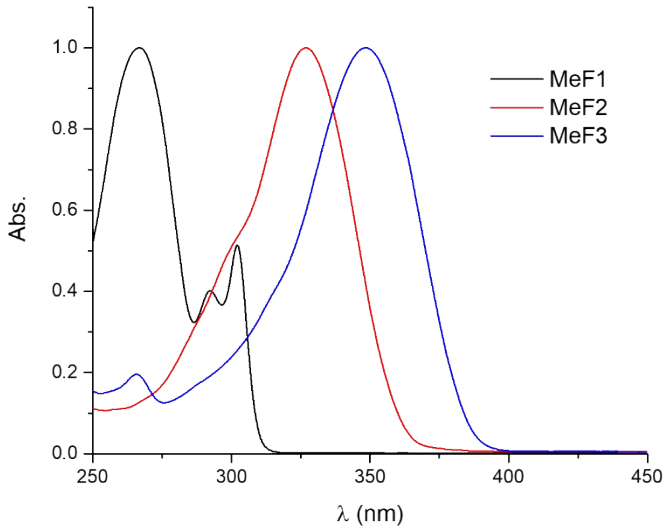

Figure S25: UV-Vis spectra of MeF1-3 in chloroform.

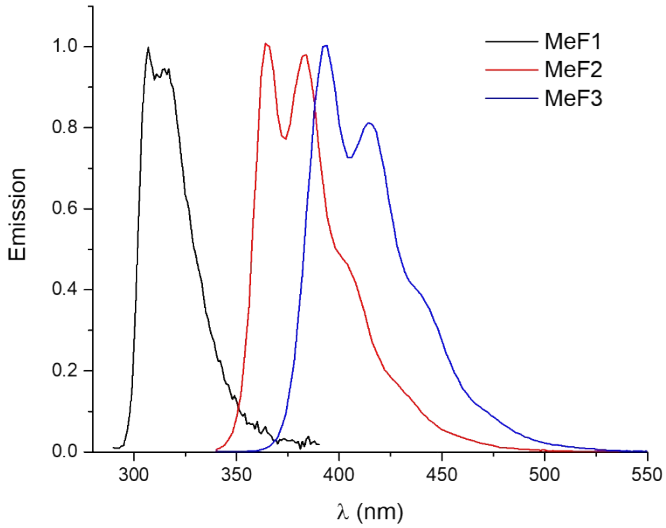

Figure S26: Emission spectra of MeF1-3 in chloroform.

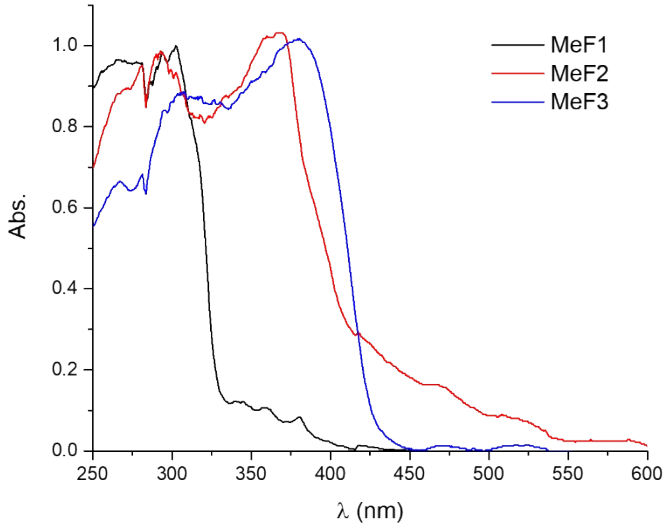

Figure S27: UV-Vis spectra of MeF1-3 in the solid-state.

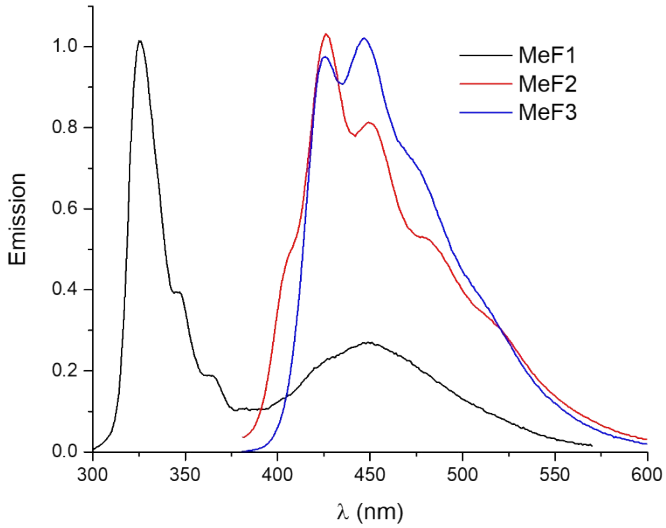

Figure S28: Emission spectra of MeF1-3 in the solid-state.

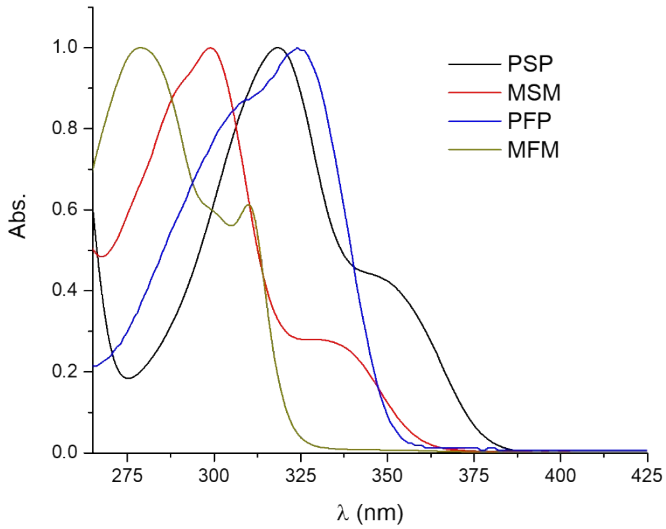

Figure S29: UV-Vis spectra of PSP, MSM, PFP and MFM in chloroform.

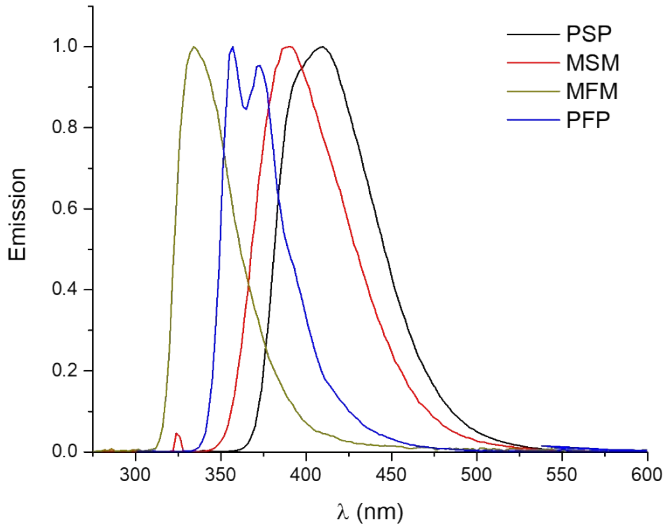

Figure S30: Emission spectra of PSP, MSM, PFP and MFM in chloroform.

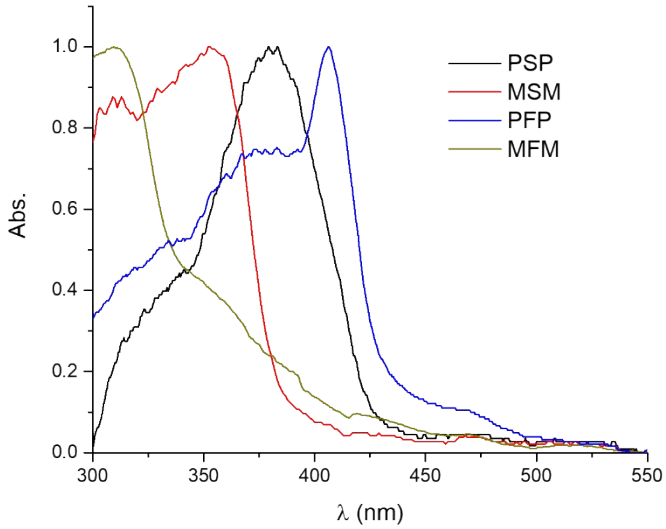

Figure S31: UV-Vis spectra of PSP, MSM, PFP and MFM in the solid-state.

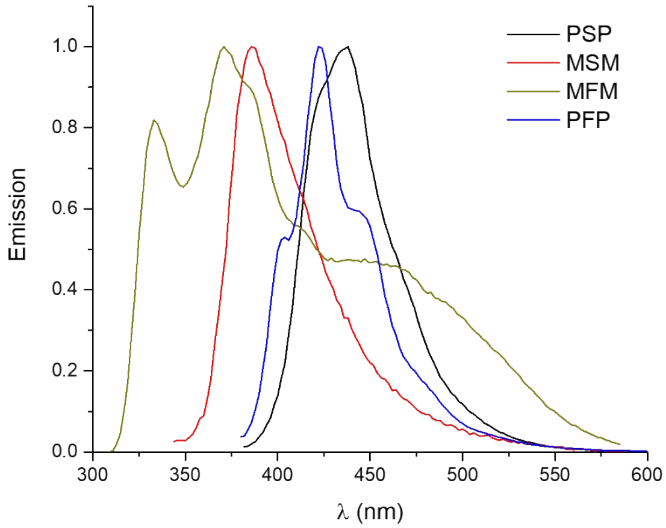

Figure S32: Emission spectra of PSP, MSM, PFP and MFM in the solid-state.

9. Time Correlated Single Photon Counting

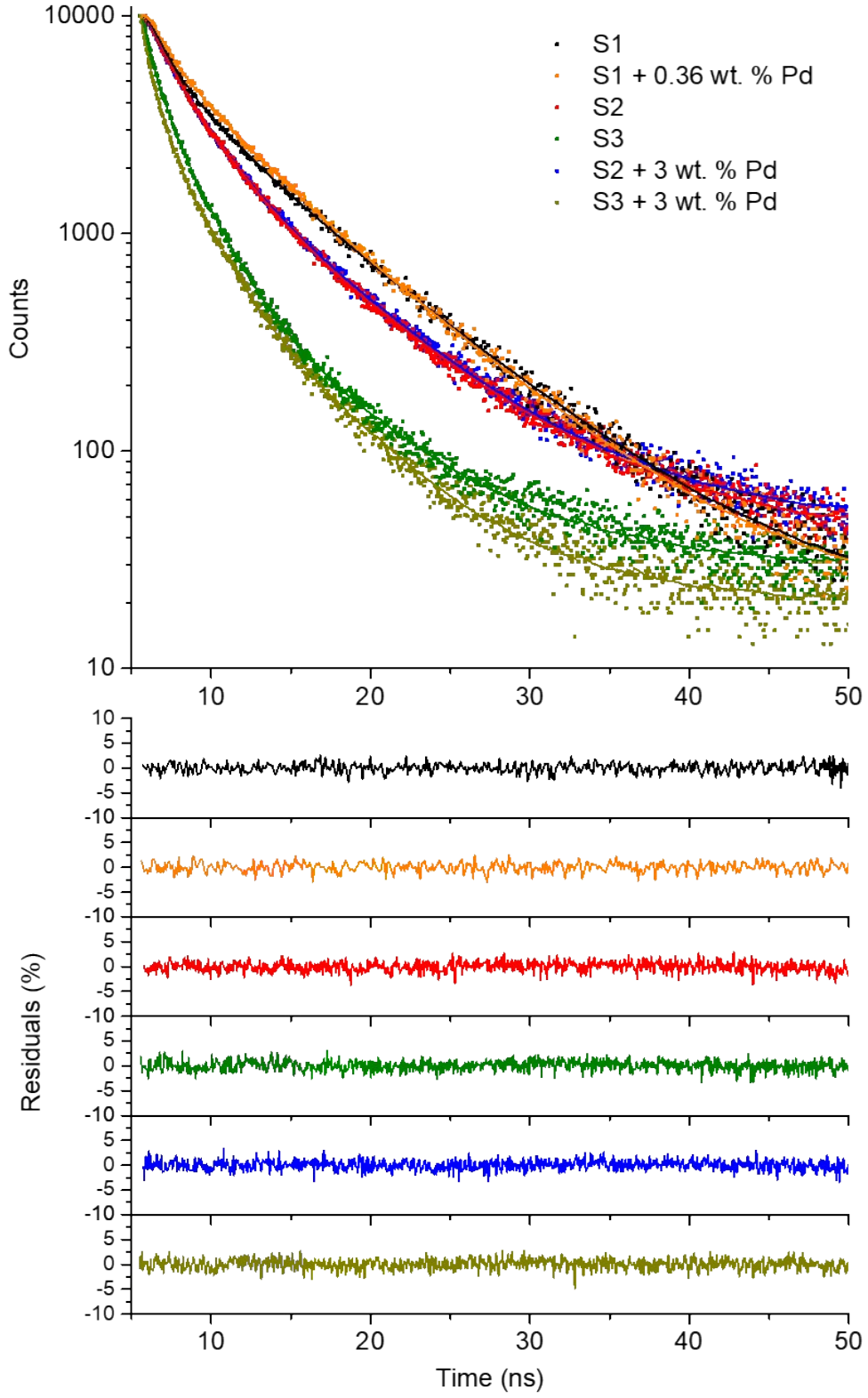

Figure S33: TCSPC spectra of S1, S2 and S3 in the solid state. Excitation with either a 295 nm (S1) or 375 nm (S2 and S3) laser, emission measured at the maxima for each material. Raw data (points), fit (line) and residual (bottom).

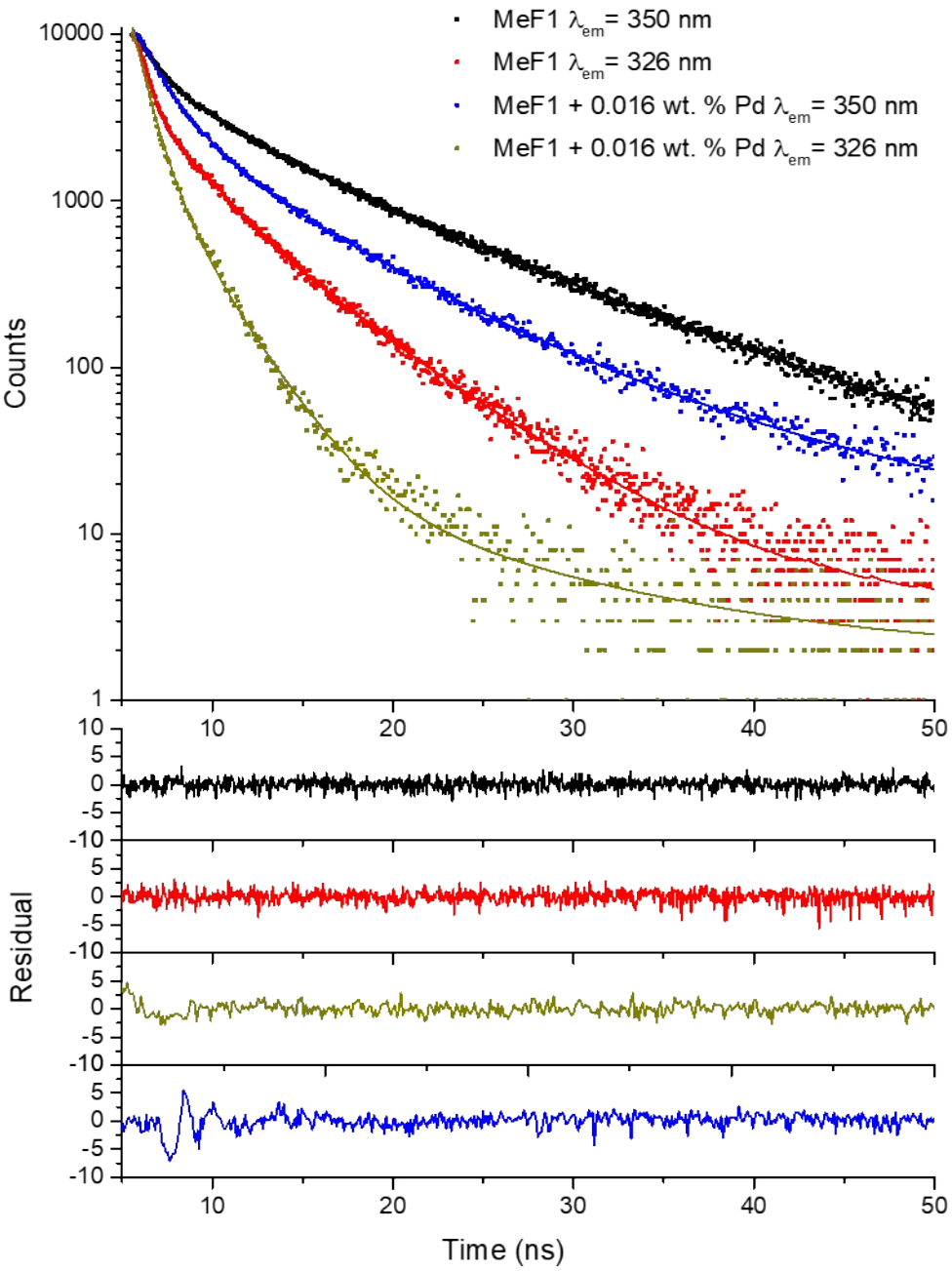

Figure S34: TCSPC spectra of MeF1 in the solid state. Excitation with a 295 nm laser. Emission measured at 325 nm or 350 nm. Raw data (points), fit (line) and residual (bottom).

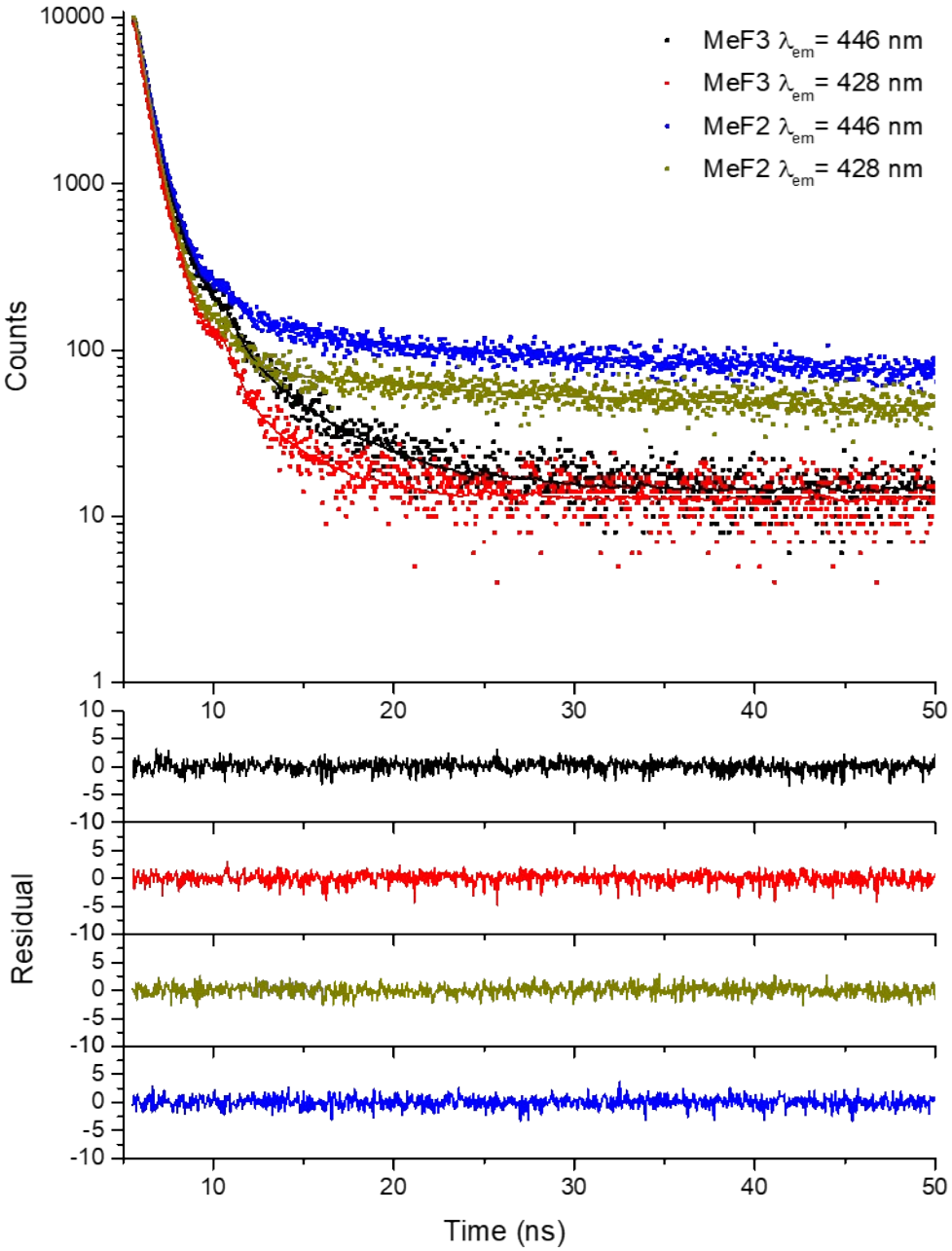

Figure S35: TCSPC spectra of MeF2 and MeF3 in the solid state. Excitation with a 375 nm laser. Raw data (points), fit (line) and residual (bottom).

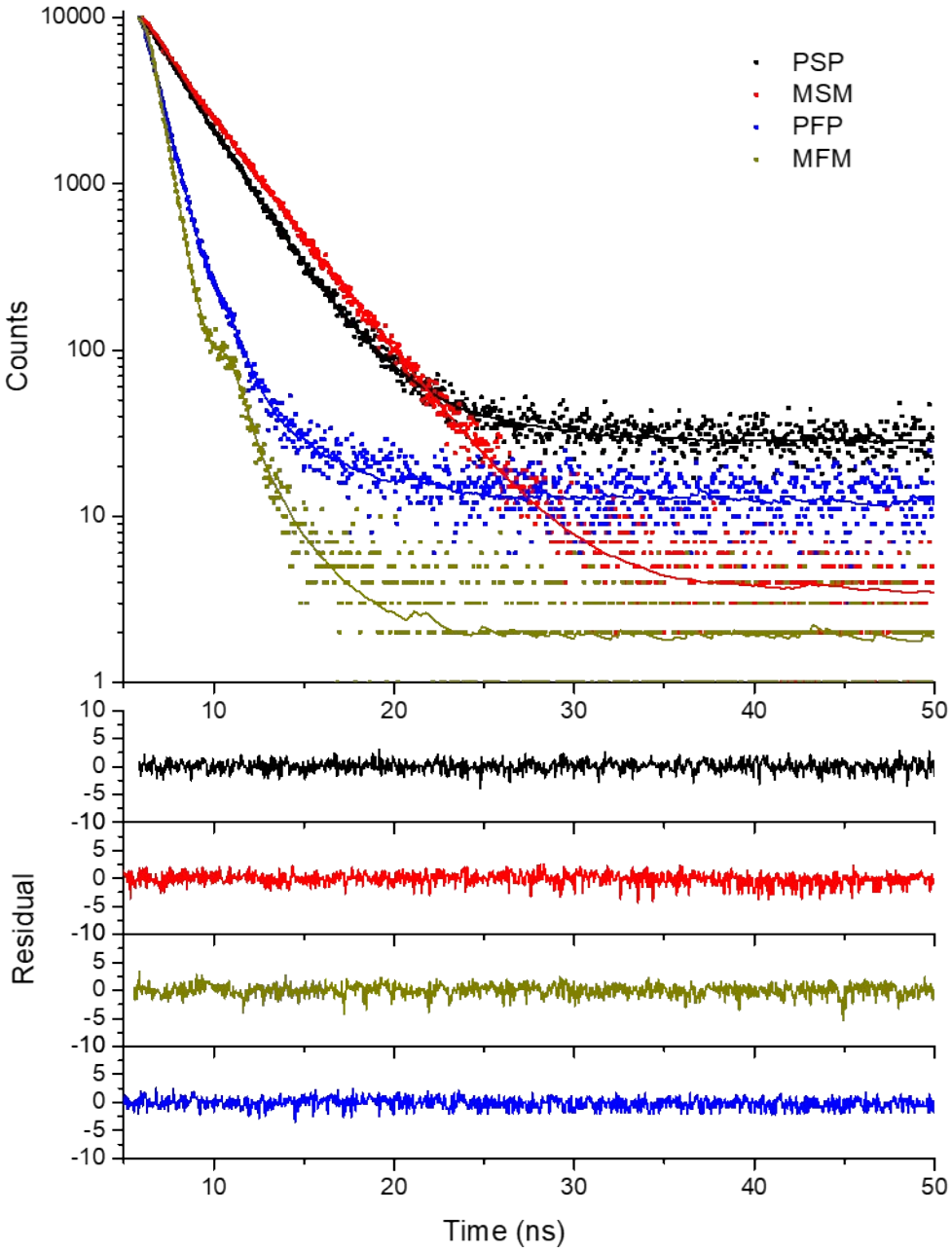

Figure S36: TCSPC spectra of PSP, MSM, PFP and MFM in the solid state. Excitation with either a 295 nm (MSM and MFM) or 375 nm (PSP and PFP) laser. Emission measured at the maxima for each material. Raw data (points), fit (line) and residual (bottom).

Table S5: Fluorescence lifetime properties of the oligomers in the solid state.

Material	Excitation (nm)	Emission (nm)	τ_1 (ns)	f_1	τ_2 (ns)	f_2	τ_3 (ns)	f_3	χ^2	τ_{Av} (ns) [a]
S1	295	394	1.27	15.17	3.07	19.27	7.51	65.56	1.06	5.71
S1 + 0.36 wt. % Pd	295	394	1.33	13.01	3.85	27.64	7.41	59.36	1.05	5.64
S2	375	460	0.60	2.33	2.30	41.64	6.93	56.02	1.04	4.85
S2 + 3 wt. % Pd	375	460	0.94	3.41	2.48	46.01	7.27	50.57	1.03	4.85
S3	375	492	0.44	14.25	1.99	59.03	6.60	26.73	1.09	3.00
S3 + 3 wt. % Pd	375	492	0.43	21.51	1.85	47.34	5.74	31.16	1.15	2.76
MeF1	295	326	0.51	35.58	2.54	33.96	6.01	30.47	1.27	2.87
MeF1	295	350	1.04	14.96	3.71	24.25	10.0	60.79	0.98	7.15
MeF1 + 0.016 wt. % Pd	295	326	0.83	58.91	2.45	38.62	11.2	2.47	1.76	1.71
MeF1 + 0.016 wt. % Pd	295	350	1.75	39.67	6.30	49.10	15.5	11.22	1.44	5.53
MeF2	375	428	0.44	45.99	0.93	48.55	5.45	14.24	1.05	1.43
MeF2	375	446	0.48	47.77	1.12	42.58	12.9	9.65	1.09	1.95
MeF3	375	428	0.39	50.10	0.92	44.62	3.42	5.28	1.14	0.78
MeF3	375	446	0.44	52.61	1.16	38.71	4.48	8.67	1.08	1.07
PSP	375	438	0.50	3.49	2.38	90.61	4.95	5.91	1.03	2.47
MSM	295	387	0.13	6.67	1.70	19.90	3.18	73.43	1.34	2.68
PFP	375	423	0.06	3.62	0.96	93.17	4.00	3.21	1.25	1.02
MFM	295	372	0.26	21.22	0.63	76.93	2.52	1.86	1.03	0.58

[a] $\tau_{Av} = (1/i)\ (\sum f_i\, \tau_i)$

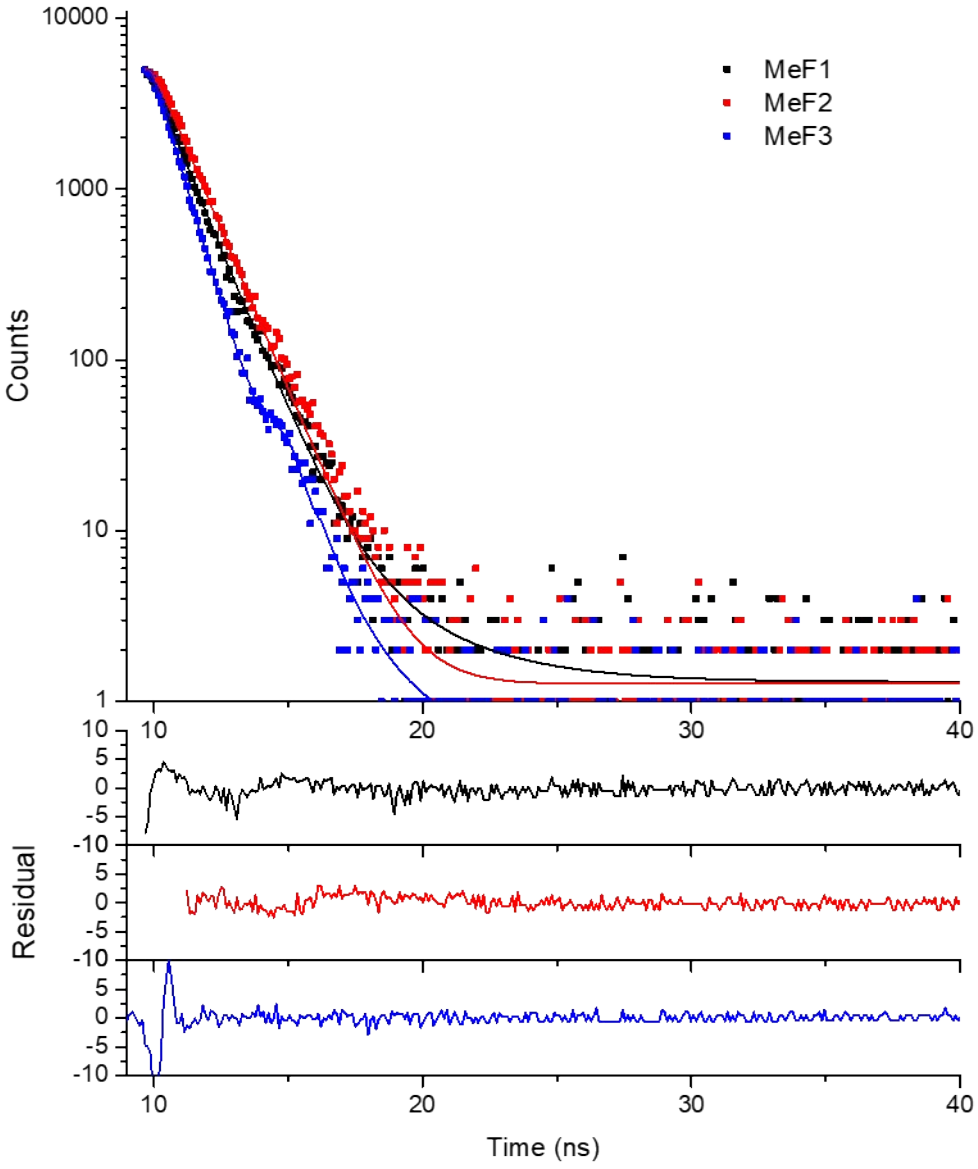

Figure S37: TCSPC spectra of MeF oligomers in chloroform solution. Excitation with a 295 nm laser. Emission measured at 400 nm (MeF1) or 475 nm (MeF2 and MeF3). Raw data (points), fit (line) and residual (bottom).

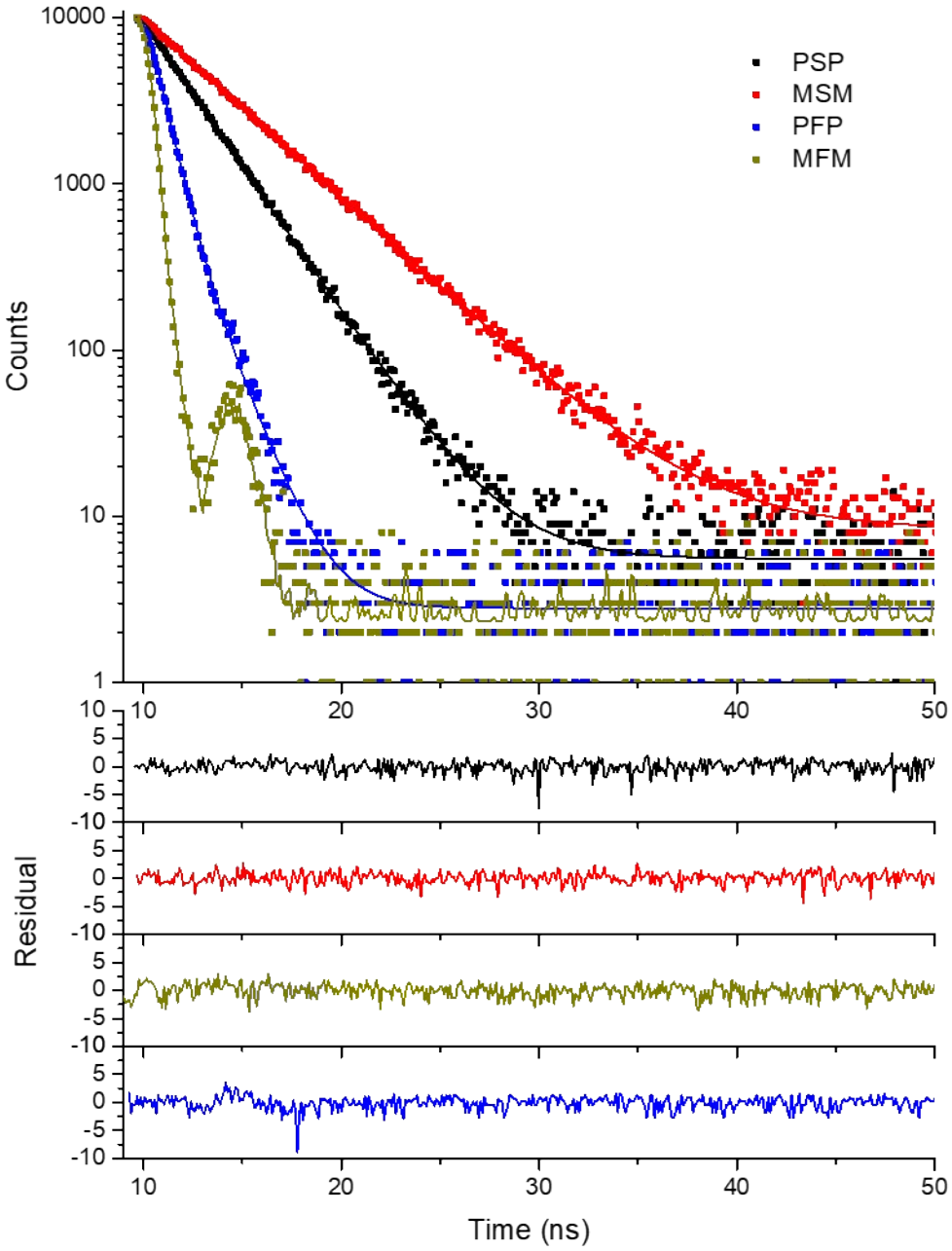

Figure S38: TCSPC spectra of PSP, MSM, PFP and MFM in the chloroform solution. Excitation with a 295 nm laser. Emission measured at the maxima for each material. Raw data (points), fit (line) and residual (bottom).

Table S6: Fluorescence lifetime properties of the oligomers dissolved in chloroform.

Material	Excitation (nm)	Emission (nm)	τ_1 (ns)	f_1	τ_2 (ns)	f_2	τ_3 (ns)	f_3	χ^2	τ_{Av} (ns) [a]
MeF1	295	312	1.11	98.23	3.19	1.78	-	-	1.11	1.15
MeF2	295	363	0.28	9.48	1.16	90.52	-	-	0.86	1.07
MeF3	295	393	0.79	97.0	1.95	2.96	-	-	1.25	0.83
PSP	295	409	0.09	0.65	0.16	1.80	2.47	97.56	1.40	2.42
MSM	295	390	0.16	0.40	3.02	7.03	3.95	92.58	1.36	3.87
PFP	295	357	0.51	44.55	0.56	52.10	1.43	3.35	1.42	0.57
MFM	295	334	0.05	58.40	0.05	41.59	0.81	0.01	1.80	0.05

[a] $\tau_{Av} = (1/i) (\sum f_i \tau_i)$

10. Static Light Scattering

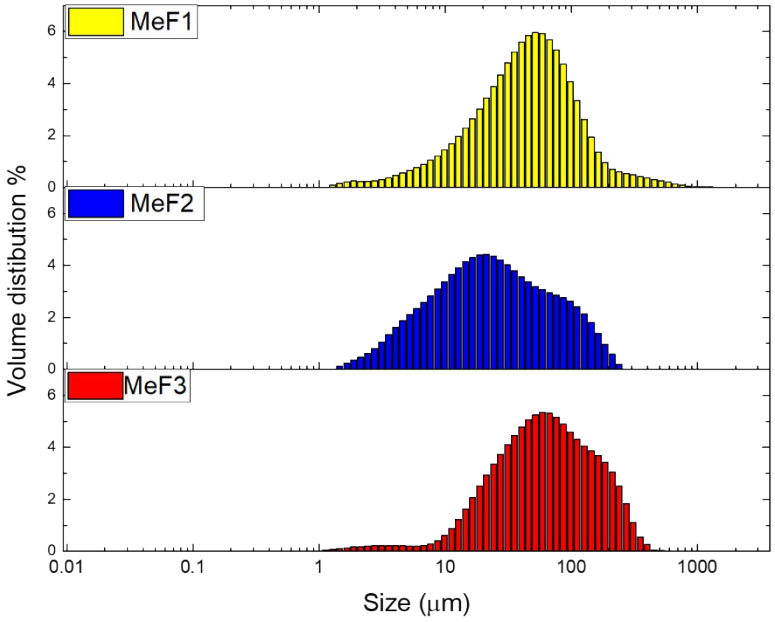

Figure S39: Catalyst particle size distribution in water.

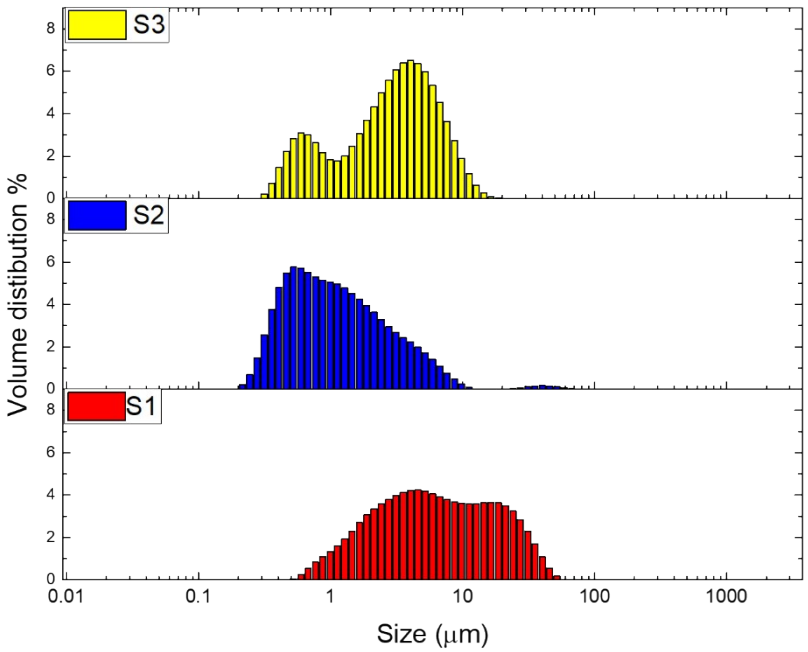

Figure S40: Catalyst particle size distribution in water.

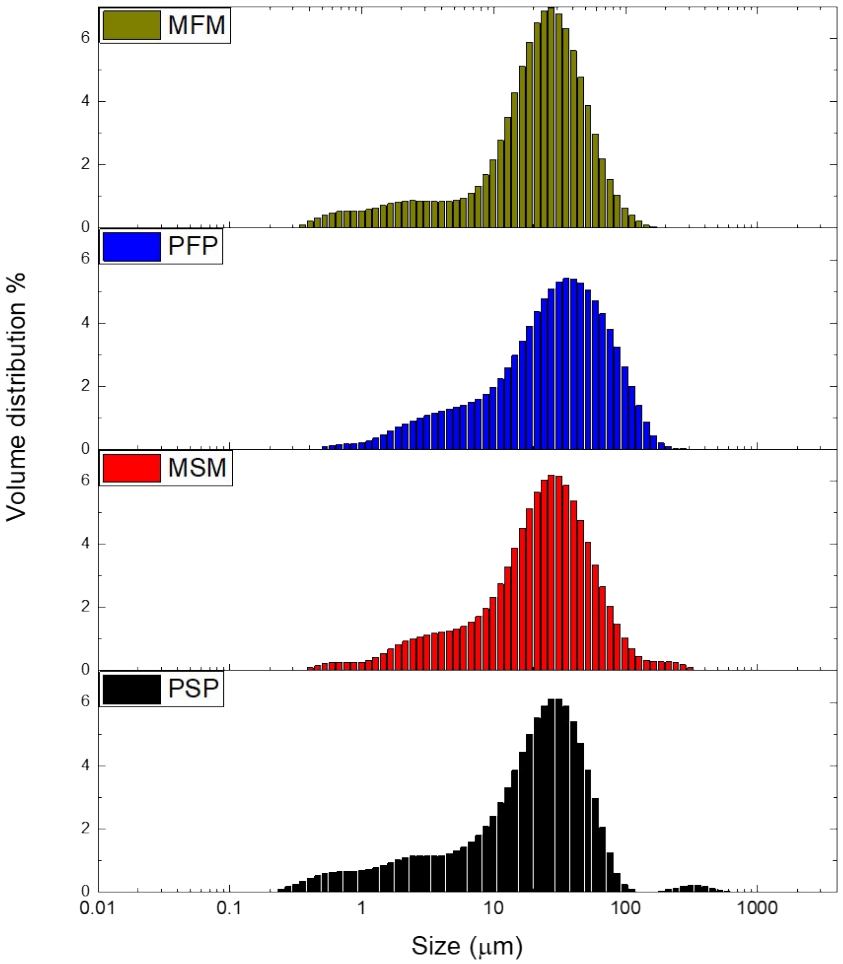

Figure S41: Catalyst particle size distributions in water.

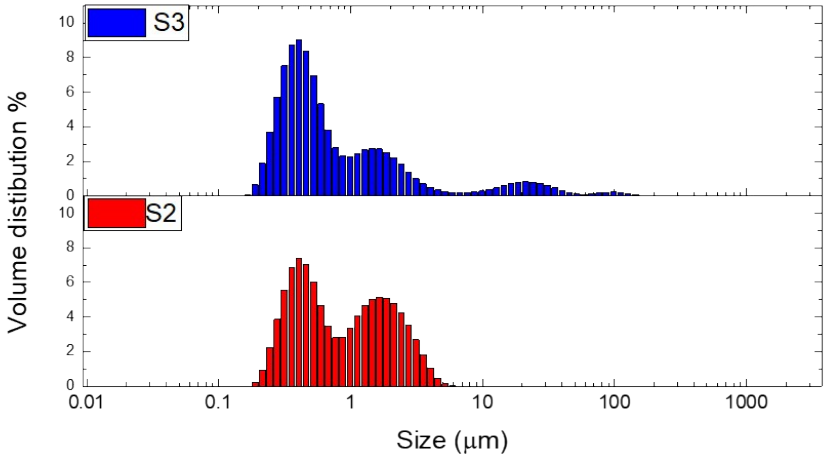

Figure S42: Catalyst particle size distribution in TEA/MeOH/water.

11. Thermogravimetric Analysis

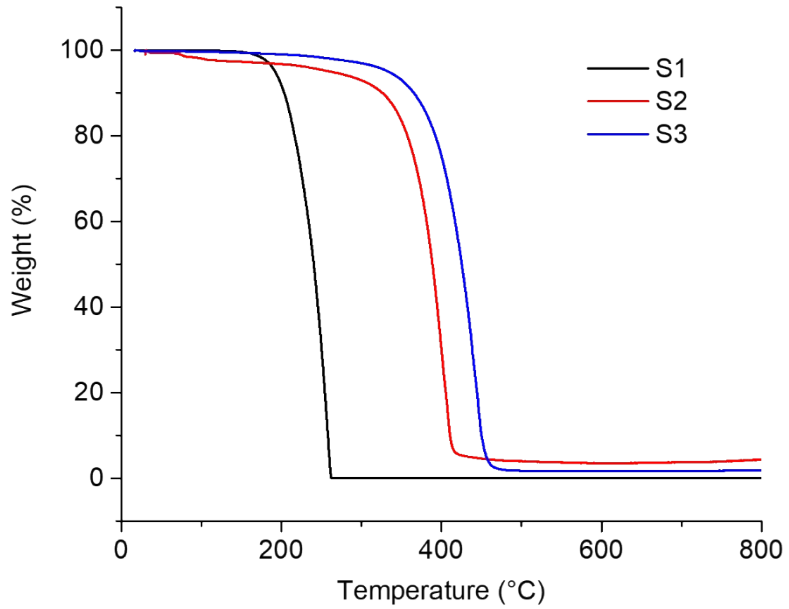

Figure S43: Thermogravimetric analysis of S1-3 under air.

12. Characteristics of Filters / Light Sources

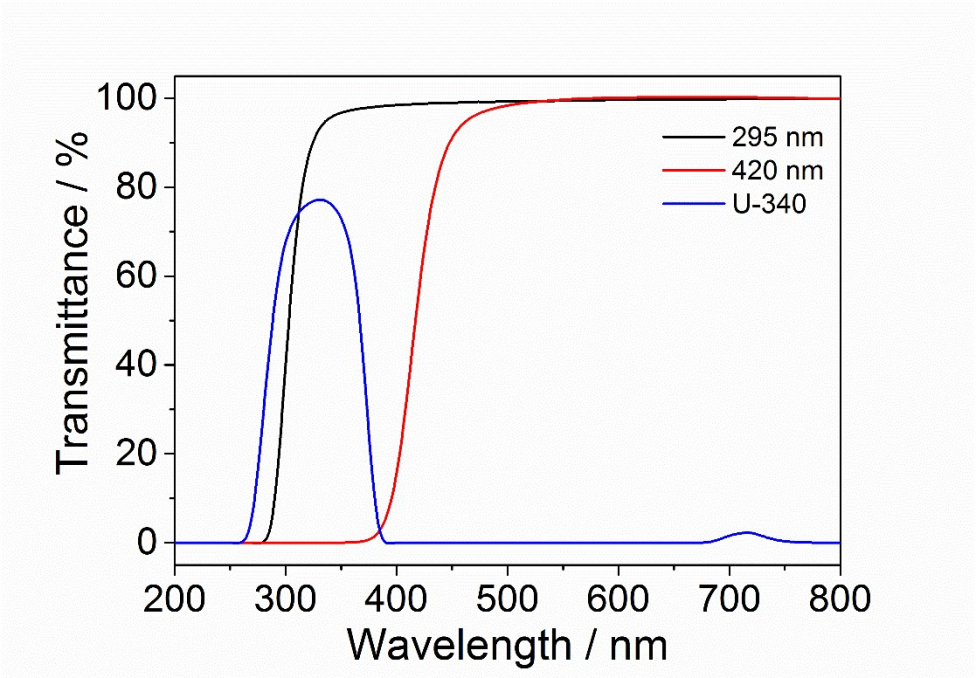

Figure S44: Transmittance characteristics of the λ > 420 nm, λ > 295 nm and U-340 nm filter used in this study.

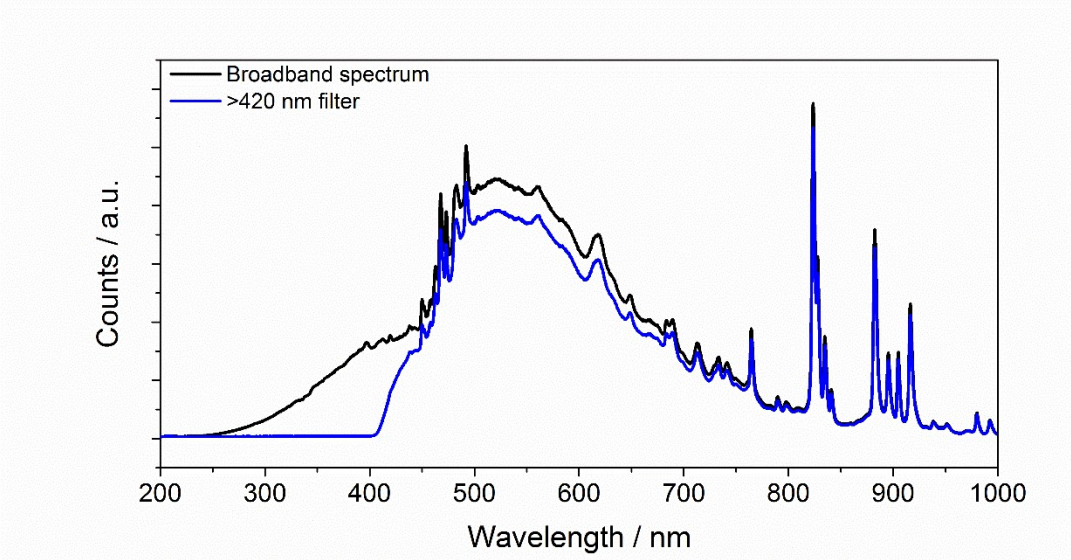

Figure S45: Output of the Xe light source used in this study.

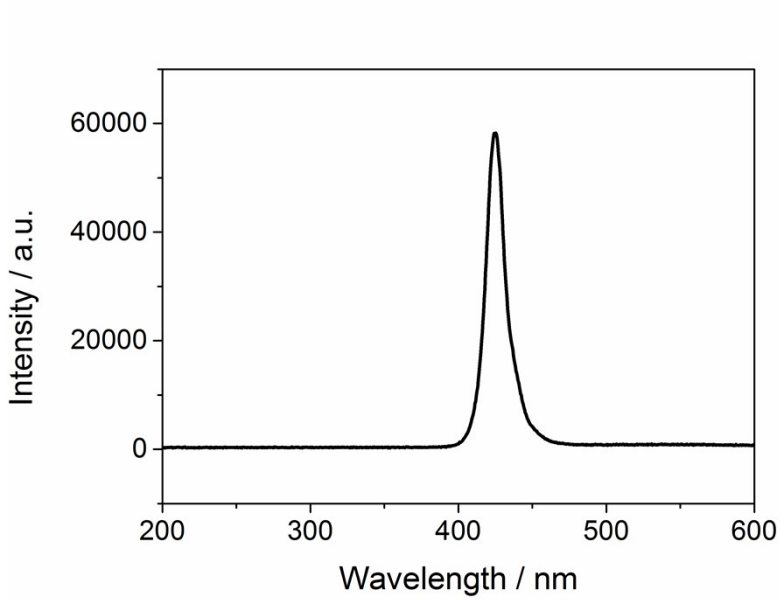

Figure S46. Output of the 420 nm LED used in this study.

13. Hydrogen Evolution Experiments

Water for hydrogen evolution experiments was purified using an ELGA LabWater system with a Purelab Option S filtration and ion exchange column (ρ = 15 MΩ cm) without pH level adjustment. A quartz flask was charged with the catalyst, Pd co-catalysts (if applicable) and dispersants as described and sealed with a septum. The resulting suspension was ultrasonicated until the photocatalyst was dispersed before degassing by N_2 bubbling for 30 minutes. For standard measurements the reaction mixture was illuminated with a 300 W Newport Xe light-source (Model: 6258, Ozone free) for the time specified. The lamp was cooled by water circulating through a metal jacket. Gas samples were taken with a gas-tight syringe, and run on a Bruker 450-GC gas chromatograph equipped with a Molecular Sieve 13X 60-80 mesh 1.5 m × ⅛" × 2 mm ss column at 50 °C with an argon flow of 40.0 mL min^{-1}. Hydrogen was detected with a thermal conductivity detector referencing against standard gas with a known concentration of hydrogen. Hydrogen dissolved in the reaction mixture was not measured and the pressure increase generated by the evolved hydrogen was neglected in the calculations. The rates were determined from a linear regression fit and the error is given as the standard deviation of the amount of hydrogen evolved.

Table S7: Summary of Photocatalytic Testing

Material	Pd[a] (wt. %)	HER (µmol h^{-1} g^{-1}) TEA/MeOH/Water[b] λ > 295 nm filter[c]	HER (µmol h^{-1} g^{-1}) TEA/MeOH/Water[b] 400 > λ > 275 nm filter[c]	HER (µmol h^{-1} g^{-1}) Na_2S / Na_2SO_3 (aq)[d] λ > 295 nm filter	HER (µmol h^{-1} g^{-1}) Na_2S / Na_2SO_3 (aq)[d] 400 > λ > 275 nm filter[c]	HER (µmol h^{-1} g^{-1}) Homogeneous[e] 400 > λ > 275 nm filter[c]
PSP	< 0.001[f]			24.1 ± 0.8	29.6 ± 0.4	14 ± 0.5
MSM	0.002			5.5 ± 0.2	20.4 ± 0.7	44 ± 4[h]
PFP	0.003			13.8 ± 0.8	8.7 ± 0.3	120 ± 13
MFM	0.014			4.8 ± 0.4	10.0 ± 0.5	13 ± 1
MeF1	< 0.001[f]	4.7 ± 0.2[g]	2.6 ± 0.3[g]	4.1 ± 0.3	6.5 ± 0.6	107 ± 8
MeF2	0.011	12.9 ± 0.4	4.3 ± 0.3	3.4 ± 0.2	4.4 ± 0.2	93 ± 5
MeF3	0.017	37 ± 1	28 ± 1	10.1 ± 0.3	6.6 ± 0.3	30 ± 1
MeF1+ 0.02 % Pd	0.016	9.6 ± 0.5	4.9 ± 0.3	14.2 ± 0.3	28 ± 1	**HER (µmol h^{-1} g^{-1}) TEA/MeOH/Water[b] λ > 420 nm filter[c]**
S1	< 0.001[f]	26 ± 3[g,h]	20.1 ± 0.4[g,h]	8.1 ± 0.8	25.4 ± 0.2	< 0.1
S2	0.22	414 ± 9	101 ± 1	81 ± 2	50 ± 1	26 ± 1
S3	0.26	2073 ± 82	526 ± 9	286 ± 4	162 ± 6	1125 ± 9
S1 + 0.4 % Pd	0.36			14.7 ± 0.5	33 ± 0.7	< 0.1
S1+ 3 wt. % Pd	-[i]	43 ± 3[g,h]				
S2[i]	0.008	306 ± 9				
S2 + 3 wt. % Pd	2.1	1369 ± 24				
S3 + 3 wt. % Pd	2.5	6550 ± 150				

[a] Measured by ICP-MS after microwave digestion with HNO_3, present from $[Pd(PPh_3)_4]$ used in synthesis via Suzuki-Miayura coupling or loaded by photodepostion using $[Pd(NH_4)_2Cl_4]$; [b] Photocatalyst (1 mg mL^{-1}) suspended in TEA/MeOH/Water (1:1:1), rate calculated as linear regression fit over 5 hours; [c] See previous page for full filter characteristics. [d] Photocatalyst (1 mg mL^{-1}) suspended in Na_2S / Na_2SO_3 (aq) (0.2 M / 0.35 M, 25 mL), rate calculated as linear regression fit over 5 hours; [e] Photocatalyst (5 mg) dissolved in THF (22.5 mL), TEA (1.25 mL) and water (1.25 mL), rate calculated as linear regression fit over 5 hours; [f] Pd level below the baseline of the instrument; [g] Catalyst partially soluble in mixture used for photocatalysis experiment; [h] Rate determined as linear regression fit less than 5 hours due to non-linearity; [i] Photocatalyst washed with sodium *N,N*-diethyldithiocarbamate. [j] Accurate Pd deposition could not be determined due to dissolution of the photocatalyst.

13.2 Photocatalytic tests in Na_2S / Na_2SO_3 (aq)

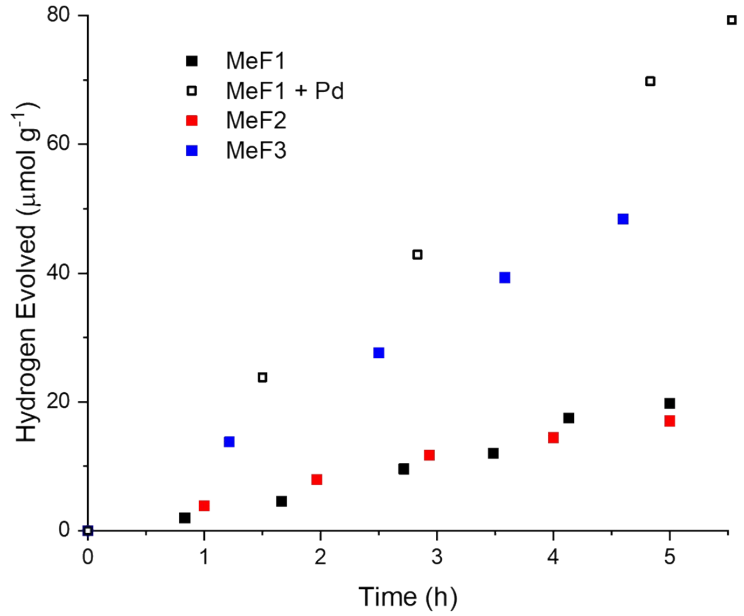

Figure S46: Photocatalytic hydrogen evolution of MeF1, MeF1 containing 0.016 wt. % Pd, MeF2 and MeF3 from from $Na_2S_{(aq)}$ (0.35 M) / $Na_2SO_{3(aq)}$ (0.2 M) using a λ > 295 nm filter (25 mg photocatalyst in 25 mL, 300 W Xe light source). Note that MeF2 and MeF3 contain 0.011 and 0.014 wt. % residual Pd from synthesis respectively.

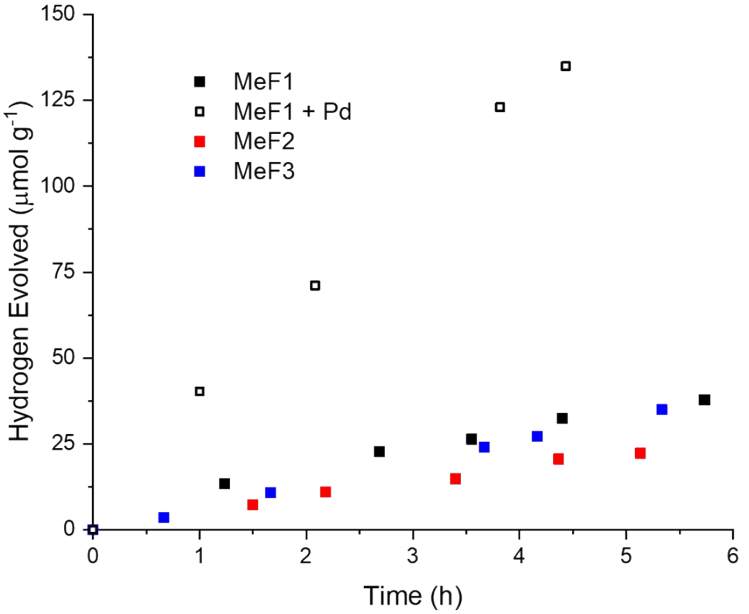

Figure S47: Photocatalytic hydrogen evolution of MeF1, MeF1 containing 0.016 wt. % Pd, MeF2 and MeF3 from from $Na_2S_{(aq)}$ (0.35 M) / $Na_2SO_{3(aq)}$ (0.2 M) using a 400 > λ > 275 nm filter (25 mg photocatalyst in 25 mL, 300 W Xe light source). Note that MeF2 and MeF3 contain 0.011 and 0.014 wt. % residual Pd from synthesis respectively.

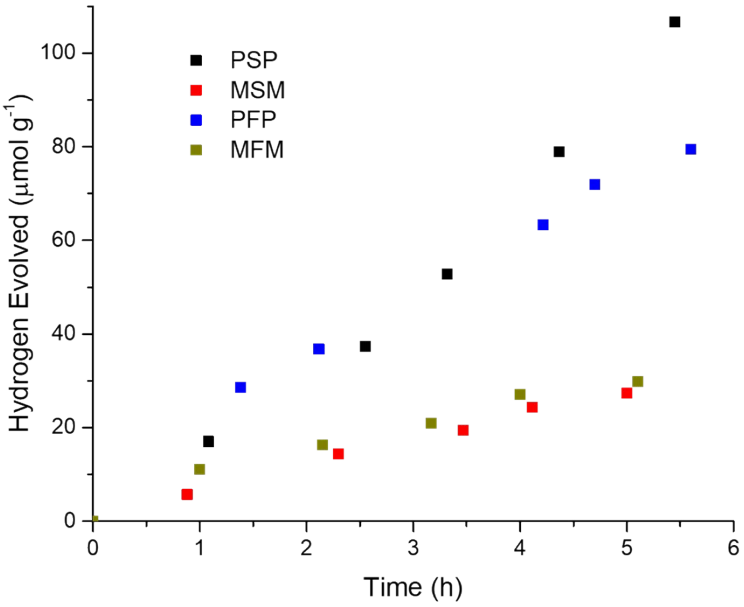

Figure S48: Photocatalytic hydrogen evolution of PSP, MSM, PFP and MFM from $Na_2S_{(aq)}$ (0.35 M) / $Na_2SO_{3(aq)}$ (0.2 M) using a $\lambda > 295$ nm filter (25 mg photocatalyst in 25 mL, 300 W Xe light source).

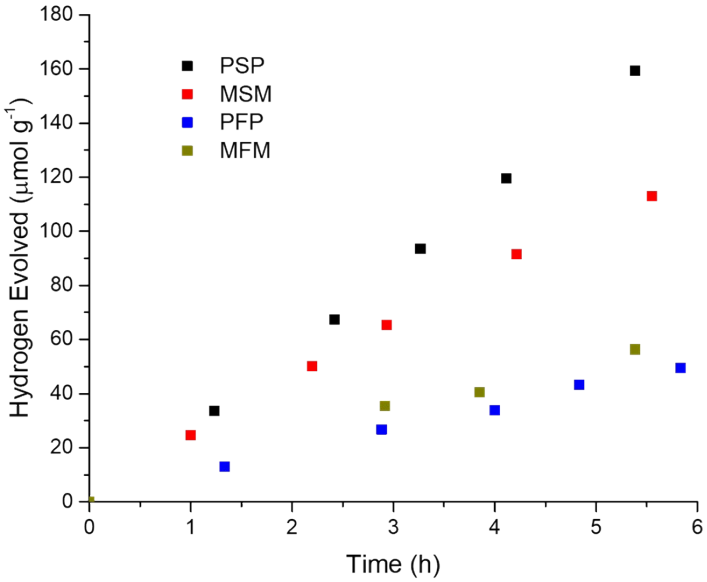

Figure S49: Photocatalytic hydrogen evolution of PSP, MSM, PFP and MFM from $Na_2S_{(aq)}$ (0.35 M) / $Na_2SO_{3(aq)}$ (0.2 M) using a $400 > \lambda > 275$ nm filter (25 mg photocatalyst in 25 mL, 300 W Xe light source).

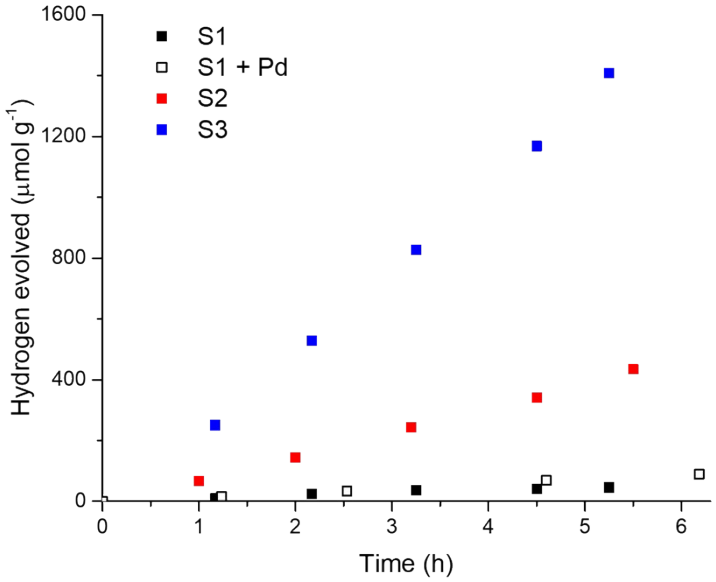

Figure S50: Photocatalytic hydrogen evolution of S1, S1 containing 0.36 wt. % Pd, S2 and S3 from $Na_2S_{(aq)}$ (0.35 M) / $Na_2SO_{3(aq)}$ (0.2 M) using a $\lambda > 295$ nm filter (25 mg photocatalyst in 25 mL, 300 W Xe light source).

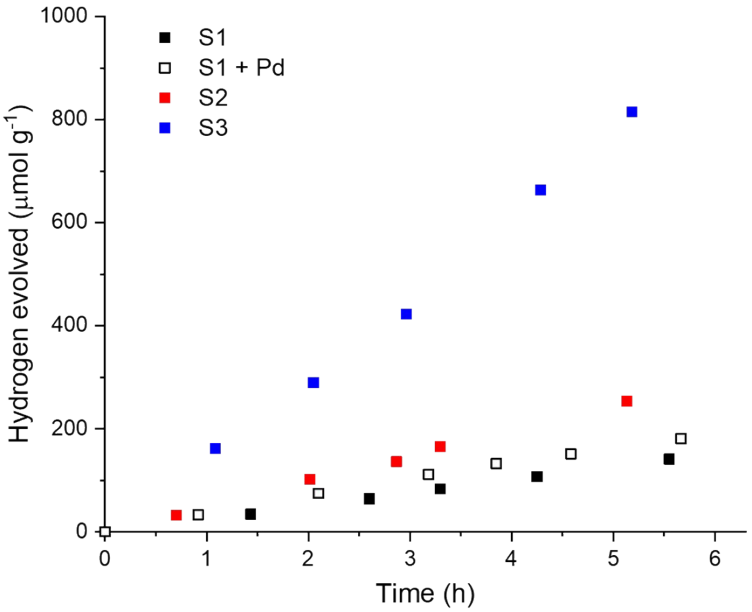

Figure S51: Photocatalytic hydrogen evolution of S1, S1 containing 0.36 wt. % Pd, S2 and S3 from $Na_2S_{(aq)}$ (0.35 M) / $Na_2SO_{3(aq)}$ (0.2 M) using a $400 > \lambda > 275$ nm filter (25 mg photocatalyst in 25 mL, 300 W Xe light source).

13.3 Photocatalytic tests in TEA / MeOH / Water

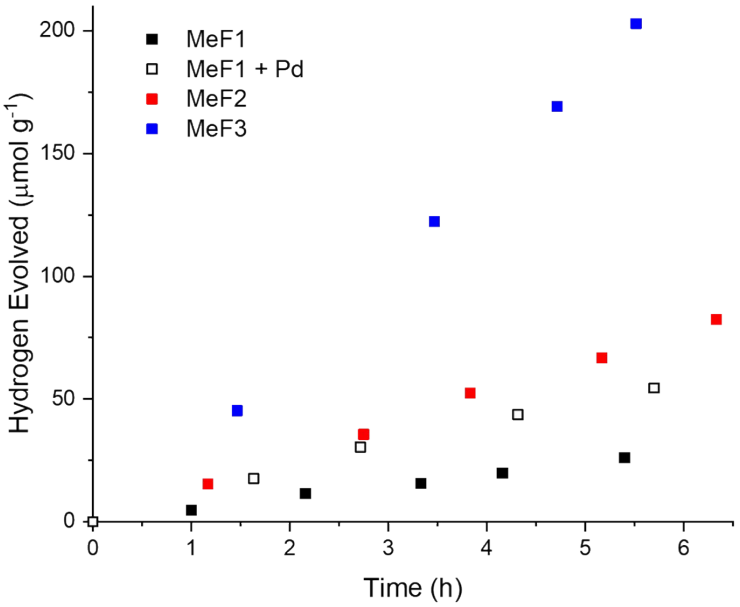

Figure S52: Photocatalytic hydrogen evolution of MeF1, MeF1 containing 0.016 wt. % Pd, MeF2 and MeF3 from water/methanol/triethylamine mixtures using a λ > 295 nm filter (25 mg photocatalyst in 25 mL, 300 W Xe light source).

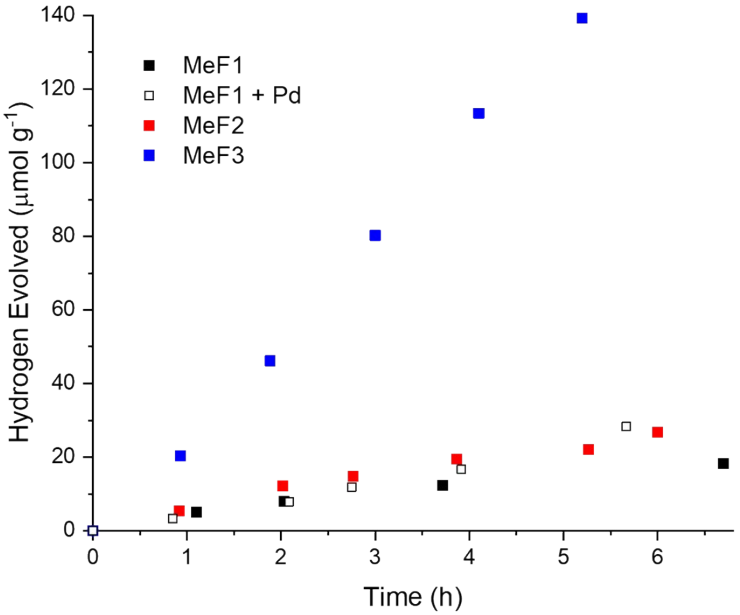

Figure S53: Photocatalytic hydrogen evolution of MeF1, MeF1 containing 0.016 wt. % Pd, MeF2 and MeF3 from water/methanol/triethylamine mixtures using a 400 > λ > 275 nm filter (25 mg photocatalyst in 25 mL, 300 W Xe light source).

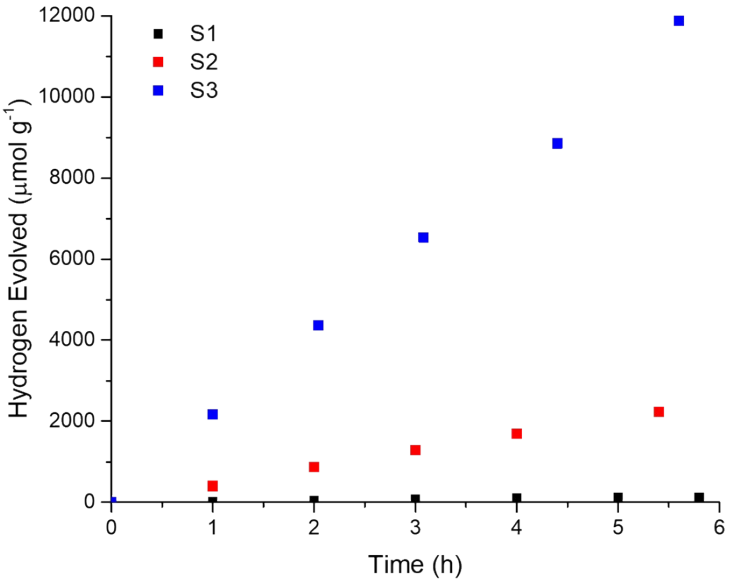

Figure S54: Photocatalytic hydrogen evolution of S1, S2 and S3 from water/methanol/triethylamine mixtures using a λ > 295 nm filter (25 mg photocatalyst in 25 mL, 300 W Xe light source).

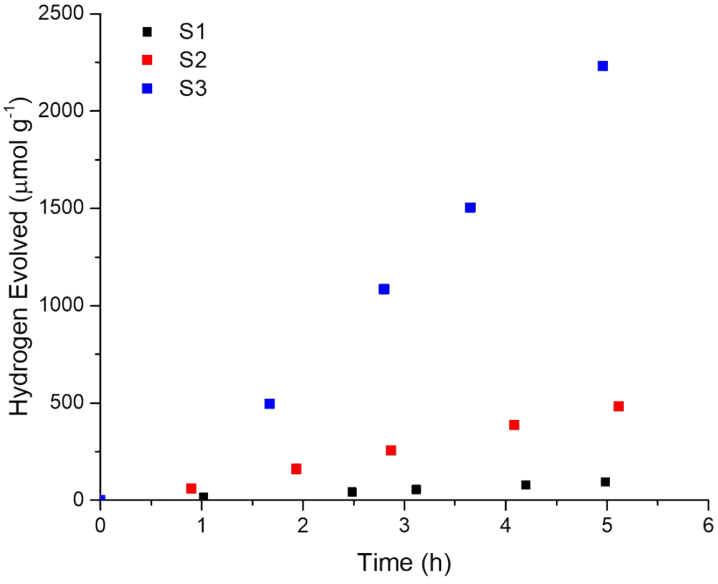

Figure S55: Photocatalytic hydrogen evolution of S1, S2 and S3 from water/methanol/triethylamine mixtures using a 400 > λ > 275 nm filter (25 mg photocatalyst in 25 mL, 300 W Xe light source).

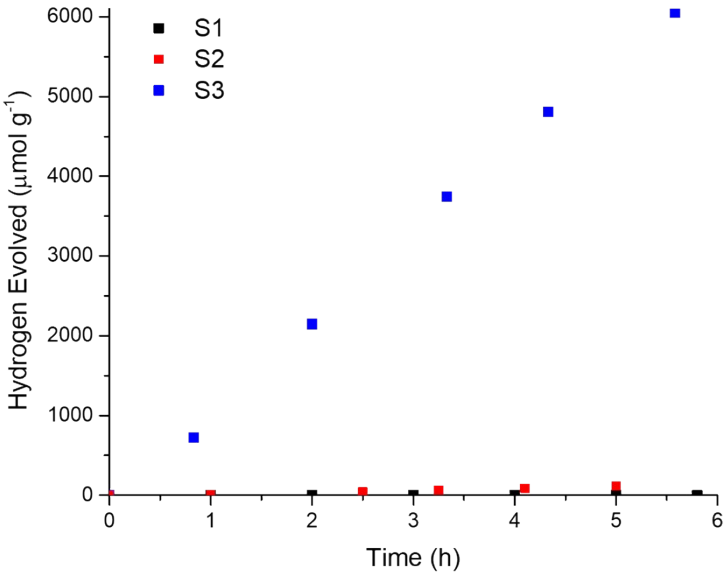

Figure S56: Photocatalytic hydrogen evolution of S1, S2 and S3 from water/methanol/triethylamine mixtures using a λ > 420 nm filter (25 mg photocatalyst in 25 mL, 300 W Xe-lamp).

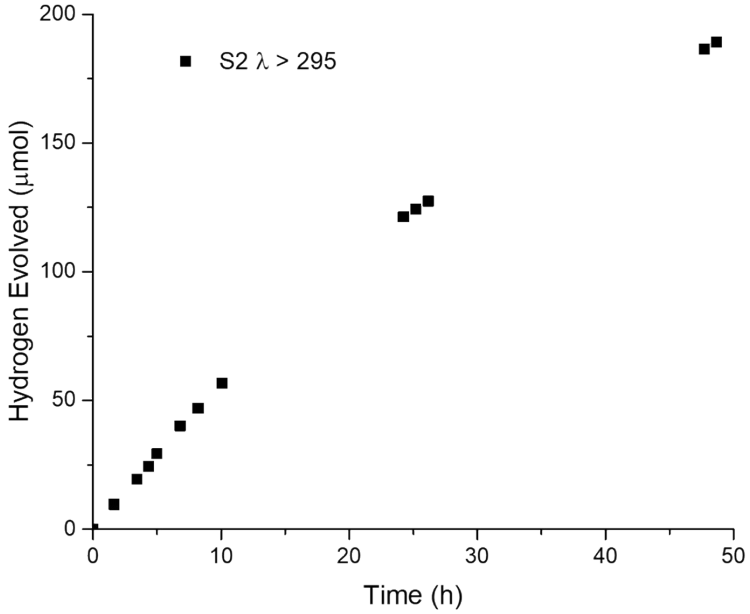

Figure S57: Photocatalytic hydrogen evolution of S2 from water/methanol/triethylamine mixtures using a λ > 295 nm filter (5 mg photocatalyst in 5 mL, 300 W Xe light source). Mixture was degassed by N_2 bubbling after 28 hours.

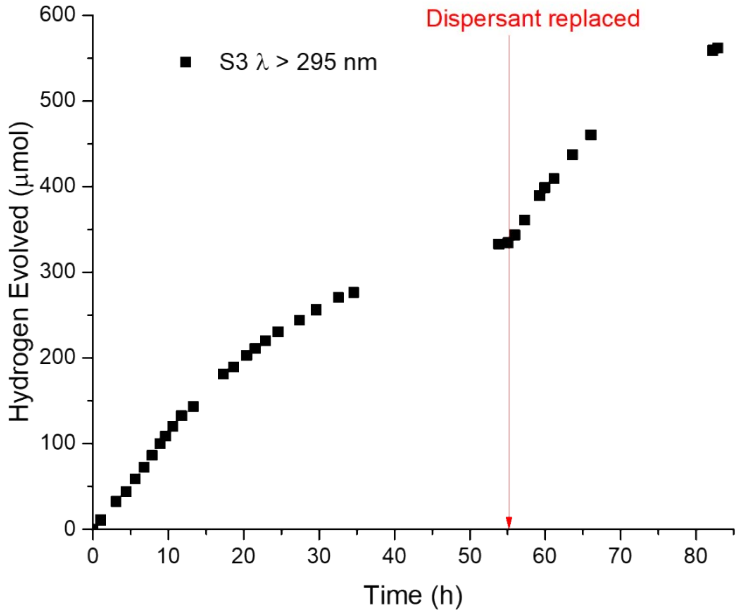

Figure S58: Photocatalytic hydrogen evolution of S3 from water/methanol/triethylamine mixtures using a λ > 295 nm filter (5 mg photocatalyst in 5 mL, 300 W Xe light source). Mixture was degassed by N_2 bubbling after 11 hours, after 55 hours catalysts was collected by filtration and photolysis mixture replaced before degassing by N_2 bubbling, the mixture was degassed after 65 hours by N_2 bubbling.

13.4 Photocatalytic tests with high palladium content

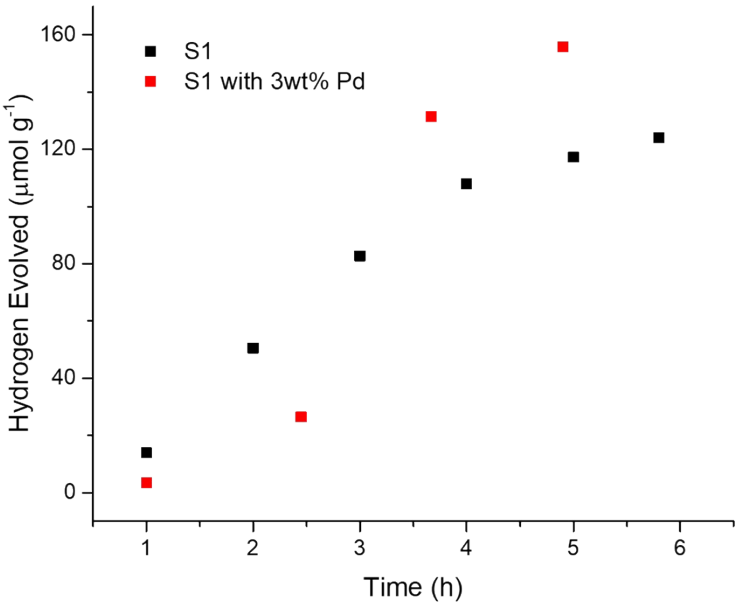

Figure S59: Photocatalytic hydrogen evolution of S1 with (red) and without (black) 3 wt. % Pd from water/methanol/triethylamine mixtures using a λ > 295 nm filter (25 mg photocatalyst in 25 mL, 300 W Xe light source).

14. Homogeneous hydrogen evolution experiments

MeF1-3, PSP, MSM, PFP and MFM are soluble in THF meaning it was possible to measure their activity as homogeneous catalysts. This is particularly pertinent given recent promising examples of homogenous catalysis by carbon nitride dissolved in organic acid[14] and using water soluble conjugated molecules for proton reduction.[15] For the homogeneous experiments the oligomers were dissolved in THF with 5 vol. % H_2O and 5 vol. % TEA. It has been previously shown that PFP degrades to 2,7-diphenyl-9*H*-fluoren-9-one under UV-light,[16] possibly through reaction with singlet oxygen. Nickel(II) dibutyldithiocarbamate successfully stabalised S1, described above, and has been shown to act as a scavenger for reactive oxygen species,[17,18] so was added to the photolysis mixture to improve catalyst stability. All samples were illuminated using the 275 – 400 nm filter, as this best matched the solution absorption spectra, and in contrast to the heterogeneous experiments PFP was the most active material, after an initial induction period (Fig. S61) a HER of 120 μmol h^{-1} g^{-1} was measured while PSP had a rate of only 14 μmol h^{-1} g^{-1}. After an initial induction period MSM had a steady HER of 44 μmol h^{-1} g^{-1} (Fig. S61), while MFM on the other hand showed a slow drop off in activity over 5 hours with an average HER of 13 μmol h^{-1} g^{-1}. It should be noted that NMR analysis of the materials collected by evaporation post catalysis showed differences in the aromatic region, indicating a degree of photocatalyst break down. This is most significant in MFM where full catalyst breakdown appears to have occurred (Fig. S84), consistent with the loss of activity over time. MSM shows significant impurity peaks (Fig. S80), PFP shows only small impurity peaks and PSP appears to be stable (Fig. S78 and S82). We believe the hydrogen produced in these experiments is from photocatalytic proton reduction rather than photodegradation of the oligomers although at this stage we cannot conclusively prove this.

The MeF 9*H*-fluorene oligomers were also tested under these conditions (Fig. S60). As under heterogenous conditions, when using UV light only (275 – 400 nm filter, 300 W Xe light source) MeF1 is the most active with a HER of 107 μmol h^{-1} g^{-1} followed by MeF2 (93 μmol h^{-1} g^{-1}) and MeF3 (30 μmol h^{-1} g^{-1}). Again, analysis of material collected post catalysis showed signs of catalyst breakdown (Fig. S72) with MeF1 significantly decomposing whilst MeF2 and MeF3 appear to be more stable, as evident from ^{1}H NMR spectra recorded after the photocatalytic experiments (Fig. S74 and S76).

To approximate the light absorbed by each material when using the 275 – 400 nm filter the average mass extinction coefficient of the oligomers from 275 to 400 nm was calculated (Table 4, see section 5 for full details). This shows MeF1 has the most limited light absorption with a value of 9.6 cm^2 g^{-1}, less than a quarter that of MeF2 and MeF3, which had values of 44.5 and 54.5 cm^2 g^{-1}, respectively. The average mass extinction coefficients over the 275 to 400 nm irradiation range for PSP and PFP were 38.8 and 49.4 cm^2 g^{-1}, considerably higher than their mesitylated analogues, which have values of 14.8 and 18.3 cm^2 g^{-1}respectively.

These values give an indication of how much light each material can absorb under photocatalytic testing and can also be used to approximate an absorption-corrected activity (ACA), which we define as the hydrogen evolution rate of the photocatalyst divided by the average mass extinction coefficient of the photocatalysts across the irradiation range (Table S4). The ACA values represent the relative activity of the photocatalysts if light absorption were removed as a factor. For MeF1 a value of 11.2 was calculated, which is decreased to 2.8 for MeF2 and 0.6 for MeF3. PSP, MSM, PFP and MFM had ACA values of 0.3, 1.9, 2.4 and 0.7 respectively.

Table S8. Optical properties and photocatalytic activity of the oligomers under homogeneous conditions.

Material	Average ε_{Molar} 275 – 400 nm [a] (M^{-1} cm^{-1})	Average ε_{mass} 275 – 400 nm [b] (g^{-1} cm^2)	HER[c] 275 – 400 nm irradiation[d] (μmol h^{-1} g^{-1})	Absorption-corrected activity[e]
PSP	14,300	38.8	14 ± 0.5	0.3
MSM	6700	14.8	44 ± 4[f]	1.9
PFP	15,700	49.4	120 ± 13	2.4
MFM	7400	18.3	13 ± 1	0.7
MeF1	1860	9.6	107 ± 8	11.2
MeF2	17,200	44.5	93 ± 5	2.8
MeF3	31,500	54.5	30 ± 1	0.6

[a] Average molar extinction coefficient over the irradiation range ($275 < \lambda < 400$ nm) see section 8 for full details; [b] Average mass extinction coefficient over the irradiation range ($275 < \lambda < 400$ nm); [c] photocatalyst (5 mg) dissolved in THF (22.5 mL), TEA (1.25 mL) and water (1.25 mL) with nickel(II) dibutyldithiocarbamate singlet oxygen scavenger (1 mg, 2.14 mmol), rate calculated as linear regression fit over 5 hours unless otherwise stated; [d] see Section 12 for filter characteristics; [e] defined as the HER divided by the average mass extinction coefficient over the irradiation range ($275 < \lambda < 400$ nm); [f] rate calculated over final 3 hours due to induction period.

When using the polymers as homogenous photocatalysts we do not observe the same trend in catalytic activity as in the heterogeneous case; PFP displays by far the highest activity, followed by MSM whilst PSP and MFM had more moderate rates respectively. The ACA values, which account for differences in absorption of the oligomers follow the same trend, suggesting that the most active materials are not necessarily the oligomers that absorb the most light but the oligomers that use the absorbed light most effectively. It is yet unclear what the origin of the difference in light utilization is between the different oligomers. All properties considered, e.g. driving force, light absorption and exciton life-time; either group by oligomer core (*i.e.* PSP/MSM vs. PFP/MFM) or terminal groups (*i.e.* PSP/PFP vs. MSM/MDF), and hence cannot explain why PFP and MSM, which differ both in core and terminal group, are the most active. It appears that the advantages provided by the dibenzo[*b*,*d*]thiophene sulfone unit are not as dominant in solution. It is possible that the crystal packing structure of these materials, which generally have greater planar overlap between aromatic units, plays a role in their improved activity in the solid state, which is not applicable in the homogenous system. Alternatively, the homogenous system, in which contact between oligomer, water and electron donor is maximized, could change the rate-limiting step for reaction.

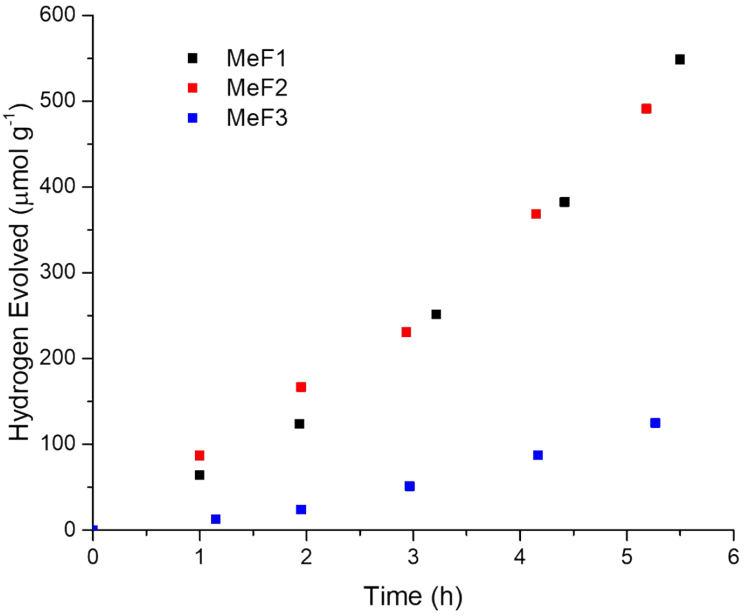

Figure S60: Photocatalytic hydrogen evolution of MeF1-3 (5 mg), and nickel(II) dibutyldithiocarbamate (1 mg) dissolved in THF (22.5 mL), water (1.25 mL) and triethylamine (1.25 mL) using a 400 > λ > 275 nm U-340 filter, 300 W Xe light source.

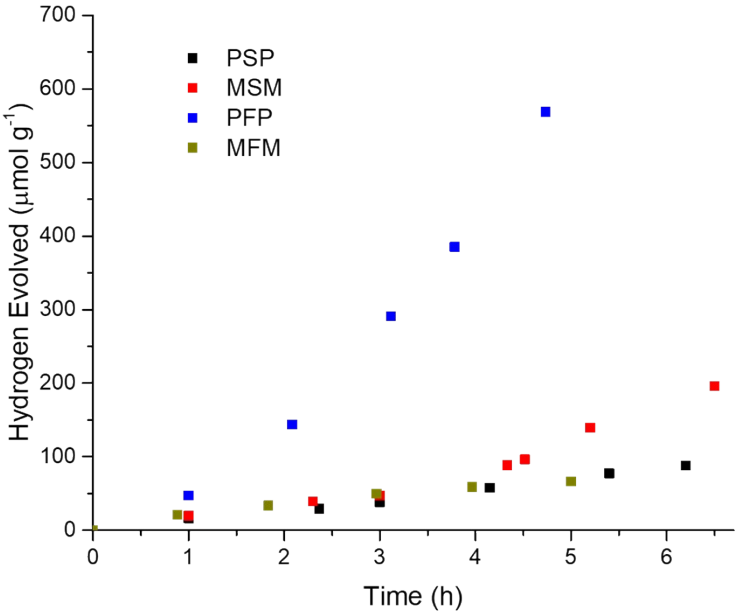

Figure S61: Photocatalytic hydrogen evolution of PSP, MSM, PFP and MFM (5 mg), and nickel(II) dibutyldithiocarbamate (1 mg) dissolved in THF (22.5 mL), water (1.25 mL) and triethylamine (1.25 mL) using a 400 > λ > 275 nm U-340 filter, 300 W Xe light source.

15. Stability of the Photocatalysts

15.1 Photostability of S1

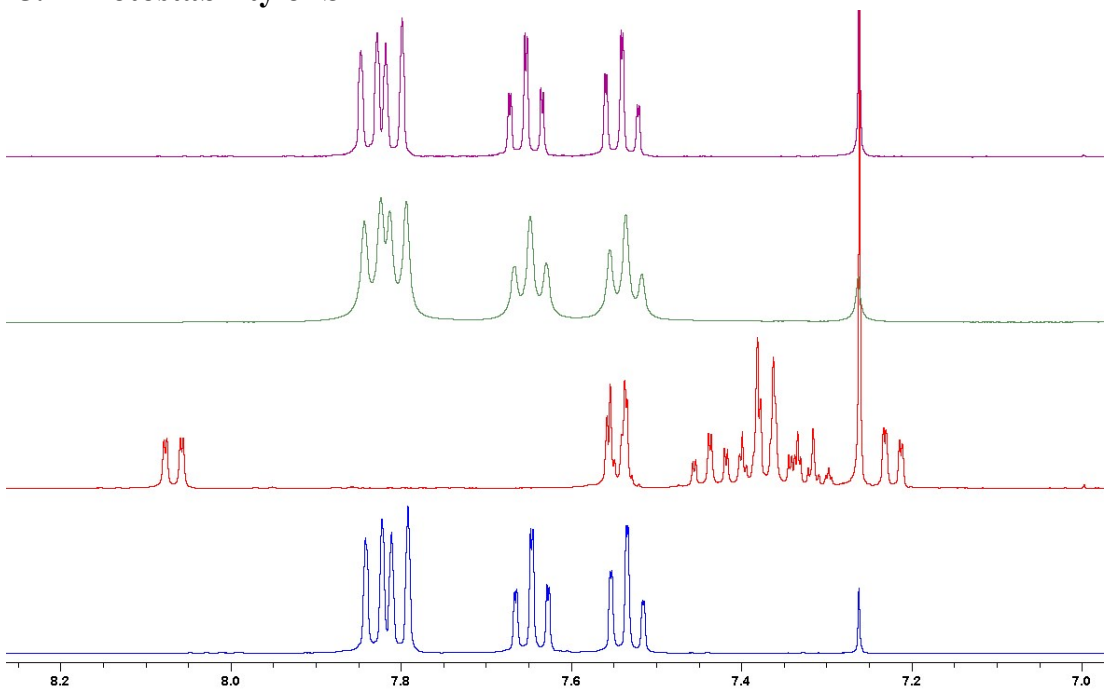

Figure S62: ^{1}H NMR in $CDCl_3$ of S1 pre (blue) and post 72 hours irradiation in TEA / MeOH / Water (1:1:1) at λ > 295 nm with (green) and without (red) nickel(II) dibutyldithiocarbamate, or post 72 hours irradiation in Na_2S / Na_2SO_3 (aq) (purple) at λ > 295 nm. X-axis in ppm.

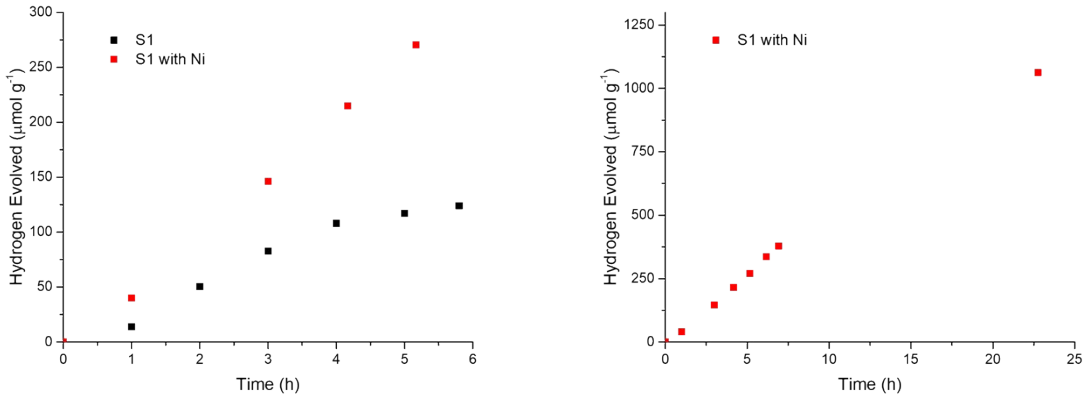

Figure S63: Photocatalytic hydrogen evolution of S1 with and without nickel(II) dibutyldithiocarbamate (left) and extended run (right) from water/methanol/triethylamine mixtures using a λ > 295 nm filter (25 mg photocatalyst in 25 mL, 300 W Xe light source).

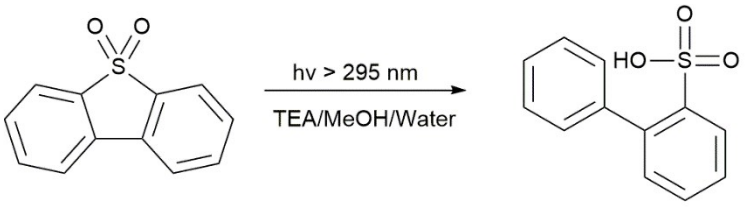

Scheme 1: Proposed catalyst breakdown.

Breakdown product analysis

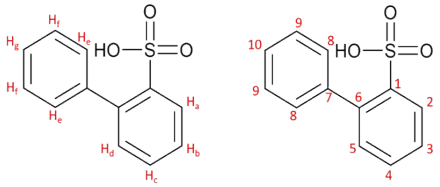

^{1}H NMR (400 MHz, $CDCl_3$): δ(ppm) = 8.08 (H_a, dd, J = 7.5, 1.5 Hz, 1H), 7.55 (H_e, d, J = 7.5 Hz, 2H), 7.45 (H_b, td, J = 7.5, 1.5 Hz, 1H,), 7.40 -7.30 (H_c, H_f, H_g, m, 4H), 7.23 (H_d dd, J = 7.5, 1.5 Hz, 1H). ^{13}C{^{1}H} NMR ($CDCl_3$): δ(ppm) = 154.07 (C_1), 139.94 (C_6), 139.80 (C_7), 130.17 (C_8), 130.05 (C_5), 129.15 (C_4), 127.84 (C_3), 127.78 (C_9), 127.04 (C_{10}), 121.81 (C_2). HR-MS Calcd for $[C_{12}H_9O_3S]^-$: m/z = 233.0278; found: m/z = 233.0274.

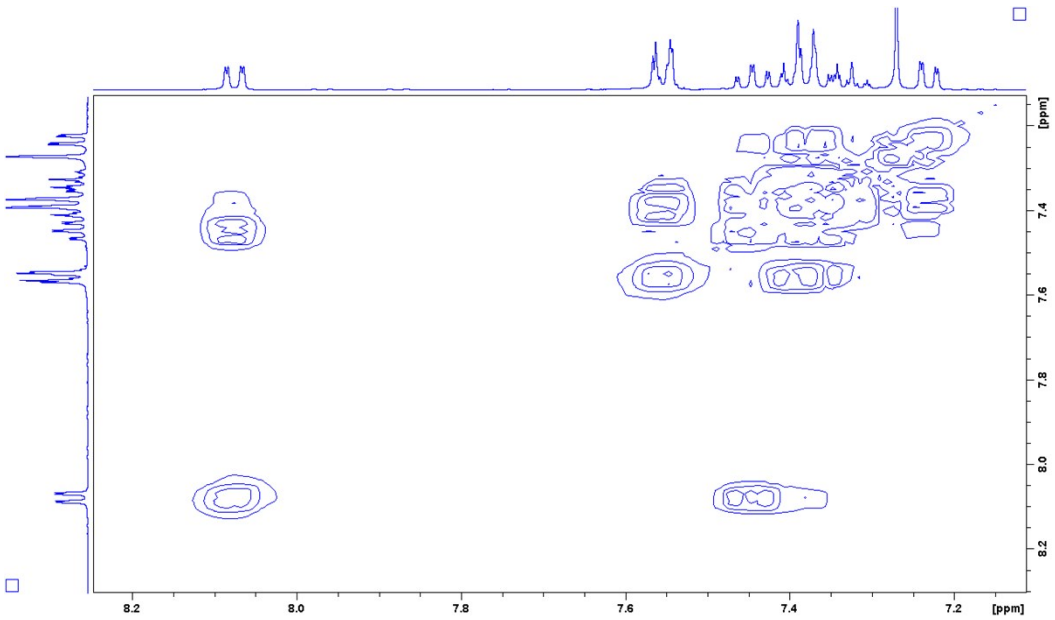

Figure S64: ^{1}H-COSY NMR spectrum of S1 breakdown product (400 MHz, $CDCl_3$).

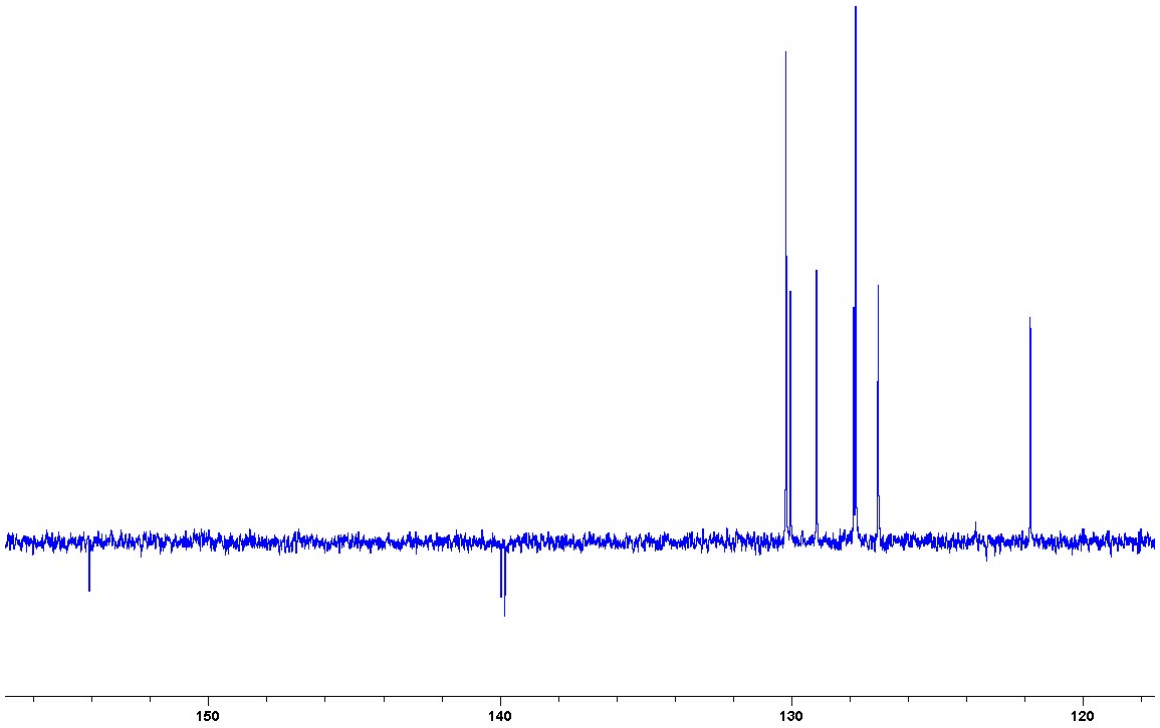

Figure S65: ^{13}C-NMR ATP spectrum of S1 breakdown product in $CDCl_3$. X-axis displays chemical shift in ppm.

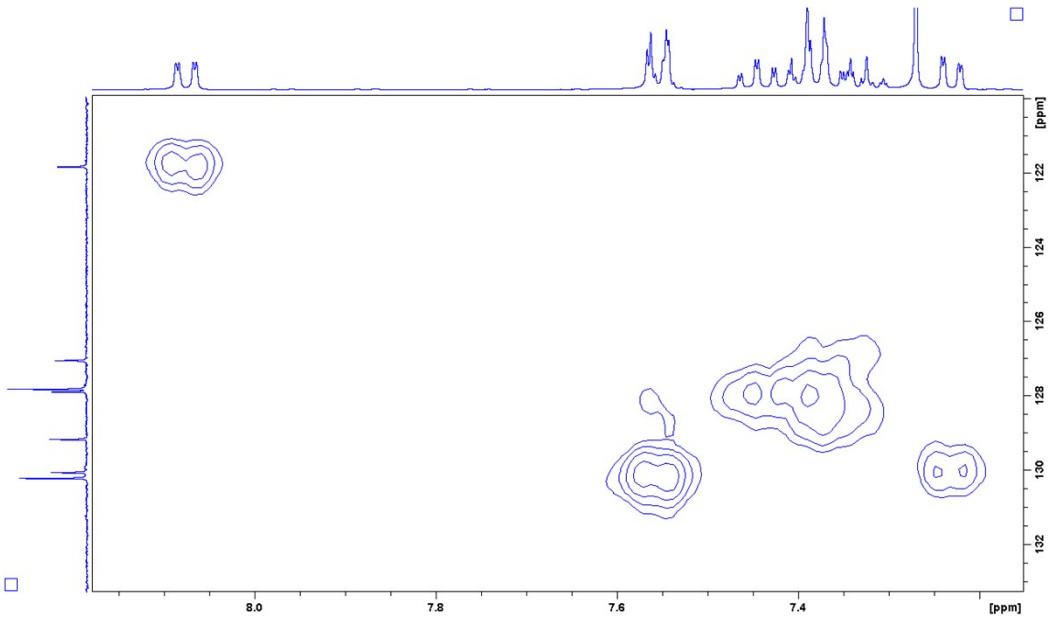

Figure S66: HSQC NMR spectra of S1 breakdown product in $CDCl_3$.

15.2 Photostability of S2

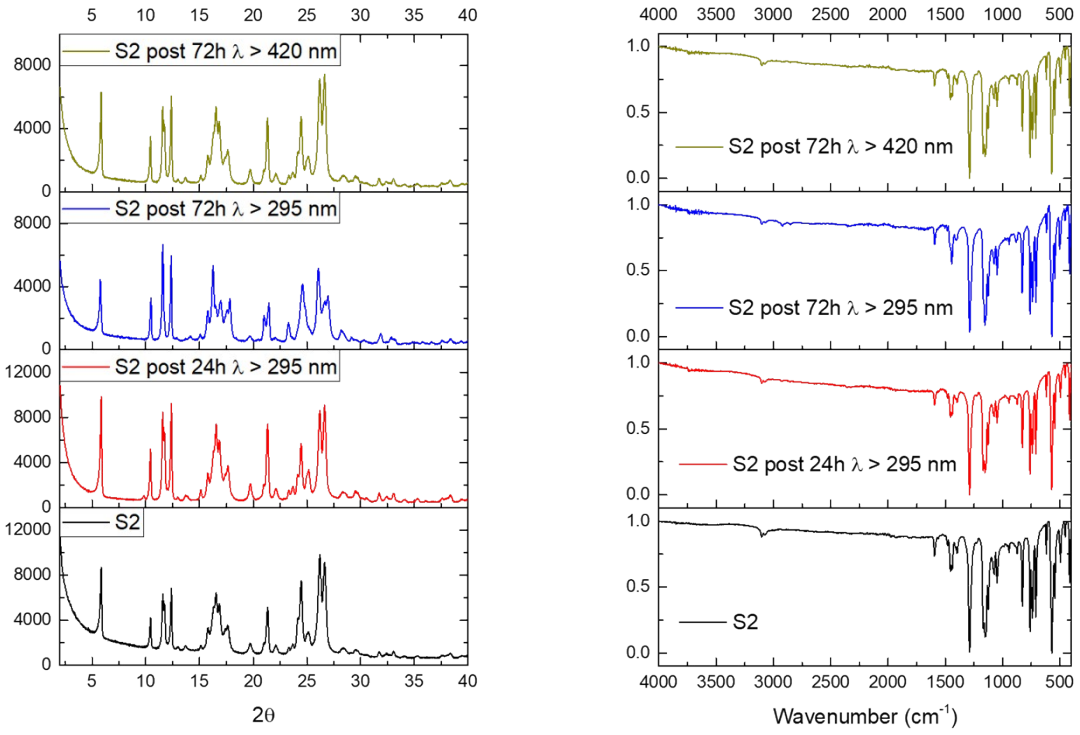

Figure S67: PXRD pattern (left) and IR spectra (right) of S2 before and after irradiation.

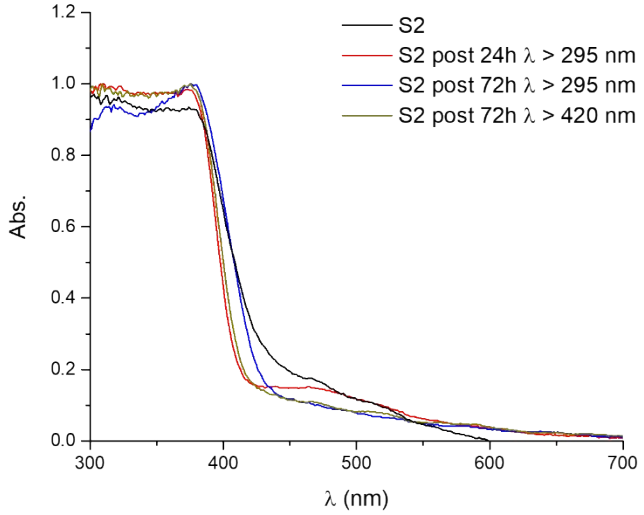

Figure S68: UV-Vis spectra of S2 before and after irradiation, 300 W Xe light source and various filters.

15.3 Photostability of S3

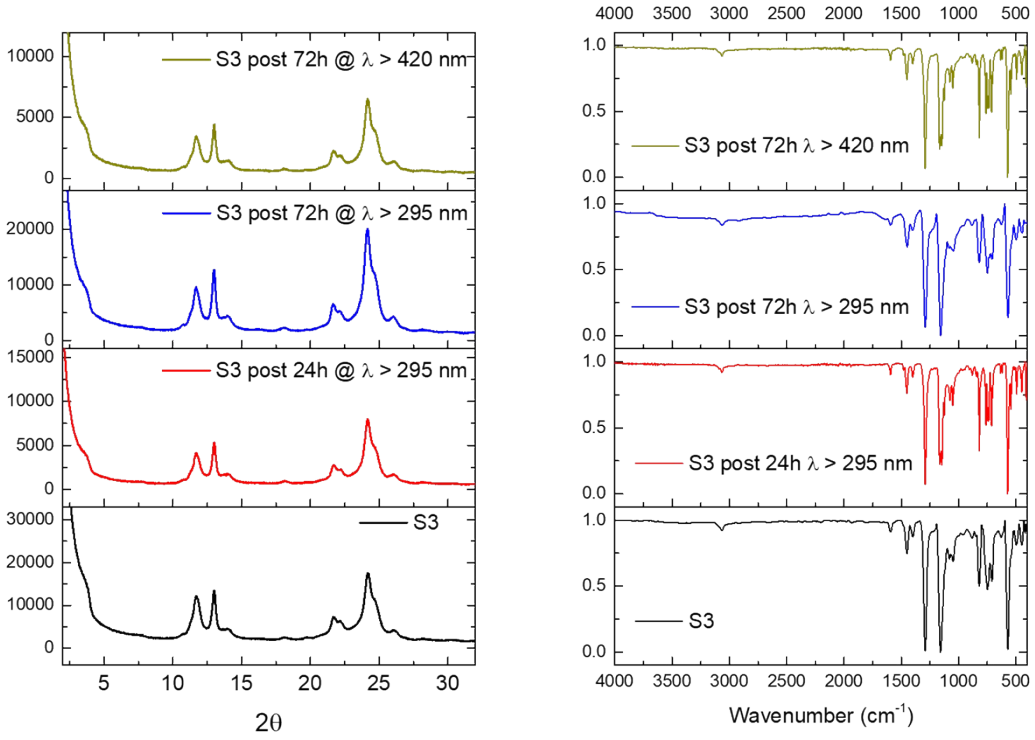

Figure S69: PXRD pattern (left) and IR spectra (right) of S3 before and after irradiation.

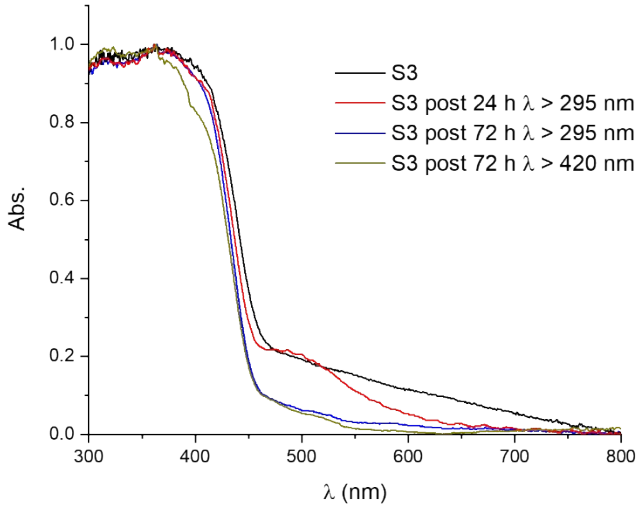

Figure S70: UV-Vis spectra of S3 before and after irradiation, 300 W Xe light source and various filters.

15.4 MeF Oligomers photostability

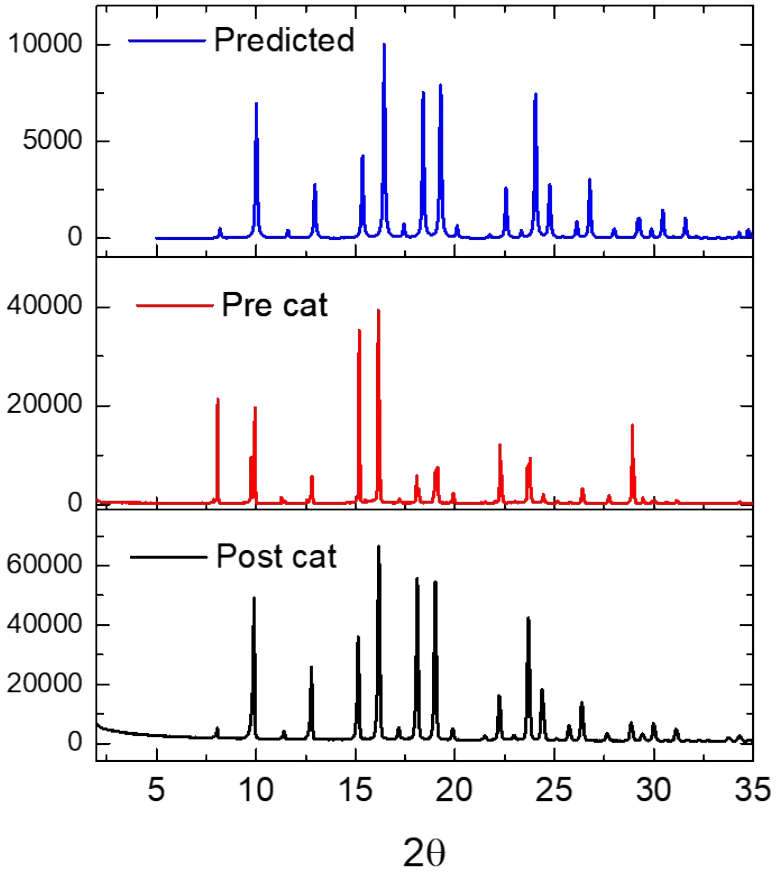

Figure S71: Predicted PXRD of MeF1 from single crystal structure (blue), measured PXRD of MeF1 pre and post 6 hours of irradiation in Na_2S / Na_2SO_3 (aq) at λ > 295 nm, 300 W Xe light source. Pre catalysis sample was comprised of large crystals measured before grinding.

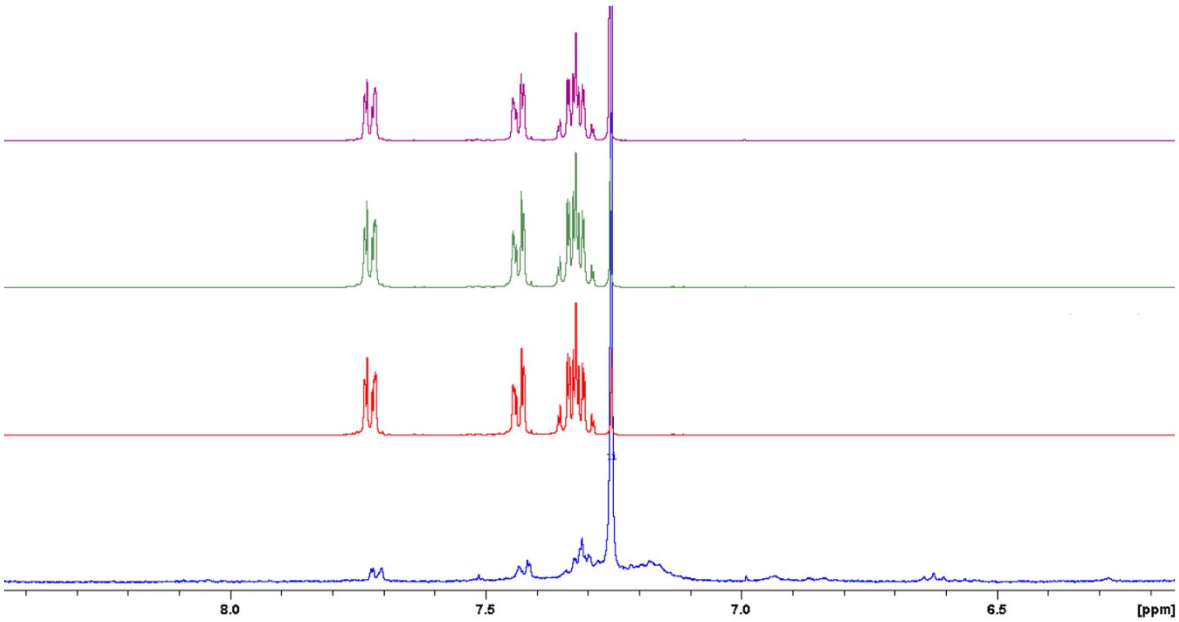

Figure S72: ^1H NMR in $CDCl_3$ of MeF1 pre (purple), post 6 hours irradiation in TEA / MeOH / water (1:1:1) at λ > 295 nm (green), post 6 hours irradiation in $Na_2S_{(aq)}$ (0.35 M) / $Na_2SO_{3(aq)}$ (0.2 M) at λ > 295 nm (red) and post 6 hours irradiation dissolved in THF / water / TEA at 400 > λ > 275 nm U-340 filter (blue). All using 300 W Xe light source. Broadening in sample from THF (blue) is thought to be due paramagnetic Ni.

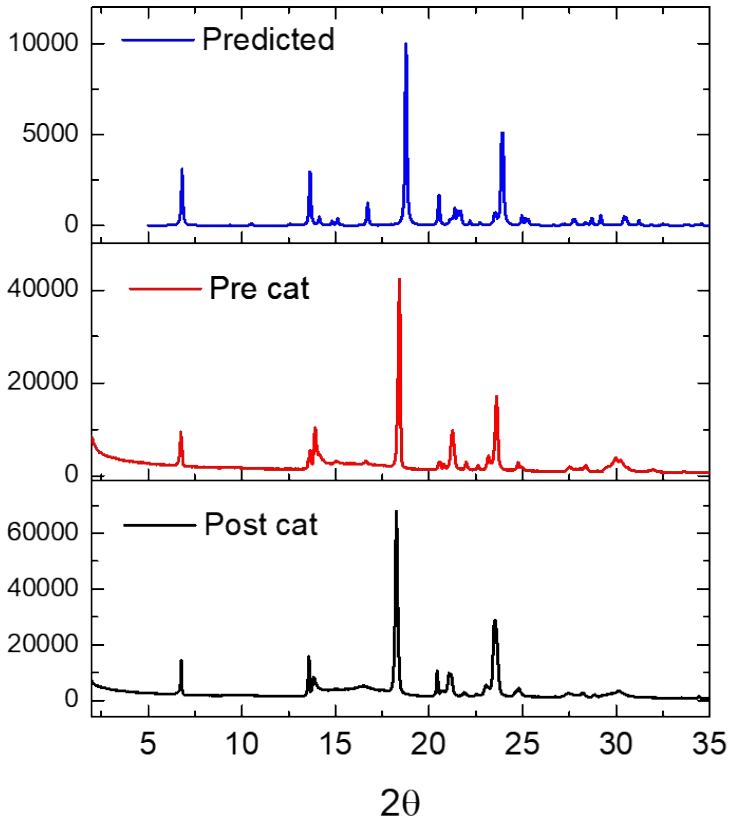

Figure S73: Predicted PXRD of MeF2 from single crystal structure (blue), measured PXRD of MeF2 pre and post 6 hours of irradiation in Na_2S / Na_2SO_3 (aq) at λ > 295 nm, 300 W Xe light source.

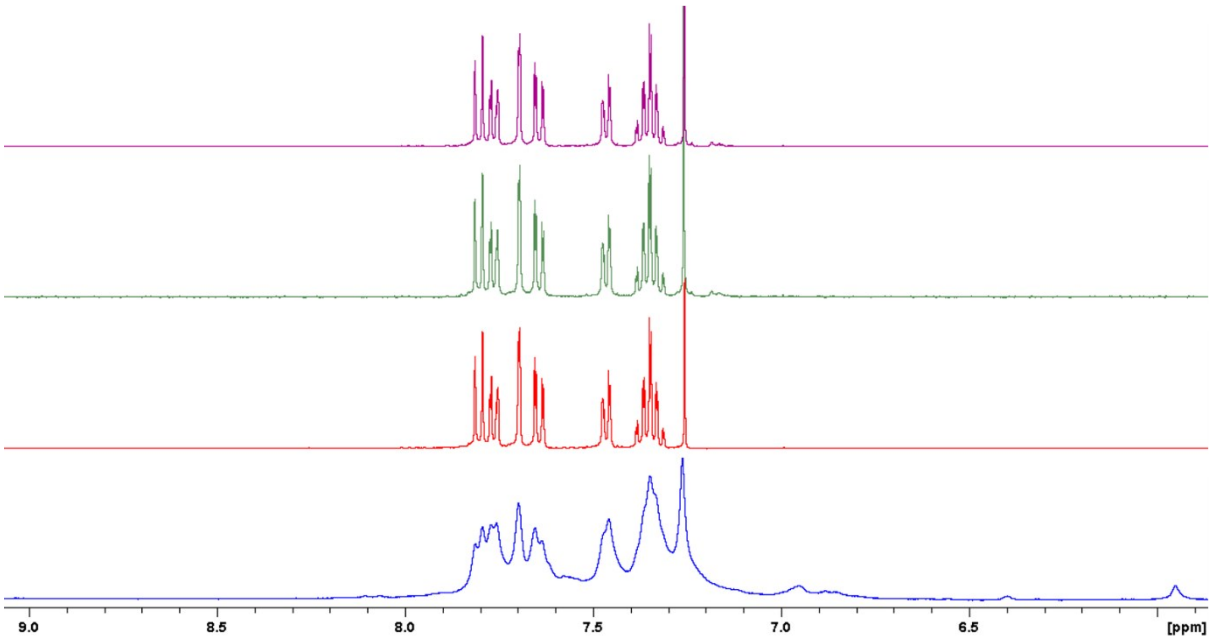

Figure S74: ^1H NMR in $CDCl_3$ of MeF2 pre (purple), post 6 hours irradiation in TEA / MeOH / water (1:1:1) at λ > 295 nm (green), post 6 hours irradiation in $Na_2S_{(aq)}$ (0.35 M) / $Na_2SO_{3(aq)}$ (0.2 M) at λ > 295 nm (red) and post 6 hours irradiation dissolved in THF / water / TEA at 400 > λ > 275 nm "U-340" filter (blue). All using 300 W Xe light source. Broadening in sample from THF (blue) is thought to be due paramagnetic Ni.

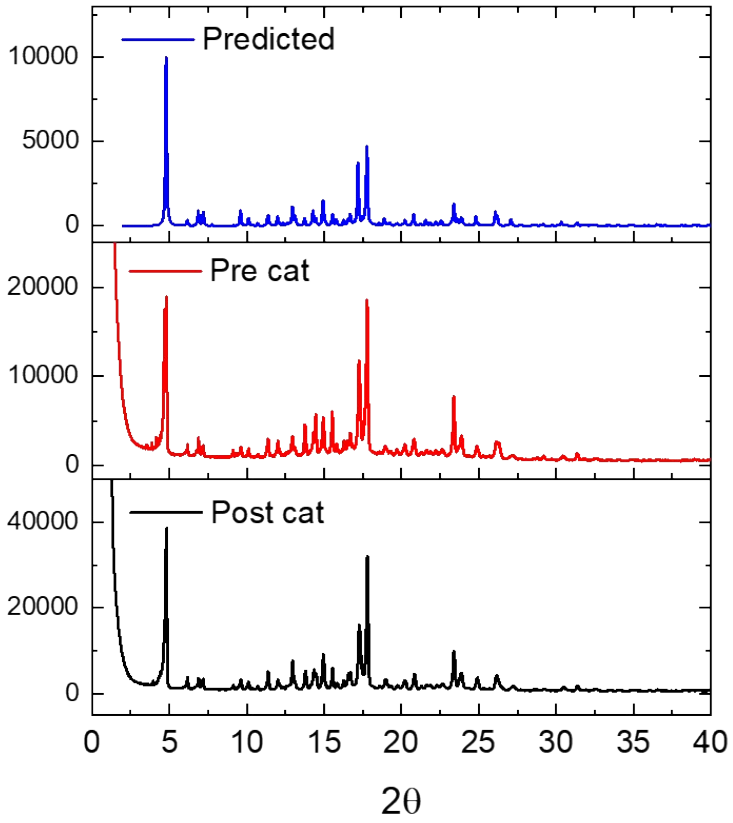

Figure S75: Predicted PXRD of MeF3 from single crystal structure (blue), measured PXRD of MeF3 pre and post 6 hours of irradiation at λ > 295 nm, 300 W Xe light source.

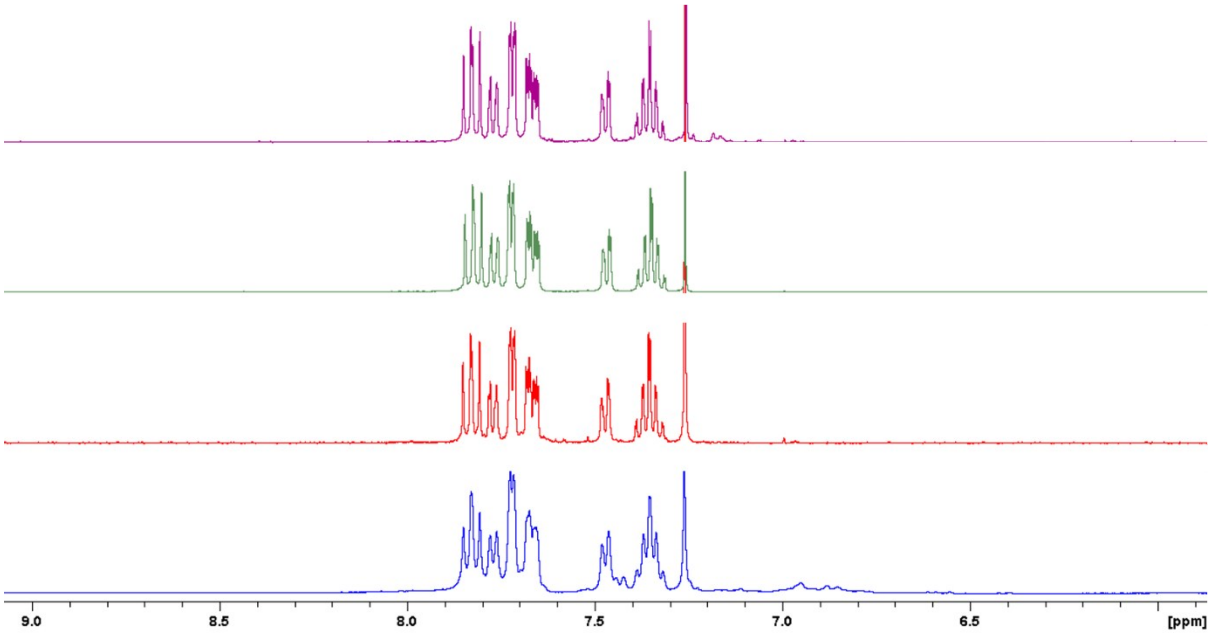

Figure S76: ^{1}H NMR in $CDCl_3$ of MeF3 pre (purple), post 6 hours irradiation in TEA / MeOH / water (1:1:1) at λ > 295 nm (green), post 6 hours irradiation in $Na_2S_{(aq)}$ (0.35 M) / $Na_2SO_{3(aq)}$ (0.2 M) at λ > 295 nm (red) and post 6 hours irradiation dissolved in THF / water / TEA at 400 > λ > 275 nm U-340 filter (blue). All using 300 W Xe light source. Broadening in sample from THF (blue) is thought to be due paramagnetic Ni.

15.5 Phenylene vs Mesitylene Oligomers photostability

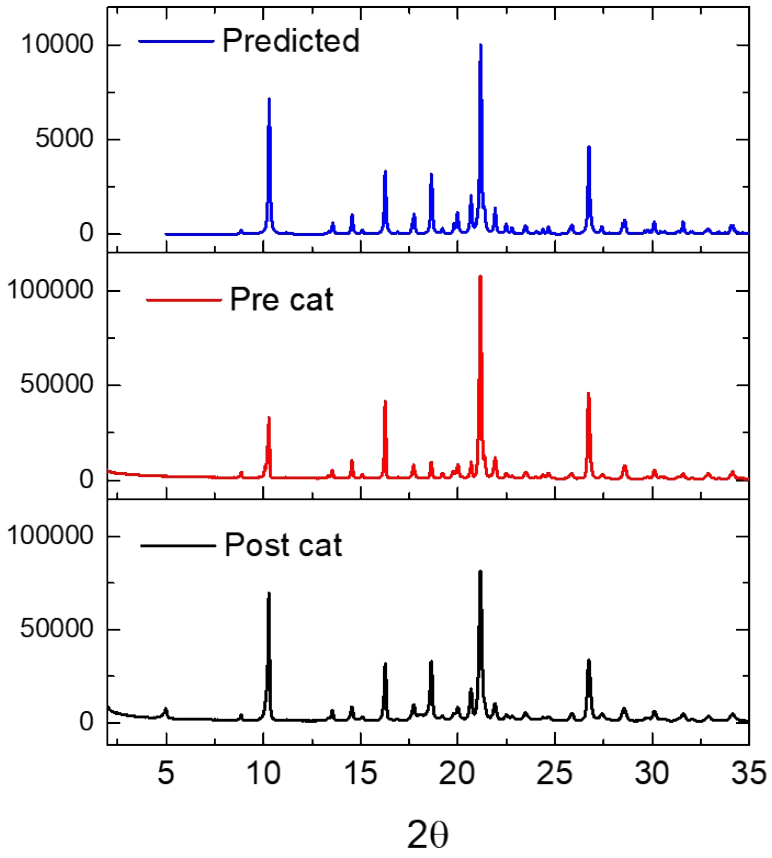

Figure S77: Predicted PXRD of PSP from single crystal structure (blue), measured PXRD of PSP pre and post 6 hours of irradiation in Na_2S / Na_2SO_3 (aq) at λ > 295 nm, 300 W Xe light source.

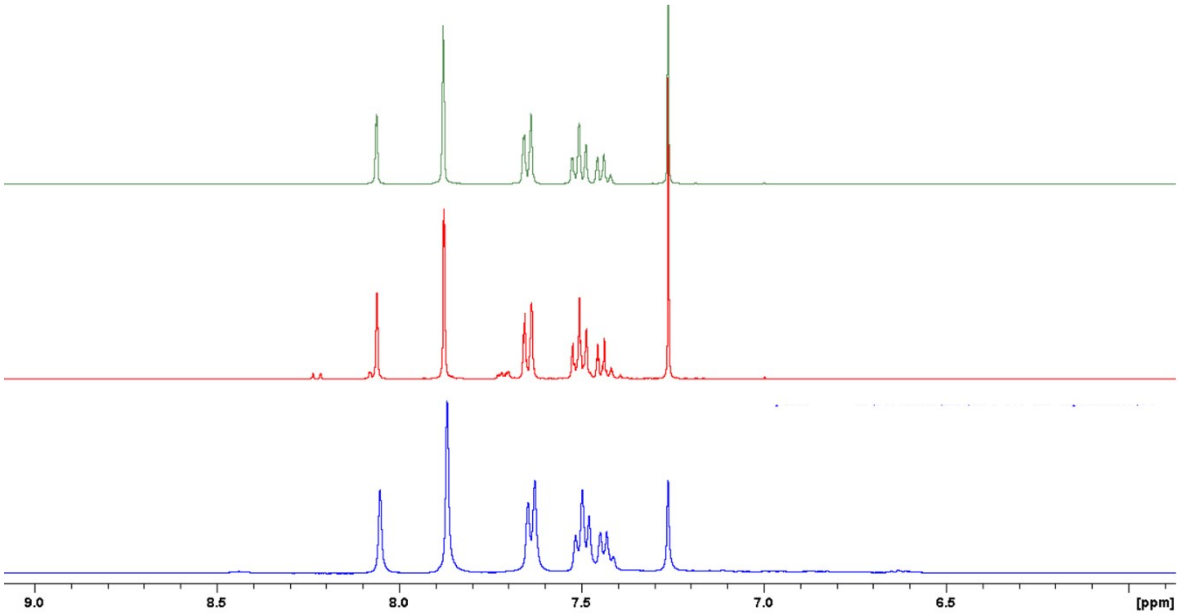

Figure S78: ^1H NMR in $CDCl_3$ of PSP pre (green), post 6 hours irradiation in $Na_2S_{(aq)}$ (0.35 M) / $Na_2SO_{3(aq)}$ (0.2 M) at λ > 295 nm (red) and post 6 hours irradiation dissolved in THF / water / TEA at 400 > λ > 275 nm U-340 filter (blue). Both using 300 W Xe light source. Broadening in sample from THF (blue) is thought to be due paramagnetic Ni.

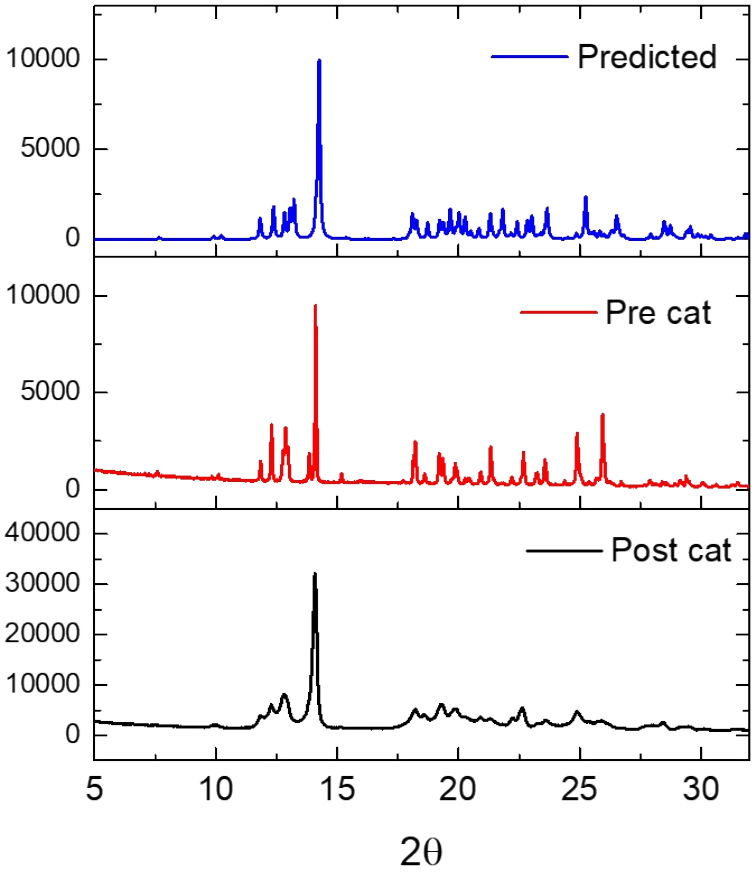

Figure S79: Predicted PXRD of MSM from single crystal structure (blue), measured PXRD of MSM pre and post 6 hours of irradiation in Na_2S / Na_2SO_3 (aq) at λ > 295 nm, 300 W Xe light source.

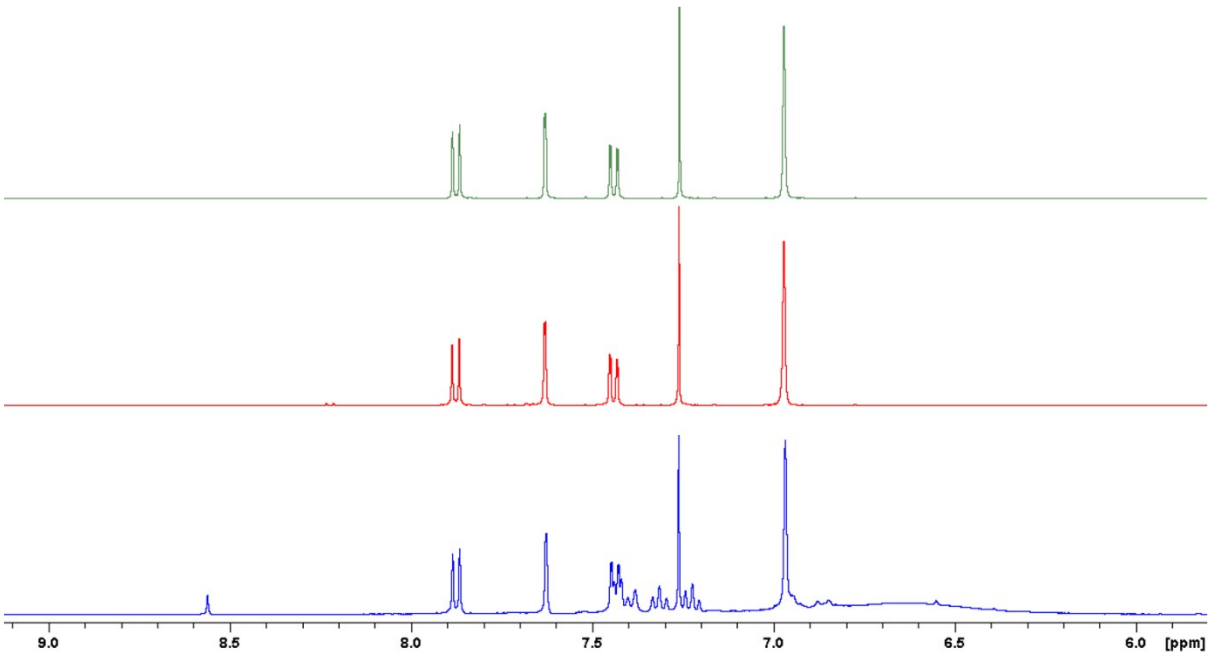

Figure S80: ^1H NMR in $CDCl_3$ of MSM pre (green), post 6 hours irradiation in $Na_2S_{(aq)}$ (0.35 M) / $Na_2SO_{3(aq)}$ (0.2 M) at λ > 295 nm (red) and post 6 hours irradiation dissolved in THF / water / TEA at 400 > λ > 275 nm U-340 filter (blue). Both using 300 W Xe light source. Broadening in sample from THF (blue) is thought to be due paramagnetic Ni.

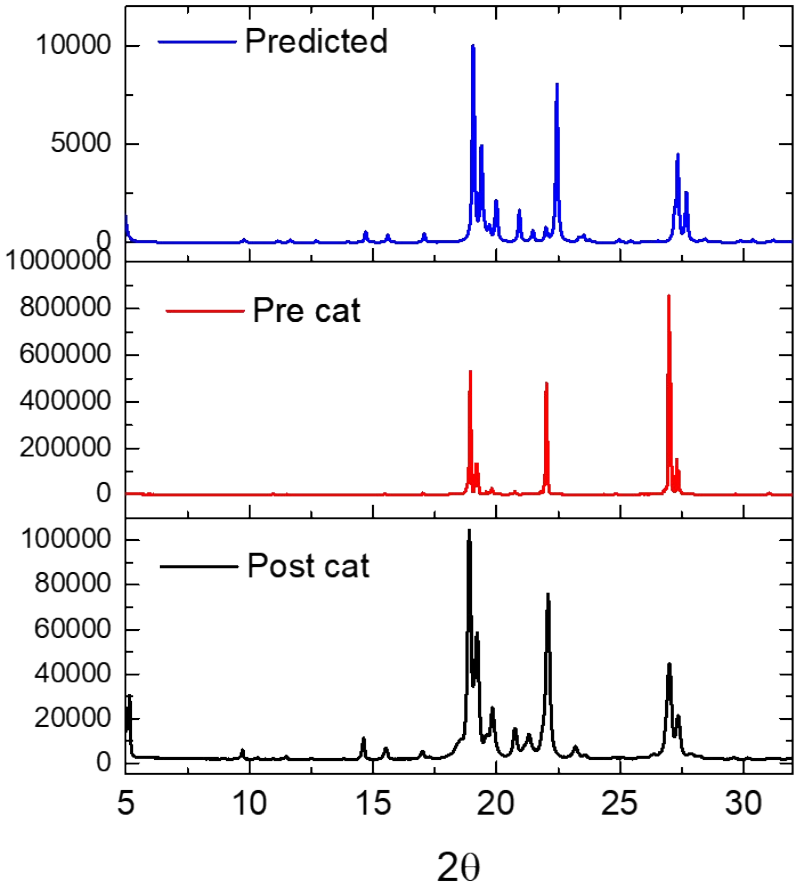

Figure S81: Predicted PXRD of PFP from single crystal structure (blue), measured PXRD of PFP pre and post 6 hours of irradiation in Na_2S / Na_2SO_3 (aq) at λ > 295 nm, 300 W Xe light source.

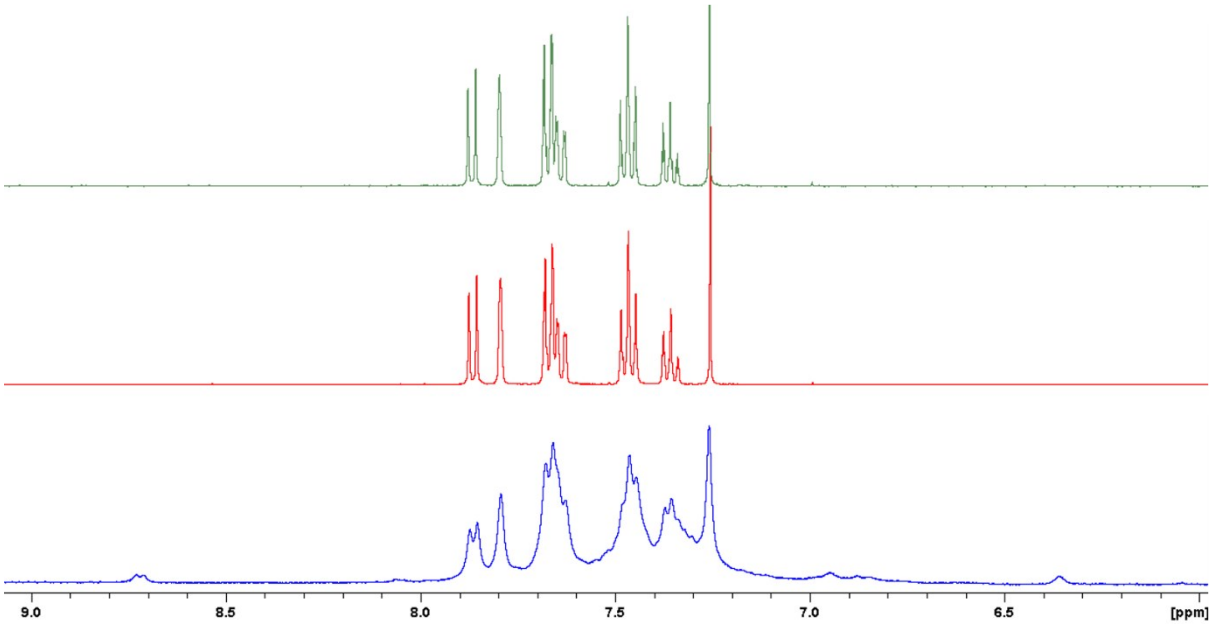

Figure S82: ^1H NMR in $CDCl_3$ of PFP pre (green), post 6 hours irradiation in $Na_2S_{(aq)}$ (0.35 M) / $Na_2SO_{3(aq)}$ (0.2 M) at λ > 295 nm (red) and post 6 hours irradiation dissolved in THF / water / TEA at 400 > λ > 275 nm U-340 filter (blue). Both using 300 W Xe light source. Broadening in sample from THF (blue) is thought to be due paramagnetic Ni.

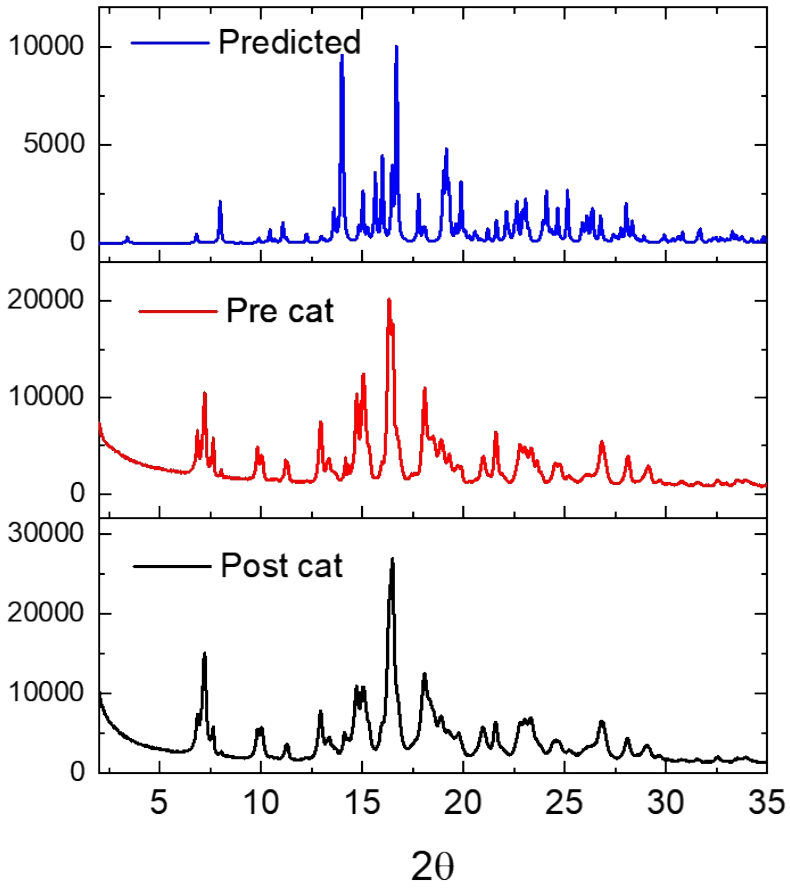

Figure S83: Predicted PXRD of MFM from single crystal structure (blue), measured PXRD of MFM pre and post 6 hours of irradiation in Na_2S / Na_2SO_3 (aq) at λ > 295 nm, 300 W Xe light source.

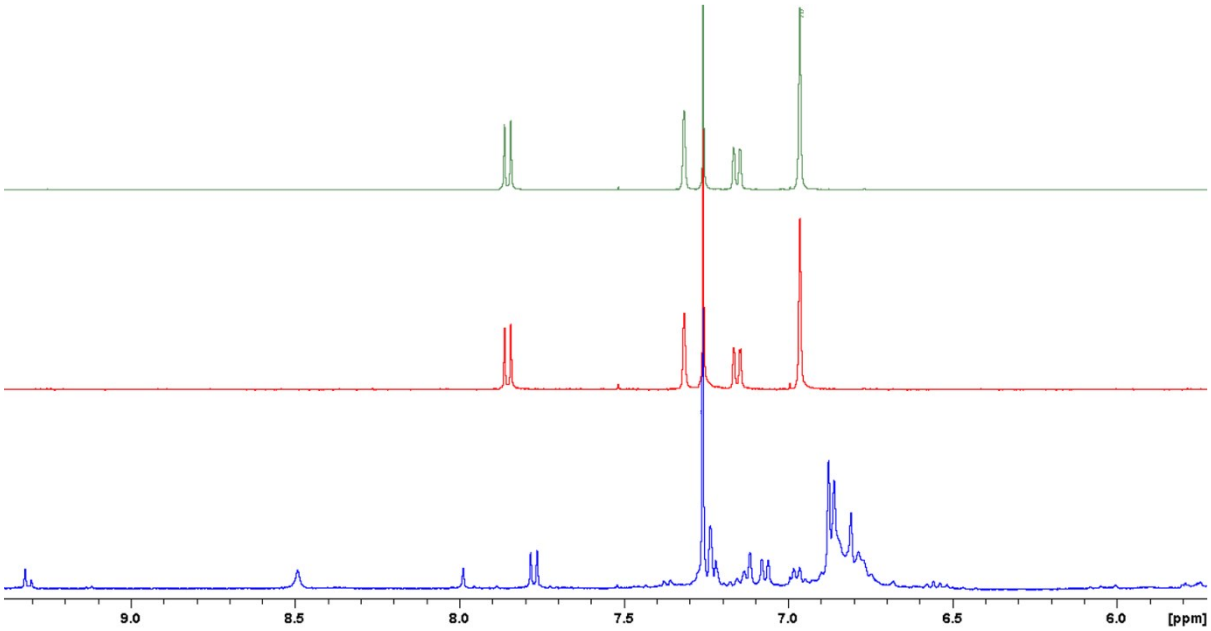

Figure S84: ^{1}H NMR in $CDCl_3$ of MFM pre (green), post 6 hours irradiation in $Na_2S_{(aq)}$ (0.35 M) / $Na_2SO_{3(aq)}$ (0.2 M) at λ > 295 nm (red) and post 6 hours irradiation dissolved in THF / water / TEA at 400 > λ > 275 nm U-340 filter (blue). Both using 300 W Xe light source. Broadening in sample from THF (blue) is thought to be due paramagnetic Ni.

16. Transmission Electron Microscopy

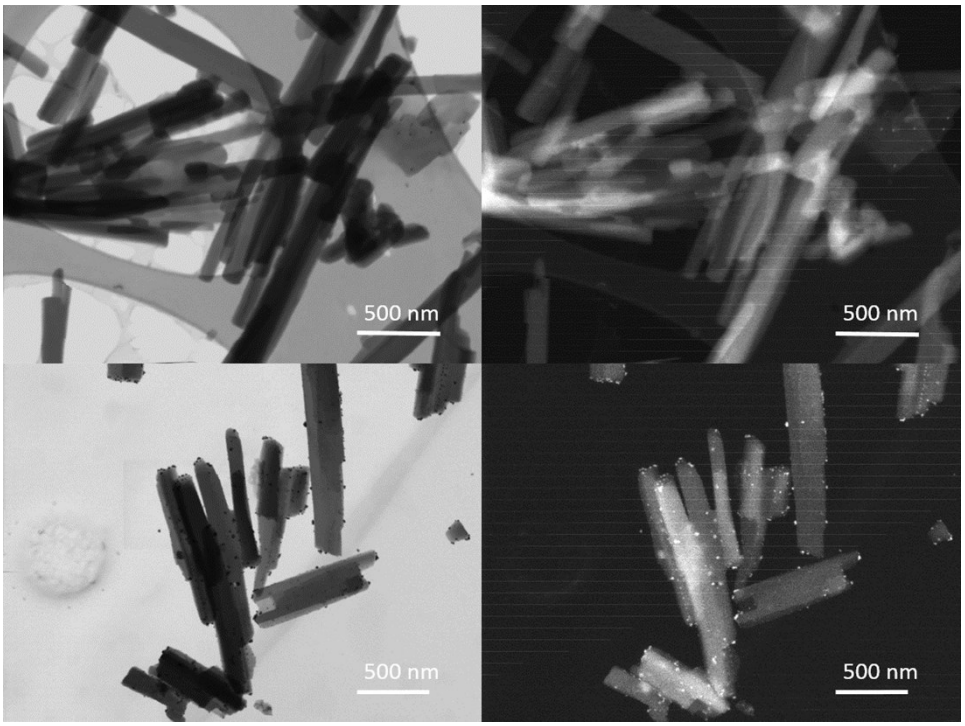

Figure S85: STEM images of S2 as synthesised (top) and with 3 wt. % Pd loaded by photodeposition (bottom) in BF mode (left) and HADF mode (right).

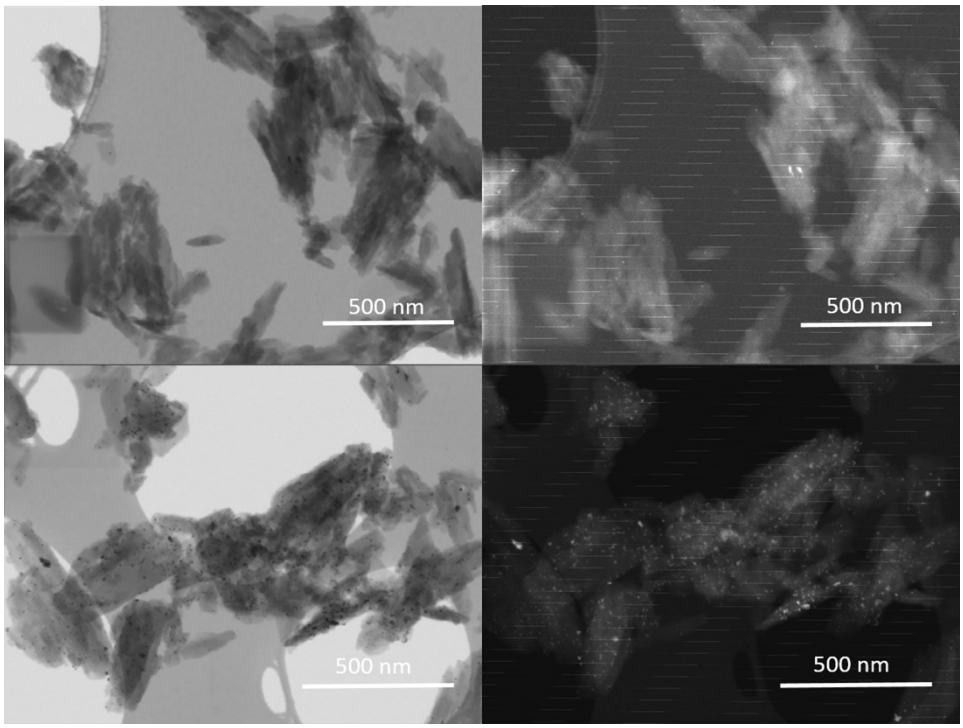

Figure S86: STEM images of S3 as synthesised (top) and with 3 wt. % Pd loaded by photodeposition (bottom) in BF mode (left) and HADF mode (right).

17.Transient Absorption Spectroscopy

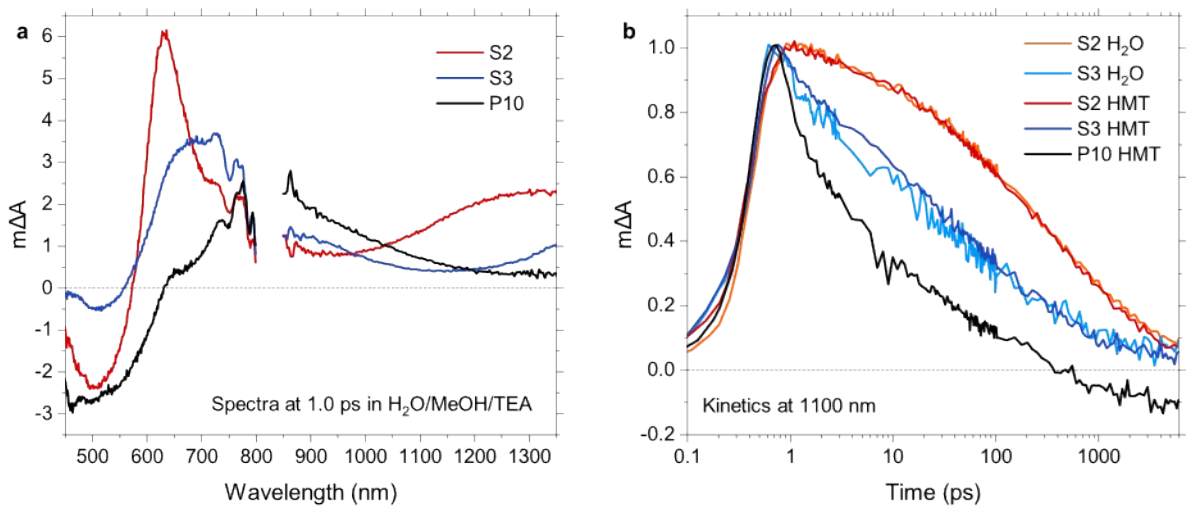

Figure S87: Exciton signatures and dynamics in S2, S3, and P10 suspensions. (a) Transient absorption spectra probed at 1.0 ps using polymer particles suspended in a H_2O/MeOH/TEA mixture, and (b) transient absorption kinetics probed at 1100 nm as obtained from suspensions in H_2O and H_2O/MeOH/TEA. All experiments were performed using an excitation wavelength of 355 nm and a fluence of 0.08 mJ cm^{-2}.

18. DFT calculations

Table S9 IP, EA, IP*, EA*, lowest vertical singlet excitation energy (optical gap, Δo) and oscillator strength of the lowest vertical singlet excitation values for the different oligomers as calculated using (TD-)DFT (B3LYP, DZP, COSMO(80.1), m3 grid, Turbomole 7.01).

	IP	EA	IP*	EA*	Δo	f
MeF1	1.26	-3.10	-3.10	1.27	4.52	0.3753
MeF2	0.85	-2.58	-2.45	0.72	3.65	1.3730
MeF3	0.74	-2.45	-2.25	0.53	3.31	2.1172
S1	1.92	-2.20	-1.81	1.53	4.12	0.1095
S2	1.55	-1.81	-1.68	1.42	3.53	1.0192
S3	1.47	-1.67	-1.49	1.29	3.25	1.7700
PFP	0.92	-2.60	-2.48	0.80	3.76	1.4283
PSP	1.37	-1.99	-1.81	1.18	3.50	0.8354
MFM	1.05	-3.03	-2.70	0.72	4.42	0.9232
MSM	1.47	-2.21	-1.89	1.15	3.90	0.1442

19. References

1 B. M. Fung, A. K. Khitrin and K. Ermolaev, *J. Magn. Reson.*, 2000, **142**, 97–101.

2 C. R. Morcombe and K. W. Zilm, *J. Magn. Reson.*, 2003, **162**, 479–86.

3 G. M. Sheldrick, *SADABS, Programs Scaling Absorpt. Correct. Area Detect. Data*, 2008, University of Göttingen: Göttingen, Germany.

4 L. Krause, R. Herbst-Irmer, G. M. Sheldrick and D. Stalke, *J. Appl. Crystallogr.*, 2015, **48**, 3-10.

5 G. Winter, D. G. Waterman, J. M. Parkhurst, A. S. Brewster, R. J. Gildea, M. Gerstel, L. Fuentes-Montero, M. Vollmar, T. Michels-Clark, I. D. Young, N. K. Sauter and G. Evans, *Acta Crystallogr. Sect. D Struct. Biol.*2018, **74**, 85-97.

6 G. M. Sheldrick, *Acta Crystallogr. Sect. A Found. Crystallogr.*, 2015, **71**, 3-8.

7 G. Sheldrick, *Acta Crystallogr., Sect. A: Found. Crystallogr*., 2008, **64**, 112-122.

8 G. Sheldrick*, Acta Crystallogr., Sect. C: Struct. Chem., 2015, 71, 3–8*

9 O. V. Dolomanov, L. J. Bourhis, R. J. Gildea, J. A. K. Howard and H. Puschmann, *J. Appl. Crystallogr.*, 2009, **42**, 339-341.

10 F. Furche, R. Ahlrichs, C. Hättig, W. Klopper, M. Sierka and F. Weigend, *Wiley Interdiscip. Rev. Comput. Mol. Sci.*, 2014, **4**, 91–100.

11 M. Sachs, C. Hyojung, J. Kosco, C. M. Aitchison, L. Francas, S. Corby, C.-L. Chiang, A. A. Wilson, R. Godin, A. Fahey-Williams, A. I. Cooper, R. S. Sprick, I. McCulloch and J. R. Durrant, *ChemRxiv*, 2020, DOI: 10.26434/chemrxiv.12273122.

12 G. A. Crosby and J. N. Demas, *J. Phys. Chem.*, 1971, **75**, 991–1024.

13 A. Samoc, *J. Appl. Phys.*, 2003, **94**, 6167–6174.

14 C. Huang, J. Wen, Y. Shen, F. He, L. Mi, Z. Gan, J. Ma, S. Liu, H. Ma and Y. Zhang, *Chem. Sci.*, 2018, **9**, 7912–7915.

15 X. Yang, Z. Hu, Q. Yin, C. Shu, X. Jiang, J. Zhang, X. Wang, J. Jiang, F. Huang and Y. Cao, *Adv. Funct. Mater.*, 2019, 1808156.

16 B. Kobin, S. Behren, B. Braun-Cula and S. Hecht, , *J. Phys. Chem. A,* 2016, **120**, 28, 5474-5480.

17 F. Waiblinger, J. Keck, A. P. Fluegge, H. E. A. Kramer, D. Leppard and G. Rytz, *J. Photochem Photobiol A,* 1999, **126**, 43-49.

18 M. Salvador, N. Gasparini, J. Darí O Perea, S. H. Paleti, A. Distler, L. N. Inasaridze, P. A. Troshin, L. Lü, H.-J. Egelhaaf and C. Brabec, *Energy Environ. Sci.*, 2017, **10**, 2005-2016.